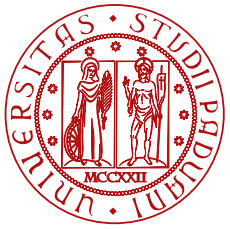

Università degli Studi di Padova

Dipartimento di Ingegneria dell'Informazione

Master Thesis in Control Systems Engineering

Extended Kalman Filter Estimation of Human Arm Configuration

Master Candidate

Gioel Adriano Maria Vencato

Student ID 2005829

Supervisor

Prof. Angelo Cenedese

University of Padova

KTH supervisor

PostDoc. Carlos Rodriguez de Cos

KTH Royal Institute of Technology

Academic Year
2022/2023

Fist of all, I would like to thank my mother, sister and Mauro who gave me the strength, their patience throughout all these years and, most importantly, their belief in me along this journey. Thanks also to uncle Robi and all the parents for their support.

Special thanks to my supervisor Prof. Cenedese who gave me the opportunity of carrying out the master thesis at the prestigious KTH Royal Institute of Technology in Sweden. Here, I could not have undertaken this journey without professor Dimorogonas, my examiner and head of the Division of Decision and Control Systems in KTH. So, a deep appreciation to him. I also would like to thank dr. Carlos Rodriguez de Cos who, as my supervisor at KTH, provided me the needed papers and clarifications in order for me to complete the given tasks.

Last but not least, a big thanks to all my friends. You will never know how helpful you have been.

Abstract

The Kalman Filter (KF) is a mathematical tool well suited for an algorithmic implementation that estimates the state of a linear dynamic system by exploiting the knowledge of the system's dynamics, its statistics and a set of measurements. In practice however, the linearity conditions are often not satisfied, but some extensions of the filter algorithm can be implemented in order to overcome this problem. One possible extension is represented by the Extended Kalman Filter (EKF) which is one of the best known non-linear filter versions.

The human arm is a highly non-linear system. Hence, the EKF algorithm can be exploited to estimate its joint-space configuration through few motion capture markers placed along the human arm. Other approaches, such as Least Squares (LS) and Linearized Kalman Filter (LKF) are tested to show how the EKF leads in general to better joint variable estimates. The design and validation of such estimation procedures are performed in a simulation environment, offered by Simulink and Simscape platforms in Matlab. Here it is possible to develop the 7 Degrees of Freedom (DoF) Robot Manipulator (RM) which models the human arm and to find a suitable combination of the number of markers on the shoulder, forearm and hand for which it is possible to compute the state estimates, namely for which singular configurations are avoided. The aforementioned estimation algorithms are implemented in the real system and they are closely compared.

Sommario

Il filtro di Kalman KF è uno strumento matematico adatto per un'implementazione algoritmica che stima lo stato di un sistema dinamico lineare sfruttando la conoscenza della dinamica del sistema, delle sue statistiche e di un insieme di misure. In pratica tuttavia, le condizioni di linearità spesso non sono soddisfatte ed alcune estensioni di tale algoritmo possono essere implementate per fare fronte al problema. Un possibile approccio è rappresentato dal filtro di Kalman esteso EKF che è una delle versioni di filtri non lineari più conosciute.

Il braccio umano è un sistema altamente non lineare. Quindi, l'algoritmo EKF può essere sfruttato per stimare la configurazione del braccio attraverso l'acquisizione di misure di alcuni sensori posti lungo di esso. Altri approcci, come il metodo dei minimi quadrati LS e il filtro di Kalman linearizzato lungo una traiettoria nominale LKF sone testati per mostrare come EKF porti in generale a una migliore stima. La progettazione e la validazione di tali procedure di stima vengono eseguite in un ambiente di simulazione, offerto dalle piattaforme Simulink e Simscape in Matlab. Qui è possibile sviluppare il 7 gradi di libertà manipolatore robotico che modella il braccio umano. Inoltre, diverse combinazioni del numero di sensori da porre sulla spalla, avambraccio e mano vengono testate. Una volta terminata la fase di simulazione, i diversi algoritmi di stima vengono applicati al sistema reale e strettamente analizzati.

Contents

List of Figures

List of Tables

List of Algorithms

List of Acronyms

ARE Algebraic Riccati Equation

DK Differential Kinematics

DoF Degrees of Freedom

EKF Extended Kalman Filter

FK Forward Kinematics

KF Kalman Filter

LKF Linearized Kalman Filter

LS Least Squares

MCS Motion Capture System

QTM Qualisys Track Manager

RF Reference Frame

RM Robot Manipulator

RMSE Root Mean Square Error

ROS Robot Operating System

SVD Singular Value Decomposition

1 Introduction

The design of control systems exploits many approaches in which all the state variables are assumed to be available for feedback. In practice, however, none or some of the state variables may be directly available for feedback. Indeed, the measurements may consist of noisy linear/non-linear combinations of the state variables which need to be estimated. Here is where estimation algorithms come into play. In systems engineering the estimation process leads to extracting information about state variables from noisy measurements. If the process does not contain any stochastic elements, then the estimation process leads to the straightforward LS estimation technique. On the other hand, if the process has non-stationary stochastic variables and it is linear then the solution to the optimal state estimation is the well known KF. The derivation of the discrete-time Kalman filter is provided in detail in Chapter 2.2. Whenever the states to estimate concern a non-linear system, one extensions of the Kalman filter, the EKF, can be used. This topic is covered in Chapter 3.1.

Since the aim of this work is to estimate the states of a highly non-linear system, such as the human arm, main focus is given to the design, validation and implementation of the EKF. However, also other approaches, namely LS and LKF, are tested. Specifically, the human arm configuration estimation is driven by the acquisition of some markers' measurements which are placed along the shoulder, forearm and hand. A good estimate of the joint-space configuration of the human arm means a better experimental outcome of the control strategy for human-robot cooperative manipulation under the collaboration of a human agent [19], about which a brief description follows.

1.1 A general overview

Human-robot collaboration is expected to play a very important role in a lot of scenarios, i.e. agricultural robotics. Therefore, flexible and robust controllers which specifically consider the interaction capabilities in their formulation are needed. Specifically, in order to cope with the human agent, an adaptive update law inferring the human contribution to the system dynamics from basic perception feedback through the human arm stiffness is used [19].

The overall system is depicted in Fig. 1.1, where the human operator arm (**H**) is assumed to be equivalent to a 7-DoF RM with flexible modes and the flexible joint RM model in [3] is employed to represent its intrinsic complexity. Given the assumption that the external forces are compensated by the elastic forces transmitted through the joints, namely

$$K\boldsymbol{\delta} = -J_H^\top \mathbf{f}_H, \tag{1.1}$$

a simplified (**H**) model is adopted:

$$K\boldsymbol{\delta} = \mathbf{d}_H - J_H^\top \mathbf{f}_H \tag{1.2}$$

Consequently, the least-squares solution is given by

$$\hat{\mathbf{f}}_H = \left(J_H^\top\right)^\dagger \left[\hat{\mathbf{d}}_H - \hat{K}\boldsymbol{\delta}\right] \tag{1.3}$$

where

- J_H is the geometric Jacobian of (**H**).
- $\left(J_H^\top\right)^\dagger = \left(J_H\, J_H^T\right)^{-1} J_H$ is the left Moore-Penrose pseudoinverse of J_H^T.
- $\mathbf{d}_H \in \mathbb{R}^7$ is an unknown slow time-varying disturbance modelling the small deviations.
- K represents the unknown stiffness of the flexible DoF of (**H**).
- $\boldsymbol{\delta}$ are the flexible deflections, namely $\boldsymbol{\delta} = \boldsymbol{\eta} - \boldsymbol{\mu}$ with $\boldsymbol{\eta} \in \mathbb{R}^7$ as the angle of the links and $\boldsymbol{\mu} \in \mathbb{R}^7$ as the angle of the motors.
- $\mathbf{f}_H$ are the forces and torques exerted by (**H**) to (**L**).

Before the collaborative manipulation, a given configuration of the human arm is assumed to be at the equilibrium, i.e. $\boldsymbol{\mu}(0) = \boldsymbol{\eta}(0)$. Moreover, from the

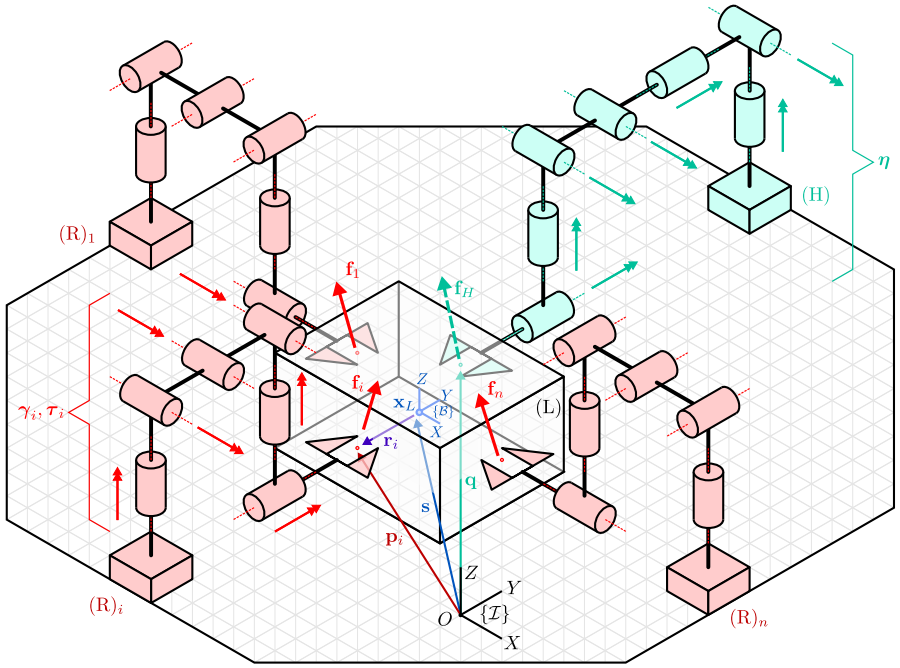

Figure 1.1: Overall system scheme -with (**H**) in aquamarine and (**R**) in red- and $\{\mathcal{B}\}$ and $\{\mathcal{I}\}$ reference frames

assumption that it does not move beyond a small area, i.e. $\boldsymbol{\mu}(t) \approx \boldsymbol{\mu}(0),\ \forall t \geq 0$, it follows that $\boldsymbol{\delta}(t) = \boldsymbol{\eta}(t) - \boldsymbol{\mu}(t) \approx \boldsymbol{\eta}(t) - \boldsymbol{\mu}(0) = \boldsymbol{\eta}(t) - \boldsymbol{\eta}(0),\ \forall t \geq 0$. In other words, at first, no flexible deflections are assumed to affect the initial joint-space configuration of (**H**) while, successively, all the movements of the arm are attributed to the flexible modes.

In [19], the quantity $\boldsymbol{\eta}(t)$ is found by simply getting the directions of the links (using some markers since the whole experiment exploited the presence of the Motion Capture System (MCS)) and estimating the angle between these vectors. An important fact to remark is that, in this scenario, no filtering is applied. Any noise in the sensors implies amplified noise for $\boldsymbol{\eta}$ and any wrong marker position creates complete new configurations. In order to make the estimate more accurate, more robust and more stable, other estimation algorithms have to be exploited. In the following, they are seen in detail.

1.2 Structure of the thesis

The thesis is structured as follows: **chapter 2** and **chapter 3** give a detailed explanation on the methods to estimate state variables for linear and non-linear systems. They give a theoretical overview concerning the Least Squares (LS), the Kalman filter (KF) and the Extended Kalman filter (EKF) approaches. As far as the human arm model is concerned, its mathematical formulation is provided by **chapter 4**, where the Forward Kinematics (FK) and Differential Kinematics (DK) equations are computed. By exploiting its mathematical system description, it is possible to simulate the human arm behaviour in the simulation environment Simulink and Simscape platforms where, the aforementioned estimation algorithms can be implemented. Different algorithm parameters are considered and closely analyzed in **chapter 5**. Finally, **chapter 6** assess that the Extended Kalman filter algorithm, verified to work in the simulations step, works in the real experiment as well. It follows a brief discussion on the obtained results.

2

Linear filters

A potential target for state estimation is any discipline that is interested in the mathematical modeling of its systems. This covers a wide range of fields, such as robotics, economics, ecology, and biology, as well as electrical engineering, mechanical engineering, chemical engineering, aerospace engineering and many others. Engineers find state estimation relevant for at least two reasons:

- In order to implement a state-feedback controller, an engineer frequently needs to estimate the system states.
- Because the system states often represents important quantities themselves, engineers frequently have to estimate them.

Methods for obtaining estimations of the state vector from the given measurements must be thought of. The study of the required state estimators is covered in this chapter, where linear state estimators are addressed, and the following one, which deals with non-linearities.

The least-squares (LS) principle is the standard approach for estimating unknown parameters from uncertain data. The parameters of interest, as well as the dominant error sources, are often time varying. If these time variations can be modeled, the parameters can be resolved based on minimum mean squared error prediction, filtering, and smoothing techniques. Of the various such techniques, the Kalman filter (KF) is most prominent. It is able to recursively estimate the state of a dynamic system.

In the following, the least-squares and its recursive version are closely addressed. The latter will serve as foundation of the kalman filter algorithm.

2.1 Least-squares

2.1.1 Least-squares estimator for linear regression models

In this section, the estimation of a constant from a number of noisy measurements of it is provided. Assume that $\boldsymbol{\theta}$ is a constant but unknown n-element vector and that $\mathbf{y}$ is a noisy m-element measurement vector. How can the "best" estimate of $\hat{\boldsymbol{\theta}}$ for $\boldsymbol{\theta}$ be determined? Each element of the measurement vector $\mathbf{y}$ is supposed to be a *linear* combination of the $\boldsymbol{\theta}$ elements plus some measurement noise:

$$\begin{aligned} y_1 &= \Phi_{11}\theta_1 + \cdots + \Phi_{1n}\theta_n + v_1 \\ &\vdots \\ y_m &= \Phi_{m1}\theta_1 + \cdots + \Phi_{mn}\theta_n + v_m \end{aligned}$$

This set of equations can be put into matrix form as

$$\mathbf{y} = \boldsymbol{\Phi}\boldsymbol{\theta} + \mathbf{v}$$

Let $\epsilon_{\mathbf{y}}$ be the difference between the noisy measurements and the vector $\boldsymbol{\Phi}\boldsymbol{\theta}$, namely the measurement residual:

$$\epsilon_{\mathbf{y}} = \mathbf{y} - \boldsymbol{\Phi}\boldsymbol{\theta}$$

Specifically, the most likely value for the vector $\boldsymbol{\theta}$, $\hat{\boldsymbol{\theta}}_{LS}$, is the one minimizing the sum of squares between the observed values of $\mathbf{y}$ and the vector $\boldsymbol{\Phi}\boldsymbol{\theta}$.
The LS estimator is given by:

$$\begin{aligned} \hat{\boldsymbol{\theta}}_{LS}(\mathbf{y}) &= \underset{\boldsymbol{\theta}\in\boldsymbol{\Theta}}{\operatorname{argmin}}\ f_{LS}(\boldsymbol{\theta}) \\ &= \underset{\boldsymbol{\theta}\in\boldsymbol{\Theta}}{\operatorname{argmin}}\ {\epsilon_{\mathbf{y}}}^T \epsilon_{\mathbf{y}} \\ &= \underset{\boldsymbol{\theta}\in\boldsymbol{\Theta}}{\operatorname{argmin}}\ \|\mathbf{y} - \boldsymbol{\Phi}\boldsymbol{\theta}\|^2 \end{aligned}$$

Theorem 2.1.1. *Let*

$$\begin{aligned} f_{LS} : \mathbb{R}^n &\to \mathbb{R} \\ \boldsymbol{\theta} &\mapsto \|\mathbf{y} - \boldsymbol{\Phi}\boldsymbol{\theta}\|^2 \end{aligned}$$

Then, f_{LS} is a convex function. Moreover, $\boldsymbol{\theta}$ is a global minimum of f_{LS} if and only if $\boldsymbol{\theta}$ is a stationary point of f_{LS}.

Proof. A sufficient condition for convexity is

$$\frac{\partial^2 f_{LS}(\boldsymbol{\theta})}{\partial \boldsymbol{\theta}^2} = \left[\frac{\partial^2 f_{LS}(\boldsymbol{\theta})}{\partial \boldsymbol{\theta}_i \partial \boldsymbol{\theta}_j} \right]_{ij} \geq 0$$

Notice that

$$\begin{aligned} \frac{\partial^2 f_{LS}(\boldsymbol{\theta})}{\partial \boldsymbol{\theta}^2} &= \frac{\partial^2 \left(\mathbf{y}^T\mathbf{y} - \boldsymbol{\theta}^T\boldsymbol{\Phi}^T\mathbf{y} - \mathbf{y}^T\boldsymbol{\Phi}\boldsymbol{\theta} + \boldsymbol{\theta}^T\boldsymbol{\Phi}^T\boldsymbol{\Phi}\boldsymbol{\theta} \right)}{\partial \boldsymbol{\theta}^2} \\ &= \boldsymbol{\Phi}^T\boldsymbol{\Phi} \geq 0 \end{aligned}$$

which proves that f_{LS} is convex. The remaining part of the statement follows from the next proposition.

Proposition 2.1.1. *Let $f(\boldsymbol{\theta})$: $\mathbb{R}^n \to \mathbb{R}$ be convex. Then, $\boldsymbol{\theta}$ is a global minimum for f if and only if $\boldsymbol{\theta}$ is a stationary point for f.*

□

Therefore, all its minimum points are given by setting its gradient equal to zero. The latter is:

$$\begin{aligned} \frac{\partial}{\partial \boldsymbol{\theta}} \|\mathbf{y} - \boldsymbol{\Phi}\boldsymbol{\theta}\|^2 &= \frac{\partial}{\partial \boldsymbol{\theta}} \left(\mathbf{y}^T\mathbf{y} - \boldsymbol{\theta}^T\boldsymbol{\Phi}^T\mathbf{y} - \mathbf{y}^T\boldsymbol{\Phi}\boldsymbol{\theta} + \boldsymbol{\theta}^T\boldsymbol{\Phi}^T\boldsymbol{\Phi}\boldsymbol{\theta} \right) \\ &= -2\boldsymbol{\Phi}^T\mathbf{y} + 2\boldsymbol{\Phi}^T\boldsymbol{\Phi}\boldsymbol{\theta} \end{aligned}$$

Then

$$\begin{aligned} &\frac{\partial}{\partial \boldsymbol{\theta}} f_{LS} = 0 \\ &\Updownarrow \\ &\boldsymbol{\Phi}^T\boldsymbol{\Phi}\hat{\boldsymbol{\theta}}_{LS} = \boldsymbol{\Phi}^T\mathbf{y} \end{aligned} \tag{2.1}$$

Two possible scenarios follow:

Scenario 1: $\mathbf{\Phi}^T\mathbf{\Phi}$ is *non-singular*
$\mathbf{\Phi}$ is a matrix over the real numbers. Since $\text{rank}\,(\mathbf{\Phi}) = \text{rank}\left(\mathbf{\Phi}^T\mathbf{\Phi}\right) = n$, $\mathbf{\Phi}$ is *full column-rank*.
In this case, Eq. 2.1 has a unique solution given by

$$\hat{\theta}_{LS} = \underbrace{\left(\mathbf{\Phi}^T\mathbf{\Phi}\right)^{-1}\mathbf{\Phi}^T}_{\mathbf{\Phi}_L^\dagger}\mathbf{y} \tag{2.2}$$

where $\mathbf{\Phi}_L^\dagger$ is the Moore-Penrose *left pseudo-inverse* of $\mathbf{\Phi}$ (see Appendix A).

Scenario 2: $\mathbf{\Phi}^T\mathbf{\Phi}$ is *singular*
Also in this second scenario, Eq. 2.1 admits solution. Indeed, it has solution if $\mathbf{\Phi}^T\mathbf{y} \in \mathcal{R}(\mathbf{\Phi}^T\mathbf{\Phi})$. This fact is always true since $\mathcal{R}(\mathbf{\Phi}^T\mathbf{\Phi}) = \mathcal{R}(\mathbf{\Phi}^T)$ and $\mathbf{\Phi}^T\mathbf{y} \in \mathcal{R}(\mathbf{\Phi}^T)$ by construction.
Let θ^* be a solution to $\mathbf{\Phi}^T\mathbf{\Phi}\theta^* = \mathbf{\Phi}^T\mathbf{y}$. Since $\mathbf{\Phi}^T\mathbf{\Phi}$ is *singular*, $\exists\ \tilde{\theta}(\tilde{\theta} \neq \mathbf{0})\ s.t.$ $\mathbf{\Phi}^T\mathbf{\Phi}\tilde{\theta} = \mathbf{0}$.
Therefore,

$$\mathbf{\Phi}^T\mathbf{\Phi}(\theta^* + \tilde{\theta}) = \mathbf{\Phi}^T\mathbf{y} \quad \forall\tilde{\theta} \in \ker(\mathbf{\Phi}^T\mathbf{\Phi})$$

where

$$\ker(\mathbf{\Phi}^T\mathbf{\Phi}) = \{\tilde{\theta} \in \mathbb{R}^n\ :\ \mathbf{\Phi}^T\mathbf{\Phi}\tilde{\theta} = \mathbf{0}\}$$

The solution to Eq. 2.1 is not unique. In particular, with reference to Appendix B, let $\mathbf{\Phi} = \mathbf{U}\mathbf{S}\mathbf{V}^T$ its Singular Value Decomposition (SVD). It follows that $\mathbf{\Phi} = \mathbf{U}_k\mathbf{S}_k\mathbf{V}_k^T$ where $\mathbf{U}_k \in \mathbb{R}^{m\times k}$, $\mathbf{S}_k \in \mathbb{R}^{k\times k}$ and $\mathbf{V}_k \in \mathbb{R}^{n\times k}$ with $k = \text{rank}\,(\mathbf{\Phi})$.

Lemma 2.1.1. *Given the SVD* $\mathbf{\Phi} = \mathbf{U}\mathbf{S}\mathbf{V}^T$, $\boldsymbol{\theta}^* = \mathbf{V}_k\mathbf{S}_k^{-1}\mathbf{U}_k^T\mathbf{y}$ *is a solution to Eq. 2.1.*

Proof.

$$\begin{aligned}\mathbf{\Phi}^T\mathbf{\Phi}\boldsymbol{\theta}^* &= (\mathbf{U}_k\mathbf{S}_k\mathbf{V}_k^T)^T(\mathbf{U}_k\mathbf{S}_k\mathbf{V}_k^T)\mathbf{V}_k\mathbf{S}_k^{-1}\mathbf{U}_k^T\mathbf{y} = \\ &= \mathbf{V}_k\mathbf{S}_k\underbrace{\mathbf{U}_k^T\mathbf{U}_k}_{\mathbf{I}_{k\times k}}\mathbf{S}_k\underbrace{\mathbf{V}_k^T\mathbf{V}_k}_{\mathbf{I}_{k\times k}}\mathbf{S}_k^{-1}\mathbf{U}_k^T\mathbf{y} \\ &= \underbrace{\mathbf{V}_k\mathbf{S}_k\mathbf{U}_k^T}_{\mathbf{\Phi}^T}\mathbf{y} \\ &= \mathbf{\Phi}^T\mathbf{y}\end{aligned}$$

□

Lemma 2.1.2. $\boldsymbol{\theta}^*$*, defined as in Lemma 2.1.1, is the minimum-norm solution to Eq. 2.1 i.e.* $\|\hat{\boldsymbol{\theta}}\|^2 \geq \|\boldsymbol{\theta}^*\|^2\ \forall\hat{\boldsymbol{\theta}}$ *solution to Eq. 2.1.*

Proof. Let $\hat{\boldsymbol{\theta}}$ be any solution to Eq. 2.1, then $\hat{\boldsymbol{\theta}} = \boldsymbol{\theta}^* + \tilde{\boldsymbol{\theta}} \quad \forall\ \tilde{\boldsymbol{\theta}} \in \ker(\mathbf{\Phi})$.
Indeed:

$$\begin{aligned}(\mathbf{\Phi}^T\mathbf{\Phi})\hat{\boldsymbol{\theta}} = \mathbf{\Phi}^T\mathbf{y} &\implies \hat{\boldsymbol{\theta}}\text{is solution} \\ (\mathbf{\Phi}^T\mathbf{\Phi})\boldsymbol{\theta}^* = \mathbf{\Phi}^T\mathbf{y} &\implies \boldsymbol{\theta}^*\text{is solution} \\ (\mathbf{\Phi}^T\mathbf{\Phi})(\underbrace{\hat{\boldsymbol{\theta}} - \boldsymbol{\theta}^*}_{\tilde{\boldsymbol{\theta}}}) = 0 &\implies \tilde{\boldsymbol{\theta}} \in \ker\left(\mathbf{\Phi}^T\mathbf{\Phi}\right)\end{aligned}$$

Since $\ker\left(\mathbf{\Phi}^T\mathbf{\Phi}\right) = \ker(\mathbf{\Phi})$, then $\tilde{\boldsymbol{\theta}} \in \ker(\mathbf{\Phi})$.
Moreover,

$$\boldsymbol{\theta}^* \ = \ \mathbf{V}_k\mathbf{S}_k^{-1}\mathbf{U}_k^T\mathbf{y} \in \mathcal{R}(\mathbf{V}_k) \ = \ \mathcal{R}\left(\mathbf{\Phi}^T\right)$$

It follows

$$\left.\begin{aligned}\hat{\boldsymbol{\theta}} &= \boldsymbol{\theta}^* + \tilde{\boldsymbol{\theta}} \\ \tilde{\boldsymbol{\theta}} &\in \ker(\mathbf{\Phi}) \\ \boldsymbol{\theta}^* &\in \mathcal{R}\left(\mathbf{\Phi}^T\right)\end{aligned}\right\} \quad \xRightarrow{\mathcal{R}\left(\mathbf{\Phi}^T\right) \perp \ker(\mathbf{\Phi})} \quad \boldsymbol{\theta}^* \ \perp \ \tilde{\boldsymbol{\theta}}$$

$\|\hat{\boldsymbol{\theta}}\|^2 = \hat{\boldsymbol{\theta}}^T\hat{\boldsymbol{\theta}} = (\boldsymbol{\theta}^* + \tilde{\boldsymbol{\theta}})^T(\boldsymbol{\theta}^* + \tilde{\boldsymbol{\theta}}) = \boldsymbol{\theta}^{*T}\boldsymbol{\theta}^* + \tilde{\boldsymbol{\theta}}^T\tilde{\boldsymbol{\theta}} = \|\boldsymbol{\theta}^*\|^2 + \|\tilde{\boldsymbol{\theta}}\|^2$.
This shows that $\|\hat{\boldsymbol{\theta}}\|^2 \geq \|\boldsymbol{\theta}^*\|^2$. □

2.1.2 Recursive least-square

In the previous section, a method for computing the estimate of a constant was seen. However, if sequentially measurements are obtained and the current estimate of $\boldsymbol{\theta}$ is needed to be updated with each new measurement, the $\boldsymbol{\Phi}$ matrix has to be augmented and $\hat{\boldsymbol{\theta}}$ has to be recomputed. This becomes a problem when the number of measurements becomes large, therefore the computational effort could become prohibitive. Recursive estimation is a method of estimating a constant without increasing the computational effort of the algorithm, regardless of how many measurements are available. Suppose $\hat{\boldsymbol{\theta}}$ is known after $(m-1)$ measurements, and a new measurement y_m is obtained. Is there a way to update the estimate without completely reworking Eq. 2.2? Firstly, consider the problem of estimating a scalar constant, θ, based on m noise corrupted measurements which are modeled as $y_i = \theta + v_i$, $i = 1, \ldots, m$. An estimate $\hat{\theta}$ can be obtained by averaging all the measurements

$$\hat{\theta}_m = \frac{1}{m}\left(\sum_{i=1}^{m} y_i\right)$$

When an additional measurement is available, the new estimate is updated as

$$\hat{\theta}_{m+1} = \frac{1}{m+1}\left(\sum_{i=1}^{m+1} y_i\right)$$

By manipulating this equation, the need to store all the measurements can be avoided. This is shown as follows

$$\begin{aligned}
\hat{\theta}_{m+1} &= \frac{m}{m+1}\left(\frac{1}{m}\sum_{i=1}^{m} y_i\right) + \frac{1}{m+1} y_{m+1} \\
\hat{\theta}_{m+1} &= \frac{m}{m+1}\hat{\theta}_m + \frac{1}{m+1} y_{m+1} \\
\hat{\theta}_{m+1} &= \hat{\theta}_m + \frac{1}{m+1}\left(y_{m+1} - \hat{\theta}_m\right)
\end{aligned}$$

Thus, we have a *recursive* linear estimator. This idea can be applied also to vectors quantities. The vector notation for the measurements available is given as:

$$y_k = \underbrace{\begin{bmatrix} \Phi_{k1} & \cdots & \Phi_{kn} \end{bmatrix}}_{\boldsymbol{\Phi}_k} \boldsymbol{\theta} + \mathbf{v}_k$$

where y_k is the k^{th} measurement, $\boldsymbol{\Phi}_k$ is the corresponding measurement matrix, $\boldsymbol{\theta}$ is the unknown constant vector and $\mathbf{v}_k$ is the measurement noise quantity. Therefore, a linear *recursive* estimator can be written in the form

$$\begin{cases} y_k &= \boldsymbol{\Phi}_k \boldsymbol{\theta} + \mathbf{v}_k \\ \hat{\boldsymbol{\theta}}_k &= \hat{\boldsymbol{\theta}}_{k-1} + \mathbf{K}_k \left(y_k - \boldsymbol{\Phi}_k \hat{\boldsymbol{\theta}}_{k-1} \right) \end{cases}$$

The new estimate $\hat{\boldsymbol{\theta}}_k$ is computed on the basis of the previous estimate $\hat{\boldsymbol{\theta}}_{k-1}$ and the new measurement y_k. $\mathbf{K}_k$ is called the estimator gain matrix. The quantity $\left(y_k - \boldsymbol{\Phi}_k \hat{\boldsymbol{\theta}}_{k-1} \right)$ is called the correction term. It is important to mention that if the correction term is zero, or if the gain matrix is zero, then the estimate does not change from time step $(k-1)$ to k.

In the following, the mean of the estimation error is computed:

$$\begin{aligned} E\left[\epsilon_{\boldsymbol{\theta},k}\right] &= E\left[\boldsymbol{\theta} - \hat{\boldsymbol{\theta}}_k\right] \\ &= E\left[\boldsymbol{\theta} - \hat{\boldsymbol{\theta}}_{k-1} - \mathbf{K}_k \left(y_k - \boldsymbol{\Phi}_k \hat{\boldsymbol{\theta}}_{k-1} \right)\right] \\ &= E\left[\epsilon_{\boldsymbol{\theta},k-1} - \mathbf{K}_k \left(\boldsymbol{\Phi}_k \boldsymbol{\theta} + \mathbf{v}_k - \boldsymbol{\Phi}_k \hat{\boldsymbol{\theta}}_{k-1} \right)\right] \\ &= E\left[\epsilon_{\boldsymbol{\theta},k-1} - \mathbf{K}_k \boldsymbol{\Phi}_k \left(\boldsymbol{\theta} - \hat{\boldsymbol{\theta}}_{k-1} \right) - \mathbf{K}_k \mathbf{v}_k\right] \\ &= \left(\mathbf{I} - \mathbf{K}_k \boldsymbol{\Phi}_k\right) E\left[\epsilon_{\boldsymbol{\theta},k-1}\right] - \mathbf{K}_k E\left[\mathbf{v}_k\right] \end{aligned} \tag{2.3}$$

The estimator is *unbiased*, namely, on average, the estimate $\hat{\boldsymbol{\theta}}$ is equal to the true value $\boldsymbol{\theta}$. Indeed, if the measurement noise $\mathbf{v}_k$ is zero-mean $\forall k$ and the initial estimate of $\boldsymbol{\theta}$ is set equal to the expected value of $\boldsymbol{\theta}$ [i.e. $\hat{\boldsymbol{\theta}}_0 = E(\boldsymbol{\theta})$], then $E\left[\epsilon_{\boldsymbol{\theta},k}\right] = 0 \; \forall k$. This property holds regardless of the value of the gain matrix $\mathbf{K}_k$, whose optimal value has to be determined. In order to do so, a cost function is needed to be defined. Specifically:

$$\hat{\mathbf{K}}_k = \underset{\mathbf{K}_k}{\operatorname{argmin}} \, f_k$$

where, the cost function f_k is chosen to be the sum of the variances of the

estimation errors at time k, namely:

$$\begin{aligned} f_k &= E\left[\left(\theta_1 - \hat{\theta}_1\right)^2\right] + \cdots + E\left[\left(\theta_n - \hat{\theta}_n\right)^2\right] \\ &= E\left[\epsilon_{\theta_1,k}^2 + \cdots + \epsilon_{\theta_n,k}^2\right] \\ &= E\left[{\epsilon_{\boldsymbol{\theta},k}}^T \epsilon_{\boldsymbol{\theta},k}\right] \\ &= E\left[\mathrm{Tr}\left(\epsilon_{\boldsymbol{\theta},k}{\epsilon_{\boldsymbol{\theta},k}}^T\right)\right] \\ &= \mathrm{Tr}\, E\left[\epsilon_{\boldsymbol{\theta},k}{\epsilon_{\boldsymbol{\theta},k}}^T\right] \\ &= \mathrm{Tr}\, \mathbf{P}_k \end{aligned}$$

where $\mathbf{P}_k$ is the estimation-error covariance. By following the same approach used in Eq. 2.3, a recursive formula for the calculation of $\mathbf{P}_k$ can be obtained:

$$\begin{aligned} \mathbf{P}_k &= E\left[\epsilon_{\boldsymbol{\theta},k}{\epsilon_{\boldsymbol{\theta},k}}^T\right] \\ &= E\left\{\left[\left(\mathbf{I} - \mathbf{K}_k\boldsymbol{\Phi}_k\right)\epsilon_{\boldsymbol{\theta},k-1} - \mathbf{K}_k\mathbf{v}_k\right]\left[\left(\mathbf{I} - \mathbf{K}_k\boldsymbol{\Phi}_k\right)\epsilon_{\boldsymbol{\theta},k-1} - \mathbf{K}_k\mathbf{v}_k\right]^T\right\} \\ &= E\Big[\left(\mathbf{I} - \mathbf{K}_k\boldsymbol{\Phi}_k\right)\epsilon_{\boldsymbol{\theta},k-1}{\epsilon_{\boldsymbol{\theta},k-1}}^T\left(\mathbf{I} - \mathbf{K}_k\boldsymbol{\Phi}_k\right)^T - \mathbf{K}_k\mathbf{v}_k{\epsilon_{\boldsymbol{\theta},k-1}}^T\left(\mathbf{I} - \mathbf{K}_k\boldsymbol{\Phi}_k\right)^T - \\ &\qquad \left(\mathbf{I} - \mathbf{K}_k\boldsymbol{\Phi}_k\right)\epsilon_{\boldsymbol{\theta},k-1}{\mathbf{v}_k}^T{\mathbf{K}_k}^T + \mathbf{K}_k\mathbf{v}_k{\mathbf{v}_k}^T{\mathbf{K}_k}^T\Big] \\ &= \left(\mathbf{I} - \mathbf{K}_k\boldsymbol{\Phi}_k\right)E\left[\epsilon_{\boldsymbol{\theta},k-1}{\epsilon_{\boldsymbol{\theta},k-1}}^T\right]\left(\mathbf{I} - \mathbf{K}_k\boldsymbol{\Phi}_k\right)^T - \mathbf{K}_k E\left[\mathbf{v}_k{\epsilon_{\boldsymbol{\theta},k-1}}^T\right]\left(\mathbf{I} - \mathbf{K}_k\boldsymbol{\Phi}_k\right)^T - \\ &\quad \left(\mathbf{I} - \mathbf{K}_k\boldsymbol{\Phi}_k\right)E\left[\epsilon_{\boldsymbol{\theta},k-1}{\mathbf{v}_k}^T\right]{\mathbf{K}_k}^T + \mathbf{K}_k E\left[\mathbf{v}_k{\mathbf{v}_k}^T\right]{\mathbf{K}_k}^T \end{aligned} \tag{2.4}$$

Since the estimation error at time $(k-1)$, i.e. $\epsilon_{\boldsymbol{\theta},k-1}$, is independent of the measurement noise at time k, i.e. $\mathbf{v}_k$, and both expected values are zero, $E\left[\mathbf{v}_k{\epsilon_{\boldsymbol{\theta},k-1}}^T\right] = E\left[\mathbf{v}_k\right]E\left[\epsilon_{\boldsymbol{\theta},k-1}\right] = 0$. Therefore, Eq. 2.4 becomes

$$\mathbf{P}_k = \left(\mathbf{I} - \mathbf{K}_k\boldsymbol{\Phi}_k\right)\mathbf{P}_{k-1}\left(\mathbf{I} - \mathbf{K}_k\boldsymbol{\Phi}_k\right)^T + \mathbf{K}_k\mathbf{R}_k{\mathbf{K}_k}^T \tag{2.5}$$

where $\mathbf{R}_k$ is the covariance of $\mathbf{v}_k$. Looking at Eq. 2.5, as the measurement noise increases (namely, $\mathbf{R}_k$ increases) the uncertainty in the estimate also increases (i.e. $\mathbf{P}_k$ increases).

The optimal value of $\mathbf{K}_k$, $\hat{\mathbf{K}}_k$, is the one minimizing $\mathrm{Tr}\,\mathbf{P}_k$ hence, the estimation error will not only be zero-mean but it will also be consistently close to zero. By combining the fact that $\frac{\partial\,\mathrm{Tr}\left(\mathbf{A}\mathbf{X}^T\right)}{\partial\mathbf{X}} = \mathbf{A}$, $\frac{\partial\,\mathrm{Tr}\left(\mathbf{X}\mathbf{A}\mathbf{X}^T\right)}{\partial\mathbf{X}} = \mathbf{X}\mathbf{A} + \mathbf{X}\mathbf{A}^T$ with $\mathbf{A}$ and $\mathbf{X}$ of

same dimension and that $\frac{\partial \operatorname{Tr}\left(\mathbf{A}\mathbf{B}\mathbf{A}^T\right)}{\partial \mathbf{A}} = 2\mathbf{A}\mathbf{B}$ with $\mathbf{B}$ symmetric, it follows

$$\begin{aligned}
\frac{\partial f_k}{\partial \mathbf{K}_k} &= \frac{\partial}{\partial \mathbf{K}_k} \operatorname{Tr}\left(\left(\mathbf{I} - \mathbf{K}_k \mathbf{\Phi}_k\right) \mathbf{P}_{k-1} \left(\mathbf{I} - \mathbf{K}_k \mathbf{\Phi}_k\right)^T + \mathbf{K}_k \mathbf{R}_k {\mathbf{K}_k}^T \right) \\
&= \frac{\partial}{\partial \mathbf{K}_k} \operatorname{Tr}\left(\mathbf{P}_{k-1} - \mathbf{K}_k \mathbf{\Phi}_k \mathbf{P}_{k-1} - \mathbf{P}_{k-1} \mathbf{\Phi}_k^T \mathbf{K}_k^T + \mathbf{K}_k \left(\mathbf{\Phi}_k \mathbf{P}_{k-1} \mathbf{\Phi}_k^T \right) \mathbf{K}_k^T \right) + \frac{\partial}{\partial \mathbf{K}_k} \operatorname{Tr}\left(\mathbf{K}_k \mathbf{R}_k \mathbf{K}_k^T \right) \\
&= -2 \frac{\partial}{\partial \mathbf{K}_k} \operatorname{Tr}\left(\mathbf{P}_{k-1} \mathbf{\Phi}_k^T \mathbf{K}_k^T \right) + 2\mathbf{K}_k \left(\mathbf{\Phi}_k \mathbf{P}_{k-1} \mathbf{\Phi}_k^T \right) + 2\mathbf{K}_k \mathbf{R}_k \\
&= -2\mathbf{P}_{k-1} \mathbf{\Phi}_k^T + 2\mathbf{K}_k \mathbf{\Phi}_k \mathbf{P}_{k-1} \mathbf{\Phi}_k^T + 2\mathbf{K}_k \mathbf{R}_k \\
&= 2\left(\mathbf{I} - \mathbf{K}_k \mathbf{\Phi}_k\right) \mathbf{P}_{k-1} \left(-\mathbf{\Phi}_k^T\right) + 2\mathbf{K}_k \mathbf{R}_k
\end{aligned}$$

By setting the above derivative equal to zero and solving for $\mathbf{K}_k$:

$$\mathbf{K}_k = \mathbf{P}_{k-1} \mathbf{\Phi}_k^T \underbrace{\left(\mathbf{\Phi}_k \mathbf{P}_{k-1} \mathbf{\Phi}_k^T + \mathbf{R}_k \right)^{-1}}_{{\mathbf{S}_k}^{-1}} \tag{2.6}$$

Alternative forms for $\mathbf{K}_k$ and $\mathbf{P}_k$

Often it is useful to write the equations for $\mathbf{K}_k$ and $\mathbf{P}_k$ in alternate forms. Although these alternate forms are mathematically identical, they can be beneficial from a computational point of view. Firstly, an alternate form for the estimation-error covariance will be found. Substituting Eq. 2.6 in Eq. 2.5:

$$\begin{aligned}
\mathbf{P}_k &= \left(\mathbf{I} - \mathbf{K}_k \mathbf{\Phi}_k\right) \mathbf{P}_{k-1} \left(\mathbf{I} - \mathbf{K}_k \mathbf{\Phi}_k\right)^T + \mathbf{K}_k \mathbf{R}_k {\mathbf{K}_k}^T \\
&= \left[\mathbf{I} - \mathbf{P}_{k-1} \mathbf{\Phi}_k^T {\mathbf{S}_k}^{-1} \mathbf{\Phi}_k\right] \mathbf{P}_{k-1} \left[\mathbf{I} - \mathbf{P}_{k-1} \mathbf{\Phi}_k^T {\mathbf{S}_k}^{-1} \mathbf{\Phi}_k\right]^T + \mathbf{P}_{k-1} \mathbf{\Phi}_k^T {\mathbf{S}_k}^{-1} \mathbf{R}_k {\mathbf{S}_k}^{-1} \mathbf{\Phi}_k \mathbf{P}_{k-1} \\
&= \mathbf{P}_{k-1} - \mathbf{P}_{k-1} \mathbf{\Phi}_k^T {\mathbf{S}_k}^{-1} \mathbf{\Phi}_k \mathbf{P}_{k-1} - \mathbf{P}_{k-1} \mathbf{\Phi}_k^T {\mathbf{S}_k}^{-1} \mathbf{\Phi}_k \mathbf{P}_{k-1} + \\
&\quad \mathbf{P}_{k-1} \mathbf{\Phi}_k^T {\mathbf{S}_k}^{-1} \underline{\mathbf{\Phi}_k \mathbf{P}_{k-1} \mathbf{\Phi}_k^T} {\mathbf{S}_k}^{-1} \mathbf{\Phi}_k \mathbf{P}_{k-1} + \mathbf{P}_{k-1} \mathbf{\Phi}_k^T {\mathbf{S}_k}^{-1} \underline{\mathbf{R}_k} {\mathbf{S}_k}^{-1} \mathbf{\Phi}_k \mathbf{P}_{k-1} \\
&= \mathbf{P}_{k-1} - \mathbf{P}_{k-1} \mathbf{\Phi}_k^T {\mathbf{S}_k}^{-1} \mathbf{\Phi}_k \mathbf{P}_{k-1} - \mathbf{P}_{k-1} \mathbf{\Phi}_k^T {\mathbf{S}_k}^{-1} \mathbf{\Phi}_k \mathbf{P}_{k-1} + \mathbf{P}_{k-1} \mathbf{\Phi}_k^T {\mathbf{S}_k}^{-1} \mathbf{S}_k {\mathbf{S}_k}^{-1} \mathbf{\Phi}_k \mathbf{P}_{k-1} \\
&= \mathbf{P}_{k-1} - \mathbf{P}_{k-1} \mathbf{\Phi}_k^T {\mathbf{S}_k}^{-1} \mathbf{\Phi}_k \mathbf{P}_{k-1} \qquad (2.7) \\
&= \mathbf{P}_{k-1} - \mathbf{K}_k \mathbf{\Phi}_k \mathbf{P}_{k-1} \\
&= \left(\mathbf{I} - \mathbf{K}_k \mathbf{\Phi}_k\right) \mathbf{P}_{k-1} \qquad (2.8)
\end{aligned}$$

Eq. 2.8 is simpler with respect to Eq. 2.5 but numerical computing problems may cause this expression for $\mathbf{P}_k$ to not be positive definite, even when $\mathbf{P}_{k-1}$ and $\mathbf{R}_k$ are positive definite. Moreover, it is possible to find an other expression for

$\mathbf{P}_k$, by exploiting the inversion lemma. Indeed, consider Eq. 2.7 and take the inverse of both sides:

$$\begin{aligned}(\mathbf{P}_k)^{-1} &= \Big(\underbrace{\mathbf{P}_{k-1}}_{\mathbf{A}} - \underbrace{\mathbf{P}_{k-1}\boldsymbol{\Phi}_k^T}_{\mathbf{B}} \Big(\underbrace{\boldsymbol{\Phi}_k\mathbf{P}_{k-1}\boldsymbol{\Phi}_k^T + \mathbf{R}_k}_{\mathbf{D}} \Big)^{-1} \underbrace{\boldsymbol{\Phi}_k\mathbf{P}_{k-1}}_{\mathbf{C}} \Big)^{-1} \\ &= \mathbf{P}_{k-1}^{-1} + \mathbf{P}_{k-1}^{-1}\mathbf{P}_{k-1}\boldsymbol{\Phi}_k^T \left(\boldsymbol{\Phi}_k\mathbf{P}_{k-1}\boldsymbol{\Phi}_k^T + \mathbf{R}_k - \boldsymbol{\Phi}_k\mathbf{P}_{k-1}\mathbf{P}_{k-1}^{-1}\mathbf{P}_{k-1}\boldsymbol{\Phi}_k^T\right)^{-1} \boldsymbol{\Phi}_k\mathbf{P}_{k-1}\mathbf{P}_{k-1}^{-1} \\ &= \mathbf{P}_{k-1}^{-1} + \boldsymbol{\Phi}_k^T\mathbf{R}_k^{-1}\boldsymbol{\Phi}_k\end{aligned}$$

Inverting both sides, one obtains:

$$\mathbf{P}_k = \left(\mathbf{P}_{k-1}^{-1} + \boldsymbol{\Phi}_k^T\mathbf{R}_k^{-1}\boldsymbol{\Phi}_k\right)^{-1} \tag{2.9}$$

Eq. 2.9 for $\mathbf{P}_k$ is more complicated that Eq. 2.8 since it requires three matrix inversions, but it may be computationally advantageous in some situations. As far as $\mathbf{K}_k$ is concerned, by using Eq. 2.6 and Eq. 2.9, one obtains

$$\begin{aligned}\mathbf{K}_k &= \mathbf{P}_{k-1}\boldsymbol{\Phi}_k^T \left(\boldsymbol{\Phi}_k\mathbf{P}_{k-1}\boldsymbol{\Phi}_k^T + \mathbf{R}_k\right)^{-1} \\ &= \mathbf{P}_k\mathbf{P}_k^{-1}\mathbf{P}_{k-1}\boldsymbol{\Phi}_k^T \left(\boldsymbol{\Phi}_k\mathbf{P}_{k-1}\boldsymbol{\Phi}_k^T + \mathbf{R}_k\right)^{-1} \\ &= \mathbf{P}_k \left(\mathbf{P}_{k-1}^{-1} + \boldsymbol{\Phi}_k^T\mathbf{R}_k^{-1}\boldsymbol{\Phi}_k\right)\mathbf{P}_{k-1}\boldsymbol{\Phi}_k^T \left(\boldsymbol{\Phi}_k\mathbf{P}_{k-1}\boldsymbol{\Phi}_k^T + \mathbf{R}_k\right)^{-1} \\ &= \mathbf{P}_k \left(\boldsymbol{\Phi}_k^T + \boldsymbol{\Phi}_k^T\mathbf{R}_k^{-1}\boldsymbol{\Phi}_k\mathbf{P}_{k-1}\boldsymbol{\Phi}_k^T\right) \left(\boldsymbol{\Phi}_k\mathbf{P}_{k-1}\boldsymbol{\Phi}_k^T + \mathbf{R}_k\right)^{-1} \\ &= \mathbf{P}_k\boldsymbol{\Phi}_k^T \left(\mathbf{I} + \mathbf{R}_k^{-1}\boldsymbol{\Phi}_k\mathbf{P}_{k-1}\boldsymbol{\Phi}_k^T\right) \left(\boldsymbol{\Phi}_k\mathbf{P}_{k-1}\boldsymbol{\Phi}_k^T + \mathbf{R}_k\right)^{-1} \\ &= \mathbf{P}_k\boldsymbol{\Phi}_k^T\mathbf{R}_k^{-1} \left(\mathbf{R}_k + \boldsymbol{\Phi}_k\mathbf{P}_{k-1}\boldsymbol{\Phi}_k^T\right) \left(\boldsymbol{\Phi}_k\mathbf{P}_{k-1}\boldsymbol{\Phi}_k^T + \mathbf{R}_k\right)^{-1} \\ &= \mathbf{P}_k\boldsymbol{\Phi}_k^T\mathbf{R}_k^{-1}\end{aligned} \tag{2.10}$$

2.2 Kalman filter

Most of the earlier section was written also to provide the foundation for this section. The Kalman filter is known as an *optimal recursive* data processing algorithm. Depending on the criteria chosen to evaluate the performance, there are many ways of defining *optimal*. Under some particular assumptions, which are analyzed in the next section, the Kalman filter is *optimal* with respect to any criterion that makes sense. Indeed, by exploting the knowledge of the system and measurement device dynamics, the statistical description of the process noise, measurement noise and any available information about initial conditions of the variables of interest, the KF is able to process all available measurements, regardless of their precision, to estimate the current value of the variables of interest.

Moreover the KF is a *recursive* algorithm. Indeed, it does not need to keep in memory all previous data and reprocess every time each measurement is taken. It operates by propagating the mean and covariance of the state through time where

- The mean of the state represents the Kalman filter estimate of the state.
- The covariance of the state is the covariance of the Kalman filter estimate of the state.

Every time that there is a new measurement, the mean and covariance of the state are updated. This is similar to the idea in the previous section where the measurements were used to recursively update the estimate of a constant. Fig. 2.1 shows a possible application of the Kalman filter. The system of interest is driven by some control inputs and the aim is to determine the system's states, which are unknown. Some measurement devices can provide the value of some pertinent quantities, which most of times, do not coincide with the variables of interest. Here is where the Kalman filter comes into play. By combining the controls and the observed measurements coming from the sensors with the prior knowledge of the system and devices' dynamics, it computes the *optimal* system's state estimate. In the following the discrete-time Kalman filter derivation is addressed.

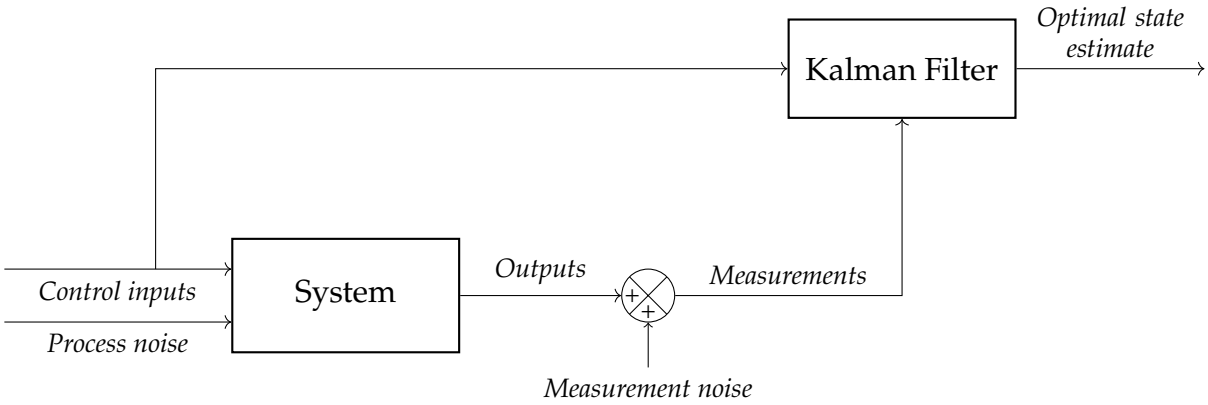

Figure 2.1: Typical Kalman filter application

2.2.1 Kalman filter dynamics for linear discrete-time systems

Let the following be a linear discrete-time system

$$\boldsymbol{\Sigma}: \begin{cases} \boldsymbol{\theta}_{k+1} = \mathbf{F}_k \boldsymbol{\theta}_k + \mathbf{G}_k \mathbf{u}_k + \mathbf{w}_k \\ \mathbf{y}_{k+1} = \boldsymbol{\Phi}_{k+1} \boldsymbol{\theta}_{k+1} + \mathbf{v}_{k+1} \end{cases} \tag{2.11}$$

$\boldsymbol{\theta}_k \in \mathbb{R}^n$, $\mathbf{u}_k \in \mathbb{R}^p$, $\mathbf{y}_k \in \mathbb{R}^m$. Let the matrices $\mathbf{F}_k$, $\mathbf{G}_k$ and $\boldsymbol{\Phi}_k$ be of appropriate size. The process noise $\{\mathbf{w}_k\}$ and the measurement noise $\{\mathbf{v}_k\}$ are white, Gaussian, zero-mean and have known covariance matrices $\mathbf{Q}_k$ and $\mathbf{R}_k$, respectively; moreover, the sequence $\{\mathbf{u}_k\}$ is deterministic and $\{\boldsymbol{\theta}_0, \mathbf{w_1}, \cdots, \mathbf{w}_k, \mathbf{v}_1, \cdots, \mathbf{v}_k\}$ are assumed to be mutually independent.

$$\begin{cases} \mathbf{w}_k \sim \mathcal{N}(0, \mathbf{Q}_k) \\ \mathbf{v}_k \sim \mathcal{N}(0, \mathbf{R}_k) \\ E\left[\mathbf{w}_k \mathbf{w}_j^T\right] = \mathbf{Q}_k \delta_{k-j} \\ E\left[\mathbf{v}_k \mathbf{v}_j^T\right] = \mathbf{R}_k \delta_{k-j} \\ E\left[\mathbf{v}_k \mathbf{w}_j^T\right] = 0 \end{cases} \quad , \quad \delta_{k-j} = \begin{cases} 1 & k = j \\ 0 & k \neq j \end{cases}$$

Based on the available information (control inputs $\mathbf{U}_0^{k-1} = \{\mathbf{u}_0, \cdots, \mathbf{u}_{k-1}\}$ and observations $\mathbf{Y}_1^k = \{\mathbf{y}_1, \cdots, \mathbf{y}_k\}$) it is required to obtain an estimate of the system's state $\hat{\boldsymbol{\theta}}_k$ that optimizes a given criteria. This is the role played by a filter. From a Bayesian viewpoint, the filter propagates the conditional probability

density function of the desired quantities, conditioned on the knowledge of the actual data coming from the measuring devices, namely the filter evaluates and propagates the conditional pdf

$$p(\boldsymbol{\theta}_k \mid \mathbf{y}_1, \cdots, \mathbf{y}_k, \mathbf{u}_0, \cdots, \mathbf{u}_{k-1}) = p(\boldsymbol{\theta}_k \mid \mathbf{Y}_1^k, \mathbf{U}_0^{k-1})$$

Once such conditional probability is propagated, it is possible to define the *optimal* estimate as:

1. The *mean*: the "center of probability mass" estimate.
2. The *mode*: the value of $\boldsymbol{\theta}_k$ that has the highest probability.
3. The *median*: the value of $\boldsymbol{\theta}_k$ such that half of the probability weight lies to the left and half to the right of it.

A Kalman filter performs this conditional probability density propagation for problems in which the system can be described as in Eq. 2.11. Under these conditions, there is a unique *best* estimate of the value of $\boldsymbol{\theta}_k$ since the mean, mode, median, and virtually any reasonable choice for an *optimal* estimate all coincide. In particular, since $\boldsymbol{\theta}_0$ is a Gaussian random vector, the process and measurement noises $\mathbf{w}_k$ and $\mathbf{v}_k$ are white and Gaussian and the system equations are linear, the conditional probability density function $p(\boldsymbol{\theta}_k \mid \mathbf{Y}_1^k, \mathbf{U}_0^{k-1})$ propagated by the filter is Gaussian for every k, hence

$$p(\boldsymbol{\theta}_k \mid \mathbf{Y}_1^k, \mathbf{U}_0^{k-1}) \sim \mathcal{N}\left(\hat{\boldsymbol{\theta}}_{k|k}, \mathbf{P}_{k|k}\right)$$

The state estimate $\hat{\boldsymbol{\theta}}_{k|k}$ is the conditional mean of the pdf and the covariance matrix $\mathbf{P}_{k|k}$ quantifies the uncertainty of the estimate.

$$\begin{aligned}
\hat{\boldsymbol{\theta}}_{k|k} &= E\left[\boldsymbol{\theta}_k \mid \mathbf{Y}_1^k, \mathbf{U}_0^{k-1}\right] \\
\mathbf{P}_{k|k} &= E\left[\left(\boldsymbol{\theta}_k - \hat{\boldsymbol{\theta}}_{k|k}\right)\left(\boldsymbol{\theta}_k - \hat{\boldsymbol{\theta}}_{k|k}\right)^T \mid \mathbf{Y}_1^k, \mathbf{U}_0^{k-1}\right]
\end{aligned}$$

Therefore, rather than propagating the entire conditional pdf, the Kalman filter only propagates the first and second moments, hence the filter dynamics defines the general transition from $p(\boldsymbol{\theta}_k \mid \mathbf{Y}_1^k, \mathbf{U}_0^{k-1})$ to $p(\boldsymbol{\theta}_{k+1} \mid \mathbf{Y}_1^{k+1}, \mathbf{U}_0^k)$. This transition is implemented as a two step-procedure, a prediction cycle (time-update) and a filtering cycle (measurement-update), where

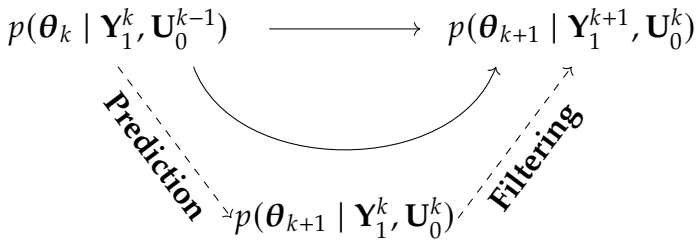

Figure 2.2: Prediction and Filtering cyles in the Kalman Filter dynamics

- $p(\boldsymbol{\theta}_{k+1} \mid \mathbf{Y}_1^k, \mathbf{U}_0^k)$ represents what can be said about $\boldsymbol{\theta}_{k+1}$ without exploiting the measurement $\mathbf{y}_{k+1}$.
- $p(\boldsymbol{\theta}_{k+1} \mid \mathbf{Y}_1^{k+1}, \mathbf{U}_0^k)$ states how to improve the estimate by exploiting the measurement $\mathbf{y}_{k+1}$.

Let

$$
\begin{aligned}
p(\boldsymbol{\theta}_k \mid \mathbf{Y}_1^k, \mathbf{U}_0^{k-1}) &\sim \mathcal{N}\left(\hat{\boldsymbol{\theta}}_{k|k}, \mathbf{P}_{k|k}\right) \\
p(\boldsymbol{\theta}_{k+1} \mid \mathbf{Y}_1^k, \mathbf{U}_0^k) &\sim \mathcal{N}\left(\hat{\boldsymbol{\theta}}_{k+1|k}, \mathbf{P}_{k+1|k}\right) \\
p(\boldsymbol{\theta}_{k+1} \mid \mathbf{Y}_1^{k+1}, \mathbf{U}_0^k) &\sim \mathcal{N}\left(\hat{\boldsymbol{\theta}}_{k+1|k+1}, \mathbf{P}_{k+1|k+1}\right)
\end{aligned}
$$

Fig. 2.3 highlights the fact that, after the measurement at time k is processed, the estimate of $\boldsymbol{\theta}_k$ and covariance of that state estimate, denoted as $\hat{\boldsymbol{\theta}}_{k|k}$ and $\mathbf{P}_{k|k}$, become available. As soon as time $(k+1)$ arrives, the state estimate and corresponding covariance are computed without using the measurement at time $k+1$. These are denoted by $\hat{\boldsymbol{\theta}}_{k+1|k}$, also called *a-priori* state-estimate, and $\mathbf{P}_{k+1|k}$. The measurement $\mathbf{y}_{k+1}$ is used to refine these estimates and are defined as $\hat{\boldsymbol{\theta}}_{k+1|k+1}$, also called *a-posteriori* state-estimate, and $\mathbf{P}_{k+1|k+1}$.

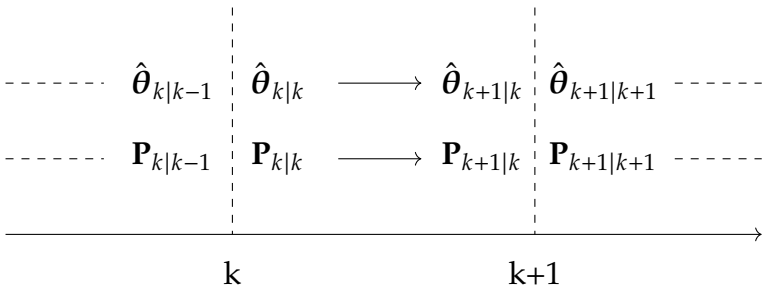

Figure 2.3: Timeline showing *a-priori* and *a-posteriori* state estimates and estimation error covariance

In the following the **prediction** and **filtering** errors are defined respectively as

$$\tilde{\boldsymbol{\theta}}_{k+1|k} = \boldsymbol{\theta}_{k+1} - \hat{\boldsymbol{\theta}}_{k+1|k}, \quad \tilde{\boldsymbol{\theta}}_{k+1|k+1} = \boldsymbol{\theta}_{k+1} - \hat{\boldsymbol{\theta}}_{k+1|k+1}$$

Prediction: *evaluating* $p(\boldsymbol{\theta}_{k+1} \mid \mathbf{Y}_1^k, \mathbf{U}_0^k)$
$p(\boldsymbol{\theta}_{k+1} \mid \mathbf{Y}_1^k, \mathbf{U}_0^k) \sim \mathcal{N}\left(\hat{\boldsymbol{\theta}}_{k+1|k}, \mathbf{P}_{k+1|k}\right)$, where

$$\begin{aligned}
\hat{\boldsymbol{\theta}}_{k+1|k} &= E\left[\boldsymbol{\theta}_{k+1} \mid \mathbf{Y}_1^k, \mathbf{U}_0^k\right] \\
\mathbf{P}_{k+1|k} &= E\left[\left(\boldsymbol{\theta}_{k+1} - \hat{\boldsymbol{\theta}}_{k+1|k}\right)\left(\boldsymbol{\theta}_{k+1} - \hat{\boldsymbol{\theta}}_{k+1|k}\right)^T \mid \mathbf{Y}_1^k, \mathbf{U}_0^k\right]
\end{aligned}$$

By considering Eq. 2.11 and the fact that $\left\{\mathbf{w}_k,\ \mathbf{Y}_1^k\right\}$ and $\left\{\tilde{\boldsymbol{\theta}}_{k|k},\ \mathbf{w}_k\right\}$ are independent:

$$\begin{aligned}
\hat{\boldsymbol{\theta}}_{k+1|k} &= E\left[\boldsymbol{\theta}_{k+1} \mid \mathbf{Y}_1^k, \mathbf{U}_0^k\right] \\
&= E\left[\mathbf{F}_k\boldsymbol{\theta}_k + \mathbf{G}_k\mathbf{u}_k + \mathbf{w}_k \mid \mathbf{Y}_1^k, \mathbf{U}_0^k\right] \\
&= \mathbf{F}_k E\left[\boldsymbol{\theta}_k \mid \mathbf{Y}_1^k, \mathbf{U}_0^k\right] + \mathbf{G}_k\mathbf{u}_k \\
&= \mathbf{F}_k\hat{\boldsymbol{\theta}}_{k|k} + \mathbf{G}_k\mathbf{u}_k
\end{aligned} \tag{2.12}$$

$$\begin{aligned}
\mathbf{P}_{k+1|k} &= E\left[\tilde{\boldsymbol{\theta}}_{k+1|k}\tilde{\boldsymbol{\theta}}_{k+1|k}^T \mid \mathbf{Y}_1^k, \mathbf{U}_0^k\right] \\
&= E\left[\left(\mathbf{F}_k\tilde{\boldsymbol{\theta}}_{k|k} + \mathbf{w}_k\right)\left(\mathbf{F}_k\tilde{\boldsymbol{\theta}}_{k|k} + \mathbf{w}_k\right)^T \mid \mathbf{Y}_1^k, \mathbf{U}_0^k\right] \\
&= \mathbf{F}_k E\left[\tilde{\boldsymbol{\theta}}_{k|k}\tilde{\boldsymbol{\theta}}_{k|k}^T \mid \mathbf{Y}_1^k, \mathbf{U}_0^k\right]\mathbf{F}_k^T + E\left[\mathbf{w}_k\mathbf{w}_k^T\right] \\
&= \mathbf{F}_k\mathbf{P}_{k|k}\mathbf{F}_k^T + \mathbf{Q}_k
\end{aligned} \tag{2.13}$$

Notice that the prediction dynamics follows exactly the system's dynamics. The predicted estimate and the associated covariance matrix in Eq. 2.12 and Eq. 2.13 correspond to the best knowledge of the system's state at time instant $(k+1)$ before making the observation at this time instant.

Filtering: *evaluating* $p(\boldsymbol{\theta}_{k+1} \mid \mathbf{Y}_1^{k+1}, \mathbf{U}_0^k)$
$p(\boldsymbol{\theta}_{k+1} \mid \mathbf{Y}_1^{k+1}, \mathbf{U}_0^k) \sim \mathcal{N}\left(\hat{\boldsymbol{\theta}}_{k+1|k+1}, \mathbf{P}_{k+1|k+1}\right)$, where

$$\begin{aligned}\hat{\boldsymbol{\theta}}_{k+1|k+1} &= E\left[\boldsymbol{\theta}_{k+1} \mid \mathbf{Y}_1^{k+1}, \mathbf{U}_0^k\right] \\ \mathbf{P}_{k+1|k+1} &= E\left[\left(\boldsymbol{\theta}_{k+1} - \hat{\boldsymbol{\theta}}_{k+1|k+1}\right)\left(\boldsymbol{\theta}_{k+1} - \hat{\boldsymbol{\theta}}_{k+1|k+1}\right)^T \mid \mathbf{Y}_1^{k+1}, \mathbf{U}_0^k\right]\end{aligned}$$

One note that $\mathbf{Y}_1^{k+1} = \left\{\mathbf{Y}_1^k,\ \mathbf{y}_{k+1}\right\}$. Moreover, $\mathbf{Y}_1^k$ and $\mathbf{y}_{k+1}$ are statistically dependent, while $\boldsymbol{\theta}_{k+1}$, $\mathbf{Y}_1^k$ and $\mathbf{y}_{k+1}$ are jointly Gaussian random vectors. Recalling [13, Theorem 12-4 on p. 105],

$$\hat{\boldsymbol{\theta}}_{k+1|k+1} = E\left[\boldsymbol{\theta}_{k+1} \mid \mathbf{Y}_1^k, \mathbf{y}_{k+1}, \mathbf{U}_0^k\right] = E\left[\boldsymbol{\theta}_{k+1} \mid \mathbf{Y}_1^k, \tilde{\mathbf{y}}_{k+1|k}, \mathbf{U}_0^k\right] \tag{2.14}$$

where

$$\tilde{\mathbf{y}}_{k+1|k} = \mathbf{y}_{k+1} - E\left[\mathbf{y}_{k+1} \mid \mathbf{Y}_1^k, \mathbf{U}_0^k\right] \tag{2.15}$$

Hence

$$\hat{\boldsymbol{\theta}}_{k+1|k+1} = E\left[\boldsymbol{\theta}_{k+1} \mid \mathbf{Y}_1^k, \mathbf{U}_0^k\right] + E\left[\boldsymbol{\theta}_{k+1} \mid \tilde{\mathbf{y}}_{k+1|k}, \mathbf{U}_0^k\right] - E\left[\boldsymbol{\theta}_{k+1} \mid \mathbf{U}_0^k\right] \tag{2.16}$$

Eq. 2.15 is called the *innovation process*. By manipulating this expression and using the measurement Eq. 2.11, one obtains the following equivalent assertion

$$\tilde{\mathbf{y}}_{k+1|k} = \boldsymbol{\Phi}_{k+1}\tilde{\boldsymbol{\theta}}_{k+1|k} + \mathbf{v}_{k+1}$$

The associated covariance matrix follows, knowing that $E\left[\tilde{\mathbf{y}}_{k+1|k} \mid \mathbf{Y}_1^k, \mathbf{U}_0^k\right] = 0$ and the fact that $\tilde{\boldsymbol{\theta}}_{k+1|k}$ does not depend on the measurement $\mathbf{y}_{k+1}$

$$\begin{aligned}\mathbf{P}_{\tilde{\mathbf{y}}_{k+1|k}} &= E\left[\tilde{\mathbf{y}}_{k+1|k}\tilde{\mathbf{y}}_{k+1|k}^T \mid \mathbf{Y}_1^k, \mathbf{U}_0^k\right] \\ &= E\left[\left(\boldsymbol{\Phi}_{k+1}\tilde{\boldsymbol{\theta}}_{k+1|k} + \mathbf{v}_{k+1}\right)\left(\boldsymbol{\Phi}_{k+1}\tilde{\boldsymbol{\theta}}_{k+1|k} + \mathbf{v}_{k+1}\right)^T \mid \mathbf{Y}_1^k, \mathbf{U}_0^k\right] \\ &= \boldsymbol{\Phi}_{k+1}\mathbf{P}_{k+1|k}\boldsymbol{\Phi}_{k+1}^T + \mathbf{R}_{k+1}\end{aligned}$$

Eq. 2.16 is the starting point for the derivation of the Kalman filter. Recall that $\boldsymbol{\theta}_{k+1}$ and $\mathbf{y}_{k+1}$ are jointly Gaussian. In Eq. 2.14 $\mathbf{y}_{k+1}$ has been replaced by $\tilde{\mathbf{y}}_{k+1|k}$. In particular, one can show that $\tilde{\mathbf{y}}_{k+1|k}$ is computable from $\mathbf{y}_{k+1}$, and that $\mathbf{y}_{k+1}$ is computable from $\tilde{\mathbf{y}}_{k+1|k}$. Because of this fact, $\boldsymbol{\theta}_{k+1}$ and $\tilde{\mathbf{y}}_{k+1|k}$ are also jointly

Gaussian. By exploiting [13, Theorem 12-1 on p. 102],

$$E\left[\boldsymbol{\theta}_{k+1} \mid \tilde{\mathbf{y}}_{k+1|k}, \mathbf{U}_0^k\right] = E\left[\boldsymbol{\theta}_{k+1} \mid \mathbf{U}_0^k\right] + \mathbf{P}_{\boldsymbol{\theta}_{k+1},\, \tilde{\mathbf{y}}_{k+1|k}} \mathbf{P}_{\tilde{\mathbf{y}}_{k+1|k}}^{-1} \tilde{\mathbf{y}}_{k+1|k} \tag{2.17}$$

with

$$\begin{aligned}
\mathbf{P}_{\tilde{\mathbf{y}}_{k+1|k}} &= \boldsymbol{\Phi}_{k+1} \mathbf{P}_{k+1|k} \boldsymbol{\Phi}_{k+1}^T + \mathbf{R}_{k+1} \\
\mathbf{P}_{\boldsymbol{\theta}_{k+1}, \tilde{\mathbf{y}}_{k+1|k}} &= E\left[\left(\boldsymbol{\theta}_{k+1} - E\left[\boldsymbol{\theta}_{k+1} \mid \mathbf{U}_0^k\right]\right) \tilde{\mathbf{y}}_{k+1|k}^T \mid \mathbf{Y}_1^k, \mathbf{U}_0^k\right] \\
&= E\left[\boldsymbol{\theta}_{k+1} \tilde{\mathbf{y}}_{k+1|k}^T \mid \mathbf{Y}_1^k, \mathbf{U}_0^k\right] \\
&= E\left[\boldsymbol{\theta}_{k+1} \tilde{\boldsymbol{\theta}}_{k+1|k}^T \mid \mathbf{Y}_1^k, \mathbf{U}_0^k\right] \boldsymbol{\Phi}_{k+1}^T \\
&= \mathbf{P}_{k+1|k} \boldsymbol{\Phi}_{k+1}^T
\end{aligned}$$

In the above computation $E\left[\tilde{\mathbf{y}}_{k+1|k} \mid \mathbf{Y}_1^k, \mathbf{U}_0^k\right] = 0$, $E\left[\boldsymbol{\theta}_{k+1} \mathbf{v}_{k+1} \mid \mathbf{U}_0^k\right] = 0$ and the *innovation* expression were used.
By combining Eq. 2.16 and Eq. 2.17, one obtains:

$$\hat{\boldsymbol{\theta}}_{k+1|k+1} = \hat{\boldsymbol{\theta}}_{k+1|k} + \underbrace{\mathbf{P}_{k+1|k} \boldsymbol{\Phi}_{k+1}^T \left(\boldsymbol{\Phi}_{k+1} \mathbf{P}_{k+1|k} \boldsymbol{\Phi}_{k+1}^T + \mathbf{R}_{k+1}\right)^{-1}}_{\mathbf{K}_{k+1}} \tilde{\mathbf{y}}_{k+1|k} \tag{2.18}$$

$\mathbf{K}_{k+1}$ is termed *Kalman gain*. As far as the corresponding covariance $\mathbf{P}_{k+1|k+1}$ is concerned, analogously from computing $\mathbf{P}_{k+1|k}$:

$$\begin{aligned}
\mathbf{P}_{k+1|k+1} &= E\left[\tilde{\boldsymbol{\theta}}_{k+1|k+1} \tilde{\boldsymbol{\theta}}_{k+1|k+1}^T \mid \mathbf{Y}_1^{k+1}, \mathbf{U}_0^k\right] \\
&= E\left[\left(\tilde{\boldsymbol{\theta}}_{k+1|k} - \mathbf{K}_{k+1} \tilde{\mathbf{y}}_{k+1|k}\right) \left(\tilde{\boldsymbol{\theta}}_{k+1|k} - \mathbf{K}_{k+1} \tilde{\mathbf{y}}_{k+1|k}\right)^T \mid \mathbf{Y}_1^{k+1}, \mathbf{U}_0^k\right] \\
&= E\left[\left(\tilde{\boldsymbol{\theta}}_{k+1|k} - \mathbf{K}_{k+1} \left(\boldsymbol{\Phi}_{k+1} \tilde{\boldsymbol{\theta}}_{k+1|k} + \mathbf{v}_{k+1}\right)\right) \left(\tilde{\boldsymbol{\theta}}_{k+1|k} - \mathbf{K}_{k+1} \left(\boldsymbol{\Phi}_{k+1} \tilde{\boldsymbol{\theta}}_{k+1|k} + \mathbf{v}_{k+1}\right)\right)^T \mid \right. \\
&\qquad \left. \mathbf{Y}_1^{k+1}, \mathbf{U}_0^k\right] \\
&= E\left[\left(\left(\mathbf{I} - \mathbf{K}_{k+1} \boldsymbol{\Phi}_{k+1}\right) \tilde{\boldsymbol{\theta}}_{k+1|k} - \mathbf{K}_{k+1} \mathbf{v}_{k+1}\right) \left(\left(\mathbf{I} - \mathbf{K}_{k+1} \boldsymbol{\Phi}_{k+1}\right) \tilde{\boldsymbol{\theta}}_{k+1|k} - \mathbf{K}_{k+1} \mathbf{v}_{k+1}\right)^T \mid \right. \\
&\qquad \left. \mathbf{Y}_1^{k+1}, \mathbf{U}_0^k\right] \\
&= \left(\mathbf{I} - \mathbf{K}_{k+1} \boldsymbol{\Phi}_{k+1}\right) E\left[\tilde{\boldsymbol{\theta}}_{k+1|k} \tilde{\boldsymbol{\theta}}_{k+1|k}^T \mid \mathbf{Y}_1^k, \mathbf{U}_0^k\right] \left(\mathbf{I} - \mathbf{K}_{k+1} \boldsymbol{\Phi}_{k+1}\right)^T + \mathbf{K}_{k+1} E\left[\mathbf{v}_{k+1} \mathbf{v}_{k+1}^T\right] \mathbf{K}_{k+1}^T \\
&= \left(\mathbf{I} - \mathbf{K}_{k+1} \boldsymbol{\Phi}_{k+1}\right) \mathbf{P}_{k+1|k} \left(\mathbf{I} - \mathbf{K}_{k+1} \boldsymbol{\Phi}_{k+1}\right)^T + \mathbf{K}_{k+1} \mathbf{R}_{k+1} \mathbf{K}_{k+1}^T
\end{aligned} \tag{2.19}$$

Recall from the recursive least squares development in Subsection 2.1.2 that the availability of the measurement y_{k+1} changes the estimate of a constant $\boldsymbol{\theta}$ as follows:

$$\mathbf{K}_{k+1} = \begin{cases} \mathbf{P}_k \boldsymbol{\Phi}_{k+1}^T \left(\boldsymbol{\Phi}_{k+1} \mathbf{P}_k \boldsymbol{\Phi}_{k+1}^T + \mathbf{R}_{k+1} \right)^{-1} \\ \mathbf{P}_{k+1} \boldsymbol{\Phi}_{k+1}^T \mathbf{R}_{k+1}^{-1} \end{cases}$$

$$\mathbf{P}_{k+1} = \begin{cases} \left(\mathbf{I} - \mathbf{K}_{k+1} \boldsymbol{\Phi}_{k+1} \right) \mathbf{P}_k \left(\mathbf{I} - \mathbf{K}_{k+1} \boldsymbol{\Phi}_{k+1} \right)^T + \mathbf{K}_{k+1} \mathbf{R}_{k+1} \mathbf{K}_{k+1}{}^T \\ \left(\mathbf{I} - \mathbf{K}_{k+1} \boldsymbol{\Phi}_{k+1} \right) \mathbf{P}_k \\ \left(\mathbf{P}_k^{-1} + \boldsymbol{\Phi}_{k+1}^T \mathbf{R}_{k+1}^{-1} \boldsymbol{\Phi}_{k+1} \right)^{-1} \end{cases}$$

$$\hat{\boldsymbol{\theta}}_{k+1} = \hat{\boldsymbol{\theta}}_k + \mathbf{K}_{k+1} \left(y_{k+1} - \boldsymbol{\Phi}_{k+1} \hat{\boldsymbol{\theta}}_k \right)$$

where $\hat{\boldsymbol{\theta}}_k$ and $\mathbf{P}_k$ are the estimate of the constant $\boldsymbol{\theta}$ and the corresponding estimation error covariance before the measurement y_{k+1} is processed while $\hat{\boldsymbol{\theta}}_{k+1}$ and $\mathbf{P}_{k+1}$ are the estimate and covariance after the measurement y_{k+1} is processed.

In this framework, $\hat{\boldsymbol{\theta}}_{k+1|k}$ and $\mathbf{P}_{k+1|k}$ are the estimate of $\boldsymbol{\theta}_{k+1}$ and related covariance before the measurement $\mathbf{y}_{k+1}$ is processed while $\hat{\boldsymbol{\theta}}_{k+1|k+1}$ and $\mathbf{P}_{k+1|k+1}$ are the ones after the corresponding measurement is processed. Following the same reasoning done in Subsection 2.1.2, one can obtain different expressions for $\mathbf{K}_{k+1}$ and $\mathbf{P}_{k+1|k+1}$. The expressions for $\hat{\boldsymbol{\theta}}_{k+1|k+1}$, $\hat{\boldsymbol{\theta}}_{k+1|k}$ and $\mathbf{P}_{k+1|k}$ are also reported for conveniency.

Prediction

$$\hat{\boldsymbol{\theta}}_{k+1|k} = \mathbf{F}_k \hat{\boldsymbol{\theta}}_{k|k} + \mathbf{G}_k \mathbf{u}_k$$

$$\mathbf{P}_{k+1|k} = \mathbf{F}_k \mathbf{P}_{k|k} \mathbf{F}_k^T + \mathbf{Q}_k$$

Filtering

$$\mathbf{K}_{k+1} = \begin{cases} \mathbf{P}_{k+1|k} \boldsymbol{\Phi}_{k+1}^T \left(\boldsymbol{\Phi}_{k+1} \mathbf{P}_{k+1|k} \boldsymbol{\Phi}_{k+1}^T + \mathbf{R}_{k+1} \right)^{-1} \\ \mathbf{P}_{k+1|k+1} \boldsymbol{\Phi}_{k+1}^T \mathbf{R}_{k+1}^{-1} \end{cases}$$

$$\mathbf{P}_{k+1|k+1} = \begin{cases} \left(\mathbf{I} - \mathbf{K}_{k+1} \boldsymbol{\Phi}_{k+1} \right) \mathbf{P}_{k+1|k} \left(\mathbf{I} - \mathbf{K}_{k+1} \boldsymbol{\Phi}_{k+1} \right)^T + \mathbf{K}_{k+1} \mathbf{R}_{k+1} \mathbf{K}_{k+1}{}^T \\ \left(\mathbf{I} - \mathbf{K}_{k+1} \boldsymbol{\Phi}_{k+1} \right) \mathbf{P}_{k+1|k} \\ \left(\mathbf{P}_{k+1|k}^{-1} + \boldsymbol{\Phi}_{k+1}^T \mathbf{R}_{k+1}^{-1} \boldsymbol{\Phi}_{k+1} \right)^{-1} \end{cases}$$

$$\hat{\boldsymbol{\theta}}_{k+1|k+1} = \hat{\boldsymbol{\theta}}_{k+1|k} + \mathbf{K}_{k+1} \left(\mathbf{y}_{k+1} - \boldsymbol{\Phi}_{k+1} \hat{\boldsymbol{\theta}}_{k+1|k} \right)$$

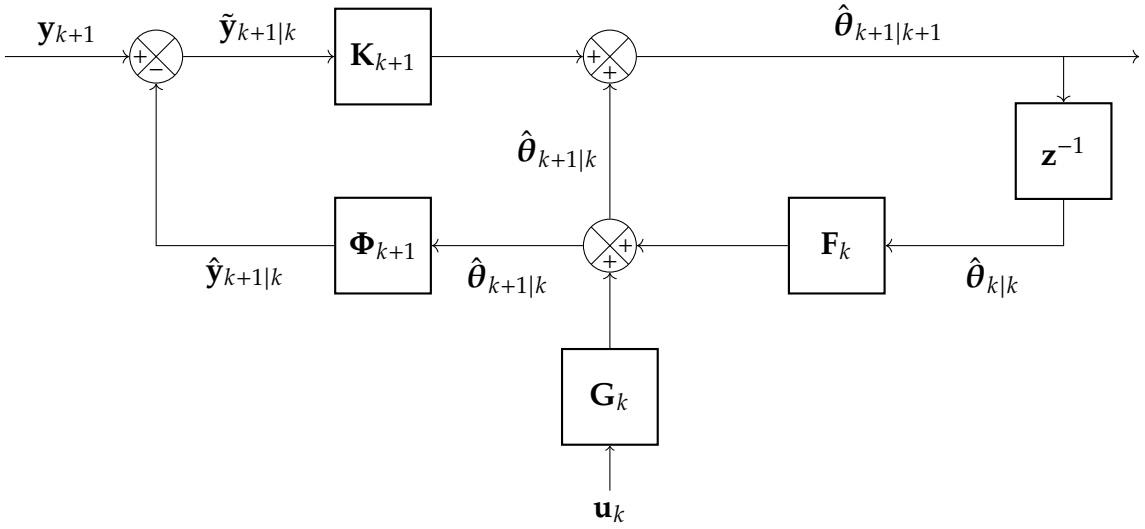

Figure 2.4: Kalman filter block diagram

Fig. 2.4 depicts the interconnection of the Kalman filter system. Note that in the prediction set of equations, the predicted state estimate and corresponding covariance depend only on the filtered state and filtered covariance at the previous step. One can observe that it is possible to obtain the predicted state estimate as function of the predicted state at the previous step, i.e $\hat{\boldsymbol{\theta}}_{k+1|k} = f_5\left(\hat{\boldsymbol{\theta}}_{k|k-1}\right)$ and the predicted covariance as $\mathbf{P}_{k+1|k} = f_6\left(\mathbf{P}_{k|k-1}\right)$. By applying the same reasoning, $\hat{\boldsymbol{\theta}}_{k+1|k+1} = f_7\left(\hat{\boldsymbol{\theta}}_{k|k}\right)$ and the predicted covariance as $\mathbf{P}_{k+1|k+1} = f_8\left(\mathbf{P}_{k|k}\right)$. Mathematically, by making use of the prediction and filtering equations, this is shown below:

$$\begin{cases} \hat{\boldsymbol{\theta}}_{k+1|k} = \mathbf{F}_k\left(\mathbf{I} - \mathbf{K}_k\boldsymbol{\Phi}_k\right)\hat{\boldsymbol{\theta}}_{k|k-1} + \mathbf{F}_k\mathbf{K}_k\mathbf{y}_k + \mathbf{G}_k\mathbf{u}_k \\ \hat{\boldsymbol{\theta}}_{k+1|k+1} = \left(\mathbf{I} - \mathbf{K}_{k+1}\boldsymbol{\Phi}_{k+1}\right)\left(\mathbf{F}_k\hat{\boldsymbol{\theta}}_{k|k} + \mathbf{G}_k\mathbf{u}_k\right) + \mathbf{K}_{k+1}\mathbf{y}_{k+1} \end{cases} \tag{2.20}$$

$$\begin{cases} \mathbf{P}_{k+1|k} = \mathbf{F}_k\mathbf{P}_{k|k-1}\mathbf{F}_k^T + \mathbf{Q}_k - \mathbf{F}_k\mathbf{P}_{k|k-1}\boldsymbol{\Phi}_k^T\left(\boldsymbol{\Phi}_k\mathbf{P}_{k|k-1}\boldsymbol{\Phi}_k^T + \mathbf{R}_k\right)^{-1}\boldsymbol{\Phi}_k\mathbf{P}_{k|k+1}\mathbf{F}_k^T \\ \mathbf{P}_{k+1|k+1} = \left\{\mathbf{I} - \left[\mathbf{F}_k\mathbf{P}_{k|k}\mathbf{F}_k^T + \mathbf{Q}_k\right]\boldsymbol{\Phi}_{k+1}^T\left[\boldsymbol{\Phi}_{k+1}\left(\mathbf{F}_k\mathbf{P}_{k|k}\mathbf{F}_k^T + \mathbf{Q}_k\right)\boldsymbol{\Phi}_{k+1}^T + \mathbf{R}_{k+1}\right]^{-1}\boldsymbol{\Phi}_{k+1}\right\} \\ \qquad\qquad \left[\mathbf{F}_k\mathbf{P}_{k|k}\mathbf{F}_k^T + \mathbf{Q}_k\right] \end{cases} \tag{2.21}$$

Eq. 2.20 represent the *recursive predictor* and *recursive filter*. Eq. 2.21 are the so called *Riccati* equations.

KF algorithm

Algorithm 1 KF algorithm

System:

$$\begin{cases} \boldsymbol{\theta}_{k+1} = \mathbf{F}_k \boldsymbol{\theta}_k + \mathbf{G}_k \mathbf{u}_k + \mathbf{w}_k \\ \mathbf{y}_{k+1} = \boldsymbol{\Phi}_{k+1} \boldsymbol{\theta}_{k+1} + \mathbf{v}_{k+1} \end{cases} \text{, where } \begin{cases} E\left[\mathbf{w}_k \mathbf{w}_j^T\right] = \mathbf{Q}_k \delta_{k-J} \\ E\left[\mathbf{v}_k \mathbf{v}_j^T\right] = \mathbf{R}_k \delta_{k-j} \\ E\left[\mathbf{v}_k \mathbf{w}_j^T\right] = 0 \end{cases}$$

Initialize:

$\hat{\boldsymbol{\theta}}_{0|0} = E[\boldsymbol{\theta}_0]$

$\mathbf{P}_{0|0} = E\left[\left(\boldsymbol{\theta}_0 - \hat{\boldsymbol{\theta}}_{0|0}\right)\left(\boldsymbol{\theta}_0 - \hat{\boldsymbol{\theta}}_{0|0}\right)^T\right]$

for $k = 0, 1, \cdots$ **do**

Prediction $\begin{cases} \hat{\boldsymbol{\theta}}_{k+1|k} \leftarrow \mathbf{F}_k \hat{\boldsymbol{\theta}}_{k|k} + \mathbf{G}_k \mathbf{u}_k \\ \mathbf{P}_{k+1|k} \leftarrow \mathbf{F}_k \mathbf{P}_{k|k} \mathbf{F}_k^T + \mathbf{Q}_k \end{cases}$

$\mathbf{y}_{k+1} \leftarrow$ new measurement

Filtering

$$\begin{cases} \mathbf{K}_{k+1} \leftarrow \begin{cases} \mathbf{P}_{k+1|k} \boldsymbol{\Phi}_{k+1}^T \left(\boldsymbol{\Phi}_{k+1} \mathbf{P}_{k+1|k} \boldsymbol{\Phi}_{k+1}^T + \mathbf{R}_{k+1}\right)^{-1} \\ \mathbf{P}_{k+1|k+1} \boldsymbol{\Phi}_{k+1}^T \mathbf{R}_{k+1}^{-1} \end{cases} \\ \mathbf{P}_{k+1|k+1} \leftarrow \begin{cases} \left(\mathbf{I} - \mathbf{K}_{k+1} \boldsymbol{\Phi}_{k+1}\right) \mathbf{P}_{k+1|k} \left(\mathbf{I} - \mathbf{K}_{k+1} \boldsymbol{\Phi}_{k+1}\right)^T + \mathbf{K}_{k+1} \mathbf{R}_{k+1} \mathbf{K}_{k+1}{}^T \\ \left(\mathbf{I} - \mathbf{K}_{k+1} \boldsymbol{\Phi}_{k+1}\right) \mathbf{P}_{k+1|k} \\ \left(\mathbf{P}_{k+1|k}^{-1} + \boldsymbol{\Phi}_{k+1}^T \mathbf{R}_{k+1}^{-1} \boldsymbol{\Phi}_{k+1}\right)^{-1} \end{cases} \\ \hat{\boldsymbol{\theta}}_{k+1|k+1} \leftarrow \hat{\boldsymbol{\theta}}_{k+1|k} + \mathbf{K}_{k+1} \left(\mathbf{y}_{k+1} - \boldsymbol{\Phi}_{k+1} \hat{\boldsymbol{\theta}}_{k+1|k}\right) \end{cases}$$

end for

The first expression for $\mathbf{P}_{k+1|k+1}$ guarantees that $\mathbf{P}_{k+1|k+1}$ will always be symmetric positive definite, as long as $\mathbf{P}_{k+1|k}$ is symmetric positive definite. The second expression for $\mathbf{P}_{k+1|k+1}$ is computationally simpler than the first expression, but its form does not guarantee symmetry or positive definiteness for $\mathbf{P}_{k+1|k+1}$. The third form for $\mathbf{P}_{k+1|k+1}$ is rarely implemented and it is used if the second expression for $\mathbf{K}_{k+1}$ is considered. Finally, the calculation of $\mathbf{P}_{k+1|k}$, $\mathbf{K}_{k+1}$, and $\mathbf{P}_{k+1|k+1}$ do not depend on the measurements $\mathbf{y}_{k+1}$, but depend only on the system parameters. This means that the *Kalman gain* $\mathbf{K}_{k+1}$ can be calculated offline. In contrast, as discussed later on, the filter gain and covariance for *non-linear* systems cannot in general be computed offline because they depend on the measurements.

2.2.2 Kalman filter dynamics for linear time-invariant stationary systems

The system of Eq. 2.11 is considered now time-invariant, namely $\mathbf{F}_k = \mathbf{F}$, $\mathbf{G}_k = \mathbf{G}$ and $\mathbf{\Phi}_k = \mathbf{\Phi}$, $\forall\ k \geq 0$. Moreover $\mathbf{Q}_k = \mathbf{Q}$ and $\mathbf{R}_k = \mathbf{R}$.

$$\mathbf{\Sigma}: \begin{cases} \boldsymbol{\theta}_{k+1} &= \mathbf{F}\boldsymbol{\theta}_k + \mathbf{G}\mathbf{u}_k + \mathbf{w}_k \\ \mathbf{y}_{k+1} &= \mathbf{\Phi}\boldsymbol{\theta}_{k+1} + \mathbf{v}_{k+1} \end{cases} \tag{2.22}$$

As before $\{\mathbf{w}_k\}$ and $\{\mathbf{v}_k\}$ are white, Gaussian, zero-mean. Their covariance is now constant, namely $E\left[\mathbf{w}_k\mathbf{w}_k^T\right] = \mathbf{Q}$ and $E\left[\mathbf{v}_k\mathbf{v}_k^T\right] = \mathbf{R}$. The Kalman filter dynamics for the time-invariant stationary case is obtained as a particularization of the general time-varying non-stationary dynamics.

Prediction

$$\hat{\boldsymbol{\theta}}_{k+1|k} = \mathbf{F}\hat{\boldsymbol{\theta}}_{k|k} + \mathbf{G}\mathbf{u}_k$$
$$\mathbf{P}_{k+1|k} = \mathbf{F}\mathbf{P}_{k|k}\mathbf{F}^T + \mathbf{Q}$$

Filtering

$$\mathbf{K}_{k+1} = \begin{cases} \mathbf{P}_{k+1|k}\mathbf{\Phi}^T\left(\mathbf{\Phi}\mathbf{P}_{k+1|k}\mathbf{\Phi}^T + \mathbf{R}\right)^{-1} \\ \mathbf{P}_{k+1|k+1}\mathbf{\Phi}^T\mathbf{R}^{-1} \end{cases}$$

$$\mathbf{P}_{k+1|k+1} = \begin{cases} \left(\mathbf{I} - \mathbf{K}_{k+1}\mathbf{\Phi}\right)\mathbf{P}_{k+1|k}\left(\mathbf{I} - \mathbf{K}_{k+1}\mathbf{\Phi}\right)^T + \mathbf{K}_{k+1}\mathbf{R}{\mathbf{K}_{k+1}}^T \\ \left(\mathbf{I} - \mathbf{K}_{k+1}\mathbf{\Phi}\right)\mathbf{P}_{k+1|k} \\ \left(\mathbf{P}_{k+1|k}^{-1} + \mathbf{\Phi}^T\mathbf{R}^{-1}\mathbf{\Phi}\right)^{-1} \end{cases}$$

$$\hat{\boldsymbol{\theta}}_{k+1|k+1} = \hat{\boldsymbol{\theta}}_{k+1|k} + \mathbf{K}_{k+1}\left(\mathbf{y}_{k+1} - \mathbf{\Phi}\hat{\boldsymbol{\theta}}_{k+1|k}\right)$$

The expression for $\hat{\boldsymbol{\theta}}_{k+1|k+1}$ is also in this case time-varying. This is due to the fact that the *Kalman gain* $\mathbf{K}_{k+1}$ is time-varying.

Steady-state Kalman filter

For time-invariant and stationary systems, if $\lim_{k\to\infty}\mathbf{P}_{k+1|k} = \bar{\mathbf{P}}$ exists, then $\lim_{k\to\infty}\mathbf{K}_{k+1} \to \bar{\mathbf{K}}$ and the Kalman filter equation $\hat{\boldsymbol{\theta}}_{k+1|k+1} = \hat{\boldsymbol{\theta}}_{k+1|k} + \mathbf{K}_{k+1}\tilde{\mathbf{y}}_{k+1|k}$ becomes a constant coefficient filter. Since $\mathbf{P}_{k+1|k}$ and $\mathbf{P}_{k+1|k+1}$ are related, then, if $\bar{\mathbf{P}}$ exists, $\lim_{k\to\infty}\mathbf{P}_{k+1|k+1}$, also exists. So, instead of computing $\mathbf{P}_{k+1|k}$, $\mathbf{P}_{k+1|k+1}$ and $\mathbf{K}_{k+1}$ at each time step, $\bar{\mathbf{K}}$ can be used as *Kalman gain* at each instant. The steady-state Kalman filter is not optimal because the optimal Kalman gain at each time step is not being used.

Asymptotic issues

As already mentioned, $\boldsymbol{\Sigma}$ is time-invariant but the predictor $\hat{\boldsymbol{\Sigma}}$ is time-variant, since the Kalman gain $\mathbf{K}_k$ varies in time. $\hat{\boldsymbol{\Sigma}}$ is reported below

$$\hat{\boldsymbol{\Sigma}} : \begin{cases} \hat{\boldsymbol{\theta}}_{k+1|k} & = \mathbf{F}\left(\mathbf{I} - \mathbf{K}_k\boldsymbol{\Phi}\right)\hat{\boldsymbol{\theta}}_{k|k-1} + \mathbf{F}\mathbf{K}_k\mathbf{y}_k + \mathbf{G}\mathbf{u}_k \\ \hat{\mathbf{y}}_{k+1|k} & = \boldsymbol{\Phi}\hat{\boldsymbol{\theta}}_{k+1|k} \end{cases}$$

Some motivations for studying the asymptotic predictor are explained below.

1. If $\lim_{k\to\infty}\mathbf{K}_k = \bar{\mathbf{K}}$ then $\bar{\mathbf{K}}$ could be used, obtaining a sub-optimal predictor converging to the optimal one. This motivates the study for $\lim_{k\to\infty}\mathbf{P}_{k|k-1}$. Specifically, if $\bar{\mathbf{P}}$ exists, it has to satisfy the Algebraic Riccati Equation (ARE):

$$\bar{\mathbf{P}} = \mathbf{F}\bar{\mathbf{P}}\mathbf{F}^T + \mathbf{Q} - \mathbf{F}\bar{\mathbf{P}}\boldsymbol{\Phi}^T\left(\boldsymbol{\Phi}\bar{\mathbf{P}}\boldsymbol{\Phi}^T + \mathbf{R}\right)^{-1}\boldsymbol{\Phi}\bar{\mathbf{P}}\mathbf{F}^T$$

   (a) When does $\lim_{k\to\infty}\mathbf{P}_{k|k-1} = \bar{\mathbf{P}}$ exist?

   (b) Does the limit $\bar{\mathbf{P}}$ (if it exists) depend on $\mathbf{P}_{0|0}$?

   (c) Can ARE admit more than one solution? Which is the right $\bar{\mathbf{P}}$ to which $\mathbf{P}_{k|k-1}$ converges?

2. Beyond computational considerations, study of $\lim_{k\to\infty}\mathbf{P}_{k|k-1}$ makes us understand if $\hat{\boldsymbol{\Sigma}}$ can predict the state with an error variance $\mathbf{P}_{k|k-1}$ which remains small.

3. Asymptotic behaviour study permits to assess if $\hat{\boldsymbol{\Sigma}}$ tends to a stable system

$$\hat{\boldsymbol{\Sigma}}_\infty : \begin{cases} \hat{\boldsymbol{\theta}}_{k+1|k} & = \mathbf{F}\left(\mathbf{I} - \bar{\mathbf{K}}\boldsymbol{\Phi}\right)\hat{\boldsymbol{\theta}}_{k|k-1} + \mathbf{F}\bar{\mathbf{K}}\mathbf{y}_k + \mathbf{G}\mathbf{u}_k \\ \hat{\mathbf{y}}_{k+1|k} & = \boldsymbol{\Phi}\hat{\boldsymbol{\theta}}_{k+1|k} \end{cases}$$

   The predictor $\hat{\boldsymbol{\Sigma}}_\infty$ is stable if $\max_i \left|\lambda_i\left(\left(\mathbf{F} - \mathbf{F}\bar{\mathbf{K}}\boldsymbol{\Phi}\right)\right)\right| < 1$

Stability of $\boldsymbol{\Sigma}$, observability of $(\mathbf{F}, \boldsymbol{\Phi})$ and controllability of $(\mathbf{F}, \mathbf{Q})$ are only a *sufficient* condition for predictor convergence. On the other hand, the general convergence theorem gives *sufficient and necessary* conditions for predictor convergence.

Theorem 2.2.1 (General convergence theorem).

$$\begin{matrix} (\mathbf{F}, \boldsymbol{\Phi}) \textit{ detectable} \\ (\mathbf{F}, \mathbf{Q}) \textit{ stabilizable} \end{matrix} \iff \begin{cases} 1. & \forall \mathbf{P}_{0|0} = \mathbf{P}_{0|0}{}^T \geq 0,\ \lim_{k\to\infty}\mathbf{P}_{k|k-1} = \bar{\mathbf{P}} \\ 2. & \hat{\boldsymbol{\Sigma}}_\infty \textit{ is stable} \\ 3. & \bar{\mathbf{P}} \textit{ is the only } \bar{\mathbf{P}} = \bar{\mathbf{P}}^T \geq 0 \textit{ which solves the ARE} \end{cases}$$

3

Non linear filters

All of previous discussion to this point has considered linear filters for linear systems. However, many real-world systems are continuous-time in nature and quite a few are also non-linear. A lot of systems are close enough to be linear such that linear estimation approaches give satisfactory results. Eventually, a system does not behave linearly even over a small range of operation, and the linear approaches for estimation no longer give good results. In this case, there is the need to explore non-linear estimators. In the following section, a very important non-linear estimator is discussed, namely the Extended Kalman Filter (EKF).

3.1 Extended Kalman filter

The Kalman filter that was discussed earlier in the previous section directly applies only to linear systems. However, a non-linear system can be linearized around a nominal trajectory so that the states of the linearized system can represent the deviation from the nominal trajectory. Thus, linear estimation technique, such as KF, can be applied. However, the linearized Kalman filter (LKF) usually gives poor results, because it relies on an open-loop strategy for choosing the nominal trajectory $\bar{\boldsymbol{\theta}}_k$, with $\boldsymbol{\theta}_k$ representing the state at time k. When $\bar{\boldsymbol{\theta}}_k$ is precomputed there is no way of forcing $\bar{\boldsymbol{\theta}}_k$ to remain close to $\boldsymbol{\theta}_k$, and this must be done or else the perturbation state-variable model is invalid. This is the reason why divergence of LKF often occurs. It does not use the non-linear nature of the original system in an active manner.

On the other hand, the EKF relinearizes the non-linear system about each new estimate as it becomes available. The purpose of relinearizing about the filter's output is to use a better reference trajectory for $\bar{\boldsymbol{\theta}}_k$. Doing this, $\boldsymbol{\theta}_k$ - $\bar{\boldsymbol{\theta}}_k$ will be held as small as possible, so that our linearization assumptions are less likely to be violated than in the case of the LKF. Consider the non-linear dynamics

$$\boldsymbol{\Sigma} : \begin{cases} \boldsymbol{\theta}_{k+1} & = \mathbf{f}_k\left(\boldsymbol{\theta}_k, \mathbf{u}_k\right) + \mathbf{w}_k \\ \mathbf{y}_{k+1} & = \boldsymbol{\phi}_{k+1}\left(\boldsymbol{\theta}_{k+1}\right) + \mathbf{v}_{k+1} \end{cases} \tag{3.1}$$

$\mathbf{w}_k$, $\mathbf{v}_k$ are white Gaussian, independent random processes with zero mean and covariance matrix

$$E\left[\mathbf{w}_k \mathbf{w}_k^T\right] = \mathbf{Q}_k, \quad E\left[\mathbf{v}_k \mathbf{v}_k^T\right] = \mathbf{R}_k$$

The initial state $\boldsymbol{\theta}_0$ is a random vector with known mean $\hat{\boldsymbol{\theta}}_{0|0}$ and covariance $\mathbf{P}_{0|0}$. The filter's goal is to obtain an estimate of the system's state based on the available information (control inputs $\mathbf{U}_0^{k-1} = \{\mathbf{u}_0, \cdots, \mathbf{u}_{k-1}\}$ and observations $\mathbf{Y}_1^k = \{\mathbf{y}_1, \cdots, \mathbf{y}_k\}$). As presented earlier, the estimator that minimizes the mean-square error evaluates the condition mean of the pdf of $\boldsymbol{\theta}_k$ given $\left(\mathbf{Y}_1^k, \mathbf{U}_0^{k-1}\right)$. Except in very particular cases, the computation of the conditional mean requires the knowledge of the entire conditional pdf. One of these particular cases is the one in which the system dynamics is linear, the initial conditional is a Gaussian random vector and system and measurement noises are mutually independent white Gaussian processes with zero mean. As a consequence, the conditional probability density functions $p\left(\boldsymbol{\theta}_k \mid \mathbf{Y}_1^k, \mathbf{U}_0^{k-1}\right)$, $p\left(\boldsymbol{\theta}_{k+1} \mid \mathbf{Y}_1^k, \mathbf{U}_0^k\right)$ and $p\left(\boldsymbol{\theta}_{k+1} \mid \mathbf{Y}_1^{k+1}, \mathbf{U}_0^k\right)$ are Gaussian.

With the non linear dynamics Eq. 3.1, these probability density functions are non Gaussian. To evaluate their first and second moments, the optimal non-linear filter has to propagate the entire pdf which, in the general case, represents a heavy computational burden. The Extended Kalman filter gives an approximation of the optimal estimate. With reference to Fig. 2.2, the prediction and filtering cycles follow.

Prediction

Assume that an estimate $\hat{\boldsymbol{\theta}}_{k|k} = E\left[\boldsymbol{\theta}_k \mid \mathbf{Y}_1^k, \mathbf{U}_0^{k-1}\right]$ and associate covariance $\mathbf{P}_{k|k}$ are given. The predictable part of $\boldsymbol{\theta}_{k+1}$ is given by

$$\begin{aligned}\hat{\boldsymbol{\theta}}_{k+1|k} &= E\left[\boldsymbol{\theta}_{k+1} \mid \mathbf{Y}_1^k, \mathbf{U}_0^k\right] \\ &= E\left[\mathbf{f}_k\left(\boldsymbol{\theta}_k, \mathbf{u}_k\right) + \mathbf{w}_k \mid \mathbf{Y}_1^k, \mathbf{U}_0^k\right] \\ &= E\left[\mathbf{f}_k\left(\boldsymbol{\theta}_k, \mathbf{u}_k\right) \mid \mathbf{Y}_1^k, \mathbf{U}_0^k\right]\end{aligned}$$

Expanding $\mathbf{f}_k(\cdot)$ around the optimal estimate $\hat{\boldsymbol{\theta}}_{k|k}$, one has

$$\mathbf{f}_k\left(\boldsymbol{\theta}_k, \mathbf{u}_k\right) \approx \mathbf{f}_k\left(\hat{\boldsymbol{\theta}}_{k|k}, \mathbf{u}_k\right) + \mathbf{F}_k \cdot \left(\boldsymbol{\theta}_k - \hat{\boldsymbol{\theta}}_{k|k}\right)$$

where the jacobian $\mathbf{F}_k$ is defined as

$$\mathbf{F}_k = \left.\frac{\partial \mathbf{f}_k}{\partial \boldsymbol{\theta}}\right|_{\left(\hat{\boldsymbol{\theta}}_{k|k}, \mathbf{u}_k\right)} = \left[\begin{array}{cccc} \frac{\partial f_{1_k}}{\partial \theta_1} & \frac{\partial f_{1_k}}{\partial \theta_2} & \cdots & \frac{\partial f_{1_k}}{\partial \theta_n} \\ \frac{\partial f_{2_k}}{\partial \theta_1} & \frac{\partial f_{2_k}}{\partial \theta_2} & \cdots & \frac{\partial f_{2_k}}{\partial \theta_n} \\ \vdots & \vdots & \cdots & \vdots \\ \frac{\partial f_{n_k}}{\partial \theta_1} & \frac{\partial f_{n_k}}{\partial \theta_2} & \cdots & \frac{\partial f_{n_k}}{\partial \theta_n} \end{array}\right]_{\left|_{\left(\hat{\boldsymbol{\theta}}_{k|k}, \mathbf{u}_k\right)}\right.}, \quad \mathbf{f}_k = \left[\begin{array}{c} f_{1_k} \\ f_{2_k} \\ \vdots \\ f_{n_k} \end{array}\right]$$

Hence,

$$\begin{aligned}\hat{\boldsymbol{\theta}}_{k+1|k} &= E\left[\mathbf{f}_k\left(\boldsymbol{\theta}_k, \mathbf{u}_k\right) \mid \mathbf{Y}_1^k, \mathbf{U}_0^k\right] \\ &\approx E\left[\mathbf{f}_k\left(\hat{\boldsymbol{\theta}}_{k|k}, \mathbf{u}_k\right) + \mathbf{F}_k \cdot \left(\boldsymbol{\theta}_k - \hat{\boldsymbol{\theta}}_{k|k}\right) \mid \mathbf{Y}_1^k, \mathbf{U}_0^k\right] \\ &= \mathbf{f}_k\left(\hat{\boldsymbol{\theta}}_{k|k}, \mathbf{u}_k\right) + \mathbf{F}_k E\left[\boldsymbol{\theta}_k - \hat{\boldsymbol{\theta}}_{k|k} \mid \mathbf{Y}_1^k, \mathbf{U}_0^k\right] \\ &= \mathbf{f}_k\left(\hat{\boldsymbol{\theta}}_{k|k}, \mathbf{u}_k\right)\end{aligned}$$

Thus, the predicted value of $\boldsymbol{\theta}_{k+1}$ is

$$\hat{\boldsymbol{\theta}}_{k+1|k} \approx \mathbf{f}_k\left(\hat{\boldsymbol{\theta}}_{k|k}, \mathbf{u}_k\right) \tag{3.2}$$

The prediction error equation results

$$\begin{aligned}\tilde{\boldsymbol{\theta}}_{k+1|k} &= \boldsymbol{\theta}_{k+1} - \hat{\boldsymbol{\theta}}_{k+1|k} \\ &\approx \mathbf{f}_k\left(\boldsymbol{\theta}_k, \mathbf{u}_k\right) + \mathbf{w}_k - \mathbf{f}_k\left(\hat{\boldsymbol{\theta}}_{k|k}, \mathbf{u}_k\right) \\ &\approx \mathbf{F}_k \cdot \left(\boldsymbol{\theta}_k - \hat{\boldsymbol{\theta}}_{k|k}\right) + \mathbf{w}_k\end{aligned}$$

The forecast error covariance is

$$\begin{aligned}\mathbf{P}_{k+1|k} &= E\left[\tilde{\boldsymbol{\theta}}_{k+1|k}\tilde{\boldsymbol{\theta}}_{k+1|k}^T \mid \mathbf{Y}_1^k, \mathbf{U}_0^k\right] \\ &\approx E\left[\left(\mathbf{F}_k\tilde{\boldsymbol{\theta}}_{k|k} + \mathbf{w}_k\right)\left(\mathbf{F}_k\tilde{\boldsymbol{\theta}}_{k|k} + \mathbf{w}_k\right)^T \mid \mathbf{Y}_1^k, \mathbf{U}_0^k\right] \\ &= \mathbf{F}_k\mathbf{P}_{k|k}\mathbf{F}_k^T + \mathbf{Q}_k\end{aligned} \tag{3.3}$$

Filtering

At time $k+1$ two pieces of information are present: the forecast value $\hat{\boldsymbol{\theta}}_{k+1|k}$ with the covariance $\mathbf{P}_{k+1|k}$ and the measurement $\mathbf{y}_{k+1}$ with the covariance $\mathbf{R}_{k+1}$. The goal is to approximate the best unbiased estimate, in the least squares sense, $\hat{\boldsymbol{\theta}}_{k+1|k+1}$ of $\boldsymbol{\theta}_{k+1}$. One way is to assume that the estimate is a linear combination of both $\hat{\boldsymbol{\theta}}_{k+1|k}$ and $\mathbf{y}_{k+1}$.

$$\hat{\boldsymbol{\theta}}_{k+1|k+1} = \boldsymbol{\delta} + \mathbf{K}_{k+1}\mathbf{y}_{k+1} \tag{3.4}$$

From the unbiasedness condition

$$\begin{aligned}\mathbf{0} &= E\left[\boldsymbol{\theta}_{k+1} - \hat{\boldsymbol{\theta}}_{k+1|k+1} \mid \mathbf{Y}_1^{k+1}, \mathbf{U}_0^k\right] \\ &= E\left[\left(\tilde{\boldsymbol{\theta}}_{k+1|k} + \hat{\boldsymbol{\theta}}_{k+1|k}\right) - \left(\boldsymbol{\delta} + \mathbf{K}_{k+1}\boldsymbol{\phi}_{k+1}\left(\boldsymbol{\theta}_{k+1}\right) + \mathbf{K}_{k+1}\mathbf{v}_{k+1}\right) \mid \mathbf{Y}_1^{k+1}, \mathbf{U}_0^k\right] \\ &= \hat{\boldsymbol{\theta}}_{k+1|k} - \boldsymbol{\delta} - \mathbf{K}_{k+1}E\left[\boldsymbol{\phi}_{k+1}\left(\boldsymbol{\theta}_{k+1}\right) \mid \mathbf{Y}_1^{k+1}, \mathbf{U}_0^k\right]\end{aligned}$$

Therefore,

$$\boldsymbol{\delta} = \hat{\boldsymbol{\theta}}_{k+1|k} - \mathbf{K}_{k+1}E\left[\boldsymbol{\phi}_{k+1}\left(\boldsymbol{\theta}_{k+1}\right) \mid \mathbf{Y}_1^{k+1}, \mathbf{U}_0^k\right] \tag{3.5}$$

Substituting Eq. 3.5 in Eq. 3.4, it holds that

$$\hat{\boldsymbol{\theta}}_{k+1|k+1} = \hat{\boldsymbol{\theta}}_{k+1|k} + \mathbf{K}_{k+1}\left(\mathbf{y}_{k+1} - E\left[\boldsymbol{\phi}_{k+1}\left(\boldsymbol{\theta}_{k+1}\right) \mid \mathbf{Y}_1^{k+1}, \mathbf{U}_0^k\right]\right)$$

The same reasoning as in the prediction step can be applied. Performing the Taylor expansion of $\boldsymbol{\phi}_{k+1}(\cdot)$ about $\hat{\boldsymbol{\theta}}_{k+1|k}$, one obtains

$$\boldsymbol{\phi}_{k+1}(\boldsymbol{\theta}_{k+1}) \approx \boldsymbol{\phi}_{k+1}\left(\hat{\boldsymbol{\theta}}_{k+1|k}\right) + \boldsymbol{\Phi}_{k+1} \cdot \left(\boldsymbol{\theta}_{k+1} - \hat{\boldsymbol{\theta}}_{k+1|k}\right)$$

where the jacobian $\boldsymbol{\Phi}_{k+1}$ is defined as

$$\boldsymbol{\Phi}_{k+1} = \left.\frac{\partial \boldsymbol{\phi}_{k+1}}{\partial \boldsymbol{\theta}}\right|_{\hat{\boldsymbol{\theta}}_{k+1|k}} = \left[\begin{array}{cccc} \frac{\partial \phi_{1_{k+1}}}{\partial \theta_1} & \frac{\partial \phi_{1_{k+1}}}{\partial \theta_2} & \cdots & \frac{\partial \phi_{1_{k+1}}}{\partial \theta_n} \\ \frac{\partial \phi_{2_{k+1}}}{\partial \theta_1} & \frac{\partial \phi_{2_{k+1}}}{\partial \theta_2} & \cdots & \frac{\partial \phi_{2_{k+1}}}{\partial \theta_n} \\ \vdots & \vdots & \cdots & \vdots \\ \frac{\partial \phi_{m_{k+1}}}{\partial \theta_1} & \frac{\partial \phi_{m_{k+1}}}{\partial \theta_2} & \cdots & \frac{\partial \phi_{m_{k+1}}}{\partial \theta_n} \end{array}\right]_{|_{\hat{\boldsymbol{\theta}}_{k+1|k}}}, \quad \boldsymbol{\phi}_{k+1} = \left[\begin{array}{c} \phi_{1_{k+1}} \\ \phi_{2_{k+1}} \\ \vdots \\ \phi_{m_{k+1}} \end{array}\right]$$

Thus,

$$\begin{aligned} E\left[\boldsymbol{\phi}_{k+1}(\boldsymbol{\theta}_{k+1}) \mid \mathbf{Y}_1^{k+1}, \mathbf{U}_0^k\right] &\approx E\left[\boldsymbol{\phi}_{k+1}\left(\hat{\boldsymbol{\theta}}_{k+1|k}\right) + \boldsymbol{\Phi}_{k+1} \cdot \left(\boldsymbol{\theta}_{k+1} - \hat{\boldsymbol{\theta}}_{k+1|k}\right) \mid \mathbf{Y}_1^{k+1}, \mathbf{U}_0^k\right] \\ &= \boldsymbol{\phi}_{k+1}\left(\hat{\boldsymbol{\theta}}_{k+1|k}\right) \end{aligned}$$

Therefore, the filtered estimate is given by

$$\hat{\boldsymbol{\theta}}_{k+1|k+1} \approx \hat{\boldsymbol{\theta}}_{k+1|k} + \mathbf{K}_{k+1} \cdot \left[\mathbf{y}_{k+1} - \boldsymbol{\phi}_{k+1}\left(\hat{\boldsymbol{\theta}}_{k+1|k}\right)\right] \tag{3.6}$$

The error in the estimate $\hat{\boldsymbol{\theta}}_{k+1|k+1}$ is

$$\begin{aligned} \tilde{\boldsymbol{\theta}}_{k+1|k+1} &= \boldsymbol{\theta}_{k+1} - \hat{\boldsymbol{\theta}}_{k+1|k+1} \\ &\approx \mathbf{f}_k(\boldsymbol{\theta}_k, \mathbf{u}_k) + \mathbf{w}_k - \hat{\boldsymbol{\theta}}_{k+1|k} - \mathbf{K}_{k+1} \cdot \left[\mathbf{y}_{k+1} - \boldsymbol{\phi}_{k+1}\left(\hat{\boldsymbol{\theta}}_{k+1|k}\right)\right] \\ &\approx \mathbf{f}_k(\boldsymbol{\theta}_k, \mathbf{u}_k) - \mathbf{f}_k\left(\hat{\boldsymbol{\theta}}_{k|k}, \mathbf{u}_k\right) + \mathbf{w}_k - \mathbf{K}_{k+1} \cdot \left[\boldsymbol{\phi}_{k+1}(\boldsymbol{\theta}_{k+1}) + \mathbf{v}_{k+1} - \boldsymbol{\phi}_{k+1}\left(\hat{\boldsymbol{\theta}}_{k+1|k}\right)\right] \\ &\approx \mathbf{F}_k \tilde{\boldsymbol{\theta}}_{k|k} + \mathbf{w}_k - \mathbf{K}_{k+1}\left(\boldsymbol{\Phi}_{k+1} \tilde{\boldsymbol{\theta}}_{k+1|k} + \mathbf{v}_{k+1}\right) \\ &\approx \mathbf{F}_k \tilde{\boldsymbol{\theta}}_{k|k} + \mathbf{w}_k - \mathbf{K}_{k+1} \boldsymbol{\Phi}_{k+1}\left(\mathbf{F}_k \tilde{\boldsymbol{\theta}}_{k|k} + \mathbf{w}_k\right) - \mathbf{K}_{k+1} \mathbf{v}_{k+1} \\ &= \left(\mathbf{I} - \mathbf{K}_{k+1} \boldsymbol{\Phi}_{k+1}\right) \mathbf{F}_k \tilde{\boldsymbol{\theta}}_{k|k} + \left(\mathbf{I} - \mathbf{K}_{k+1} \boldsymbol{\Phi}_{k+1}\right) \mathbf{w}_k - \mathbf{K}_{k+1} \mathbf{v}_{k+1} \end{aligned}$$

The posterior covariance of the new estimate is

$$\begin{aligned}\mathbf{P}_{k+1|k+1} &= E\left[\tilde{\boldsymbol{\theta}}_{k+1|k+1}\tilde{\boldsymbol{\theta}}^T_{k+1|k+1} \mid \mathbf{Y}_1^{k+1}, \mathbf{U}_0^k\right] \\ &\approx \left(\mathbf{I} - \mathbf{K}_{k+1}\boldsymbol{\Phi}_{k+1}\right)\mathbf{F}_k\mathbf{P}_{k|k}\mathbf{F}_k^T\left(\mathbf{I} - \mathbf{K}_{k+1}\boldsymbol{\Phi}_{k+1}\right)^T + \\ &\quad \left(\mathbf{I} - \mathbf{K}_{k+1}\boldsymbol{\Phi}_{k+1}\right)\mathbf{Q}_k\left(\mathbf{I} - \mathbf{K}_{k+1}\boldsymbol{\Phi}_{k+1}\right)^T + \mathbf{K}_{k+1}\mathbf{R}_{k+1}\mathbf{K}_{k+1}^T \\ &\approx \left(\mathbf{I} - \mathbf{K}_{k+1}\boldsymbol{\Phi}_{k+1}\right)\mathbf{P}_{k+1|k}\left(\mathbf{I} - \mathbf{K}_{k+1}\boldsymbol{\Phi}_{k+1}\right)^T + \mathbf{K}_{k+1}\mathbf{R}_{k+1}\mathbf{K}_{k+1}^T \end{aligned} \tag{3.7}$$

Like in the standard Kalman Filter $\mathbf{K}_{k+1}$ is found out by minimizing $\text{tr}\left(\mathbf{P}_{k+1|k+1}\right)$ with respect to $\mathbf{K}_{k+1}$. Hence, the Kalman gain is

$$\mathbf{K}_{k+1} = \mathbf{P}_{k+1|k}\boldsymbol{\Phi}_{k+1}^T\left(\boldsymbol{\Phi}_{k+1}\mathbf{P}_{k+1|k}\boldsymbol{\Phi}_{k+1}^T + \mathbf{R}_{k+1}\right)^{-1}$$

The expressions for $\hat{\boldsymbol{\theta}}_{k+1|k+1}$, $\hat{\boldsymbol{\theta}}_{k+1|k}$, $\mathbf{P}_{k+1|k+1}$, $\mathbf{P}_{k+1|k}$ are reported again below.

Prediction

$$\hat{\boldsymbol{\theta}}_{k+1|k} \approx \mathbf{f}_k\left(\hat{\boldsymbol{\theta}}_{k|k}, \mathbf{u}_k\right)$$

$$\mathbf{P}_{k+1|k} \approx \mathbf{F}_k\mathbf{P}_{k|k}\mathbf{F}_k^T + \mathbf{Q}_k$$

Filtering

$$\mathbf{K}_{k+1} = \begin{cases} \mathbf{P}_{k+1|k}\boldsymbol{\Phi}_{k+1}^T\left(\boldsymbol{\Phi}_{k+1}\mathbf{P}_{k+1|k}\boldsymbol{\Phi}_{k+1}^T + \mathbf{R}_{k+1}\right)^{-1} \\ \mathbf{P}_{k+1|k+1}\boldsymbol{\Phi}_{k+1}^T\mathbf{R}_{k+1}^{-1} \end{cases}$$

$$\mathbf{P}_{k+1|k+1} \approx \begin{cases} \left(\mathbf{I} - \mathbf{K}_{k+1}\boldsymbol{\Phi}_{k+1}\right)\mathbf{P}_{k+1|k}\left(\mathbf{I} - \mathbf{K}_{k+1}\boldsymbol{\Phi}_{k+1}\right)^T + \mathbf{K}_{k+1}\mathbf{R}_{k+1}\mathbf{K}_{k+1}^T \\ \left(\mathbf{I} - \mathbf{K}_{k+1}\boldsymbol{\Phi}_{k+1}\right)\mathbf{P}_{k+1|k} \\ \left(\mathbf{P}_{k+1|k}^{-1} + \boldsymbol{\Phi}_{k+1}^T\mathbf{R}_{k+1}^{-1}\boldsymbol{\Phi}_{k+1}\right)^{-1} \end{cases}$$

$$\hat{\boldsymbol{\theta}}_{k+1|k+1} \approx \hat{\boldsymbol{\theta}}_{k+1|k} + \mathbf{K}_{k+1}\cdot\left[\mathbf{y}_{k+1} - \boldsymbol{\phi}_{k+1}\left(\hat{\boldsymbol{\theta}}_{k+1|k}\right)\right]$$

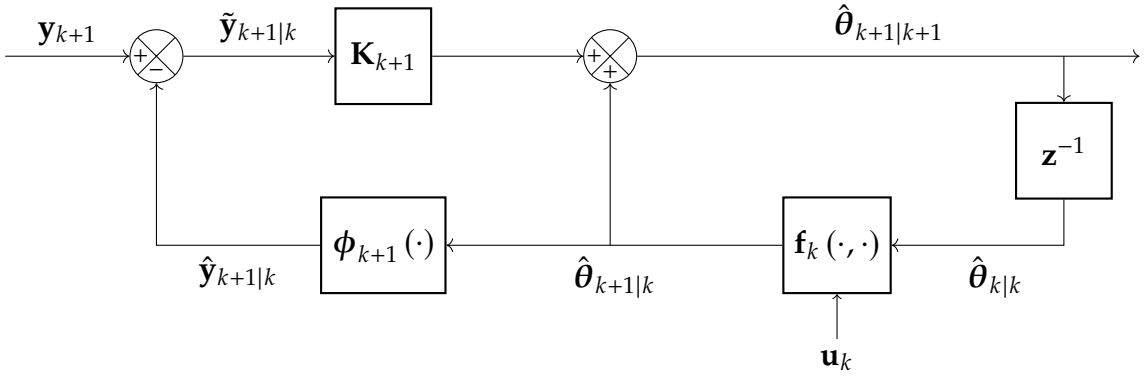

Figure 3.1: Extended Kalman filter block diagram

EKF algorithm

Algorithm 2 EKF algorithm

System:

$$\begin{cases} \boldsymbol{\theta}_{k+1} = \mathbf{f}_k\left(\boldsymbol{\theta}_k, \mathbf{u}_k\right) + \mathbf{w}_k \\ \mathbf{y}_{k+1} = \boldsymbol{\phi}_{k+1}\left(\boldsymbol{\theta}_{k+1}\right) + \mathbf{v}_{k+1} \end{cases} \text{, where } \begin{cases} E\left[\mathbf{w}_k \mathbf{w}_j^T\right] = \mathbf{Q}_k \delta_{k-j} \\ E\left[\mathbf{v}_k \mathbf{v}_j^T\right] = \mathbf{R}_k \delta_{k-j} \\ E\left[\mathbf{v}_k \mathbf{w}_j^T\right] = 0 \end{cases}$$

Initialize:

$\hat{\boldsymbol{\theta}}_{0|0} = E[\boldsymbol{\theta}_0]$

$\mathbf{P}_{0|0} = E\left[\left(\boldsymbol{\theta}_0 - \hat{\boldsymbol{\theta}}_{0|0}\right)\left(\boldsymbol{\theta}_0 - \hat{\boldsymbol{\theta}}_{0|0}\right)^T\right]$

for $k = 0, 1, \cdots$ **do**

Prediction

$$\begin{cases} \mathbf{F}_k \leftarrow \left.\frac{\partial \mathbf{f}_k}{\partial \boldsymbol{\theta}}\right|_{\left(\hat{\boldsymbol{\theta}}_{k|k}, \mathbf{u}_k\right)} \\ \hat{\boldsymbol{\theta}}_{k+1|k} \leftarrow \mathbf{f}_k\left(\hat{\boldsymbol{\theta}}_{k|k}, \mathbf{u}_k\right) \\ \mathbf{P}_{k+1|k} \leftarrow \mathbf{F}_k \mathbf{P}_{k|k} \mathbf{F}_k^T + \mathbf{Q}_k \end{cases}$$

$\mathbf{y}_{k+1} \leftarrow$ new measurement

Filtering

$$\begin{cases} \boldsymbol{\Phi}_{k+1} \leftarrow \left.\frac{\partial \boldsymbol{\phi}_{k+1}}{\partial \boldsymbol{\theta}}\right|_{\hat{\boldsymbol{\theta}}_{k+1|k}} \\ \mathbf{K}_{k+1} \leftarrow \begin{cases} \mathbf{P}_{k+1|k} \boldsymbol{\Phi}_{k+1}^T \left(\boldsymbol{\Phi}_{k+1} \mathbf{P}_{k+1|k} \boldsymbol{\Phi}_{k+1}^T + \mathbf{R}_{k+1}\right)^{-1} \\ \mathbf{P}_{k+1|k+1} \boldsymbol{\Phi}_{k+1}^T \mathbf{R}_{k+1}^{-1} \end{cases} \\ \mathbf{P}_{k+1|k+1} \leftarrow \begin{cases} \left(\mathbf{I} - \mathbf{K}_{k+1} \boldsymbol{\Phi}_{k+1}\right) \mathbf{P}_{k+1|k} \left(\mathbf{I} - \mathbf{K}_{k+1} \boldsymbol{\Phi}_{k+1}\right)^T + \mathbf{K}_{k+1} \mathbf{R}_{k+1} \mathbf{K}_{k+1}{}^T \\ \left(\mathbf{I} - \mathbf{K}_{k+1} \boldsymbol{\Phi}_{k+1}\right) \mathbf{P}_{k+1|k} \\ \left(\mathbf{P}_{k+1|k}^{-1} + \boldsymbol{\Phi}_{k+1}^T \mathbf{R}_{k+1}^{-1} \boldsymbol{\Phi}_{k+1}\right)^{-1} \end{cases} \\ \hat{\boldsymbol{\theta}}_{k+1|k+1} \leftarrow \hat{\boldsymbol{\theta}}_{k+1|k} + \mathbf{K}_{k+1} \cdot \left[\mathbf{y}_{k+1} - \boldsymbol{\phi}_{k+1}\left(\hat{\boldsymbol{\theta}}_{k+1|k}\right)\right] \end{cases}$$

end for

4

Human arm model

The human arm is modeled as a 7 DoF RM. As it is well known, a manipulator can be represented from a mechanical viewpoint as a kinematic chain of rigid bodies, known as *links*, connected by means of *revolute* or *prismatic* joints. In this framework, the 7 joint variables of the RM modeling the human arm are all *revolute*. Indeed, it can be thought as 3 *links* representing the shoulder, the forearm and the hand. At the base of each *link* the joint is placed. Specifically, the joint at the base of the shoulder is governed by 3 joint variables, called $\eta_1(t)$, $\eta_2(t)$ and $\eta_3(t)$; the joint at the base of the forearm is associated with 1 joint variable $\eta_4(t)$ while $\eta_5(t)$, $\eta_6(t)$ and $\eta_7(t)$ are placed at the base of the hand. One may be interested at the position of one object placed in the hand. This can be expressed as a function of the joint variables of the mechanical structure with respect to a reference frame. The representative model of the human arm is depicted below in Fig 4.1, where the *World* RF, RF_W, is considered fixed at the base of the shoulder link, therefore it never moves. In the figure, the joint variables are omitted for simplicity and they are discussed in the following.

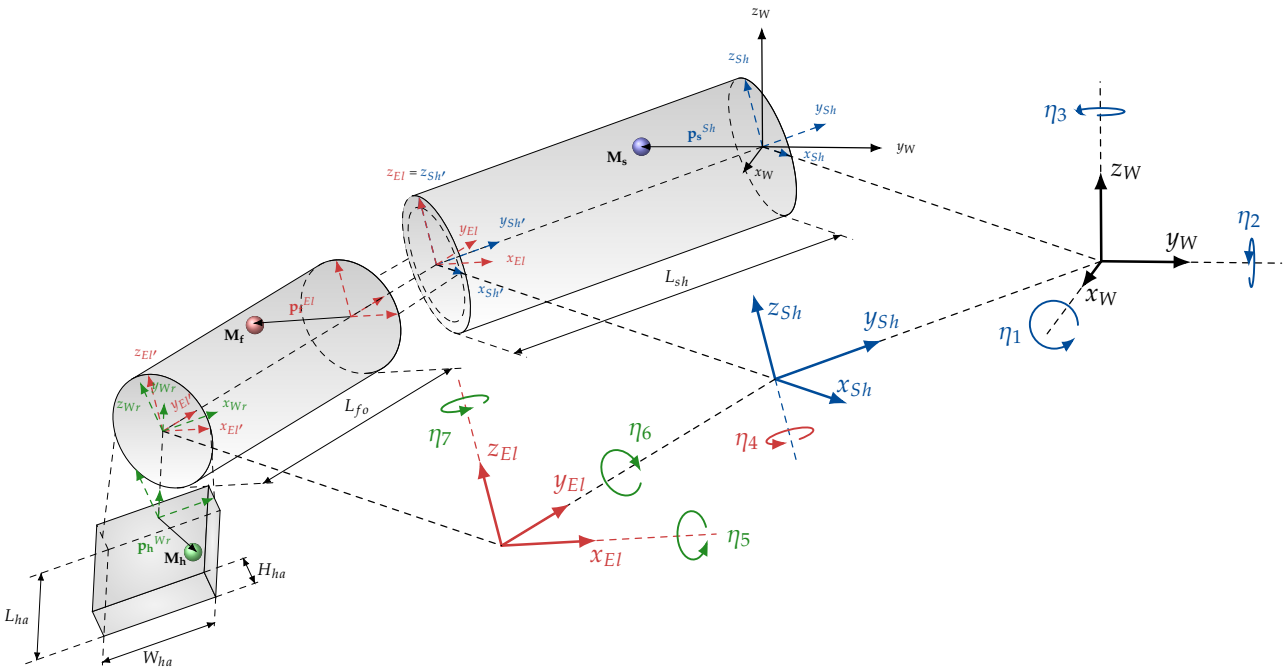

Figure 4.1: Human arm model representation

At the base of each link, a specific reference frame is attached which determines the orientation of the following links. For instance, the reference frame at the base of the shoulder, denoted as RF_{Sh} with axes $\{x_{Sh}, y_{Sh}, z_{Sh}\}$, represents the rotation of the shoulder wrt RF_W.

In the following, by *convention*, all rotations are assumed positive if they are performed counter-clockwise and each component of $\boldsymbol{\eta}$ performs a rotation around the z-axis of the corresponding frame. On the arm, some markers are attached. Specifically, let

$$\begin{aligned}
\mathcal{S} &= \{1, 2, \ldots, |\mathcal{S}|\} \\
\mathcal{F} &= \{|\mathcal{S}| + 1, |\mathcal{S}| + 2, \ldots, |\mathcal{S}| + |\mathcal{F}|\} \\
\mathcal{H} &= \{|\mathcal{S}| + |\mathcal{F}| + 1, |\mathcal{S}| + |\mathcal{F}| + 2, \ldots, |\mathcal{S}| + |\mathcal{F}| + |\mathcal{H}|\}
\end{aligned}$$

be the set of indices such that

- $|\mathcal{S}|$ is the number of markers placed on the shoulder.
- $|\mathcal{F}|$ is the number of markers placed on the forearm.
- $|\mathcal{H}|$ is the number of markers placed on the hand.

Thus,

- $\mathbf{M_s}$, $s \in \mathcal{S}$, is a marker placed on the shoulder.
- $\mathbf{M_f}$, $f \in \mathcal{F}$, is a marker placed on the forearm.
- $\mathbf{M_h}$, $h \in \mathcal{H}$, is a marker placed on the hand.

The aim of this section is twofold:

i compute the *forward kinematics* equations for each marker, namely express the position of each marker in terms of RF_W coordinates and $\boldsymbol{\eta}$.

ii compute the *differential kinematics* equations for each marker, hence find the relationship between the joint velocities and the corresponding markers' linear velocity.

4.1 Forward kinematics

Let $m = |\mathcal{S}| + |\mathcal{F}| + |\mathcal{H}|$ be the total number of markers placed on the human arm and $\mathbf{p_i}^W$ a generic marker $\mathbf{M_i}$ express wrt RF_W. With the slightly change of notation $\mathbf{p_i} = \mathbf{p_i}^W$, one has

$$\mathbf{p_i} = \mathbf{\Phi_i} = \begin{cases} \mathbf{\Phi}_{Sh}\left(\boldsymbol{\eta}_{1-3}, \mathbf{p_i}^{Sh}\right), & i \in \mathcal{S} \\ \mathbf{\Phi}_{Fo}\left(\boldsymbol{\eta}_{1-4}, \mathbf{p_i}^{El}\right), & i \in \mathcal{F} \\ \mathbf{\Phi}_{Ha}\left(\boldsymbol{\eta}, \mathbf{p_i}^{Wr}\right), & i \in \mathcal{H} \end{cases}, \quad \mathbf{p_i}^B = \begin{cases} \mathbf{p_i}^{Sh}, & i \in \mathcal{S} \\ \mathbf{p_i}^{El}, & i \in \mathcal{F} \\ \mathbf{p_i}^{Wr}, & i \in \mathcal{H} \end{cases} \qquad i = 1, \dots, m$$

Hence

$$\mathbf{p} = \begin{bmatrix} \mathbf{p_1} \\ \vdots \\ \mathbf{p_m} \end{bmatrix} = \begin{bmatrix} \mathbf{\Phi_1} \\ \vdots \\ \mathbf{\Phi_m} \end{bmatrix} = \mathbf{\Phi}\left(\boldsymbol{\eta}, \mathbf{p}^B\right), \quad \mathbf{p}^B = \begin{bmatrix} \mathbf{p_1}^B \\ \vdots \\ \mathbf{p_m}^B \end{bmatrix} \tag{4.1}$$

Before proceeding, it is important to remark that, given a generic Reference Frame (RF) O with axes $\{x, y, z\}$, if it is rotated by an angle α about axis z, obtaining the frame O' with axes $\{x', y', z'\}$, then the rotation matrix of frame O' with respect to frame O is given by:

$$\mathbf{R}_z(\alpha) = \begin{bmatrix} \cos(\alpha) & -\sin(\alpha) & 0 \\ \sin(\alpha) & \cos(\alpha) & 0 \\ 0 & 0 & 1 \end{bmatrix} = \begin{bmatrix} c_\alpha & -s_\alpha & 0 \\ s_\alpha & c_\alpha & 0 \\ 0 & 0 & 1 \end{bmatrix}$$

In a similar manner, it can be shown that the rotations by an angle β about axis y and by an angle γ about axis x are respectively given by

$$\mathbf{R}_y(\beta) = \begin{bmatrix} \cos(\beta) & 0 & \sin(\beta) \\ 0 & 1 & 0 \\ -\sin(\beta) & 0 & \cos(\beta) \end{bmatrix} = \begin{bmatrix} c_\beta & 0 & s_\beta \\ 0 & 1 & 0 \\ -s_\beta & 0 & c_\beta \end{bmatrix}$$

$$\mathbf{R}_x(\gamma) = \begin{bmatrix} 1 & 0 & 0 \\ 0 & \cos(\gamma) & -\sin(\gamma) \\ 0 & \sin(\gamma) & \cos(\gamma) \end{bmatrix} = \begin{bmatrix} 1 & 0 & 0 \\ 0 & c_\gamma & -s_\gamma \\ 0 & s_\gamma & c_\gamma \end{bmatrix}$$

In the following, depending on where the marker is placed, the corresponding FK is obtained.

4.1.1 Shoulder forward kinematics

Let $\mathbf{M_s}$, $s \in \mathcal{S}$, be a generic marker attached on the shoulder with coordinates ${\mathbf{p_s}}^{Sh} = \left(\mathbf{p_s}_x^{Sh}, \mathbf{p_s}_y^{Sh}, \mathbf{p_s}_z^{Sh}\right) \in \mathbb{R}^3$, expressed in terms of RF_{Sh}. The same marker can also be expressed wrt RF_W, obtaining ${\mathbf{p_{M_s}}}^{W}$. Since the origins of the two reference frames coincide, it follows

$${\mathbf{p_s}}^{W}(\eta_1, \eta_2, \eta_3) = \mathbf{R}_{Sh}^{W}(\eta_1, \eta_2, \eta_3)\, {\mathbf{p_s}}^{Sh}$$

where $\mathbf{R}_{Sh}^{W}$ represents the *transformation matrix* of the vector coordinates in frame RF_{Sh} into the coordinates of the same vector in frame RF_W, namely the rotation matrix of frame RF_{Sh} wrt frame RF_W and it depends on η_1, η_2 and η_3.
In order to obtain RF_{Sh}, the following rotations are performed consecutively.

Rotation by η_1

Observe Fig. 4.2a below. RF_W, as already mentioned, is a fixed RF. Specifically, η_1 represents the rotation around x_W, the x-axis of RF_W. However, because of the aforementioned *convention*, $RF_{W'} = \{x_{W'}, y_{W'}, z_{W'}\}$ is derived where $z_{W'} = x_W$, $x_{W'} = y_W$ and the frame is right-handed and it is achieved by firstly rotating RF_W by an angle of $\frac{\pi}{2}$ about z_W and secondly rotating the current frame by $\frac{\pi}{2}$ about x_W. Since composition of successive rotations is obtained by post-multiplication of the rotation matrices following the given order of rotations, it

follows that the rotation of frame $RF_{W'}$ wrt RF_W is given by

$$\mathbf{R}_{W'}^{W} = \mathbf{R}_z\left(\frac{\pi}{2}\right)\mathbf{R}_x\left(\frac{\pi}{2}\right) = \begin{bmatrix} 0 & 0 & 1 \\ 1 & 0 & 0 \\ 0 & 1 & 0 \end{bmatrix}$$

At this point, let RF_{η_1} the resulting reference frame after that the rotation by η_1 is performed about axes $z_{W'}$. Hence, the rotation of frame RF_{η_1} wrt RF_W is given by

$$\mathbf{R}_{\eta_1}^{W}(\eta_1) = \mathbf{R}_{W'}^{W}\mathbf{R}_z(\eta_1) = \begin{bmatrix} 0 & 0 & 1 \\ c_{\eta_1} & -s_{\eta_1} & 0 \\ s_{\eta_1} & c_{\eta_1} & 0 \end{bmatrix}$$

Rotation by η_2

By applying the same reasoning as before, the rotation of frame $RF_{\eta_1'}$ wrt RF_{η_1} is given by

$$\mathbf{R}_{\eta_1'}^{\eta_1} = \mathbf{R}_y\left(\frac{\pi}{2}\right)\mathbf{R}_z\left(\frac{\pi}{2}\right) = \begin{bmatrix} 0 & 0 & 1 \\ 1 & 0 & 0 \\ 0 & 1 & 0 \end{bmatrix}$$

Let RF_{η_2} the resulting reference frame after that the rotation by η_2 is performed about axes $z_{\eta_1'}$. Hence, the rotation of frame RF_{η_2} wrt RF_{η_1} is given by

$$\mathbf{R}_{\eta_2}^{\eta_1}(\eta_2) = \mathbf{R}_{\eta_1'}^{\eta_1}\mathbf{R}_z(\eta_2) = \begin{bmatrix} 0 & 0 & 1 \\ c_{\eta_2} & -s_{\eta_2} & 0 \\ s_{\eta_2} & c_{\eta_2} & 0 \end{bmatrix}$$

Rotation by η_3

With reference to Fig. 4.2c, in order to align frame RF_{η_2} to $RF_{\eta_2'}$ the following rotation matrix has to be applied

$$\mathbf{R}_{\eta_2'}^{\eta_2} = \mathbf{R}_y\left(\frac{\pi}{2}\right)\mathbf{R}_z\left(\frac{\pi}{2}\right) = \begin{bmatrix} 0 & 0 & 1 \\ 1 & 0 & 0 \\ 0 & 1 & 0 \end{bmatrix}$$

Let RF_{Sh} the resulting reference frame after that the rotation by η_3 is performed about axes $z_{\eta_2'}$. Hence, the rotation of frame RF_{Sh} wrt RF_{η_2} is given by

$$\mathbf{R}_{Sh}^{\eta_2}(\eta_3) = \mathbf{R}_{\eta_2'}^{\eta_2}\mathbf{R}_z(\eta_3) = \begin{bmatrix} 0 & 0 & 1 \\ c_{\eta_3} & -s_{\eta_3} & 0 \\ s_{\eta_3} & c_{\eta_3} & 0 \end{bmatrix}$$

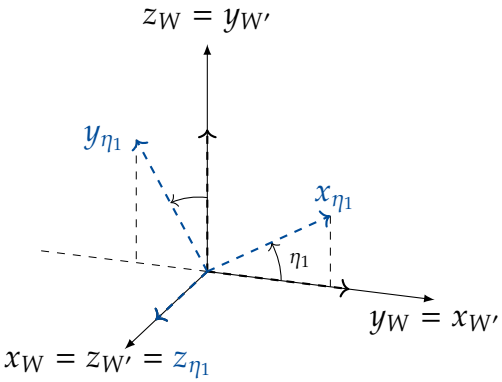

(a) Rotation by η_1 about $z_{W'}$

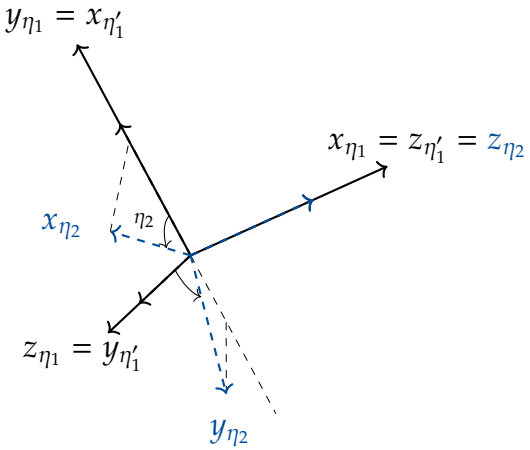

(b) Rotation by η_2 about $z_{\eta_1'}$

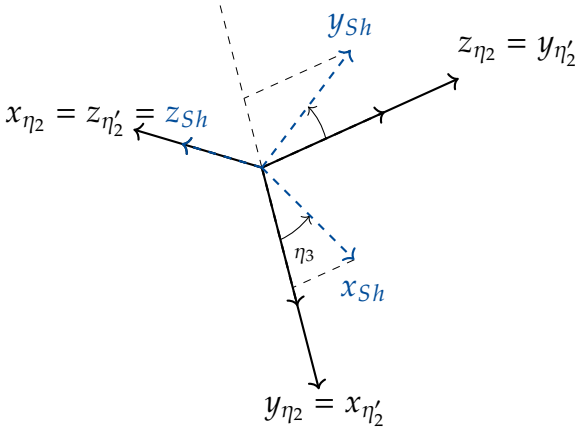

(c) Rotation by η_3 about $z_{\eta_2'}$

Figure 4.2: Shoulder rotations

At this point it is possible to compute $\mathbf{R}_{Sh}^{W}$. Since all the rotations analyzed previously are wrt the current RF, the overall rotation matrix is then obtained by post-multiplication of the rotation matrices following the order of rotations.

$$\begin{aligned}\mathbf{R}_{Sh}^{W}(\eta_1,\eta_2,\eta_3) &= \mathbf{R}_{\eta_1}^{W}(\eta_1)\,\mathbf{R}_{\eta_2}^{\eta_1}(\eta_2)\,\mathbf{R}_{Sh}^{\eta_2}(\eta_3)\\ &= \begin{bmatrix} c_{\eta_2}c_{\eta_3} & -c_{\eta_2}s_{\eta_3} & s_{\eta_2} \\ s_{\eta_1}s_{\eta_2}c_{\eta_3}+c_{\eta_1}s_{\eta_3} & -s_{\eta_1}s_{\eta_2}s_{\eta_3}+c_{\eta_1}c_{\eta_3} & -s_{\eta_1}c_{\eta_2} \\ -c_{\eta_1}s_{\eta_2}c_{\eta_3}+s_{\eta_1}s_{\eta_3} & c_{\eta_1}s_{\eta_2}s_{\eta_3}+s_{\eta_1}c_{\eta_3} & c_{\eta_1}c_{\eta_2} \end{bmatrix}\end{aligned}$$

If $\mathbf{R}_{Sh}^{W}$ is known then it is possible to express the given marker $\mathbf{M_s}$ wrt RF_W. In general, since the position of each marker placed on the shoulder only depends on the rotation of RF_{Sh} wrt RF_W, the forward kinematics of the general marker $\mathbf{M_s}$ on the shoulder is given by

$$\begin{aligned}{\mathbf{p_s}}^{W} &= \mathbf{\Phi}_{Sh}\left(\eta_1,\eta_2,\eta_3,{\mathbf{p_s}}^{Sh}\right)\\ &= \mathbf{R}_{Sh}^{W}(\eta_1,\eta_2,\eta_3)\,{\mathbf{p_s}}^{Sh}\\ &= \begin{bmatrix} \mathbf{p_s}_x^{W} \\ \mathbf{p_s}_y^{W} \\ \mathbf{p_s}_z^{W} \end{bmatrix}\end{aligned} \tag{4.2}$$

with

$$\begin{aligned}\mathbf{p_s}_x^{W} &= c_{\eta_2}c_{\eta_3}\mathbf{p_s}_x^{Sh} - c_{\eta_2}s_{\eta_3}\mathbf{p_s}_y^{Sh} + s_{\eta_2}\mathbf{p_s}_z^{Sh}\\ \mathbf{p_s}_y^{W} &= \left(s_{\eta_1}s_{\eta_2}c_{\eta_3}+c_{\eta_1}s_{\eta_3}\right)\mathbf{p_s}_x^{Sh} + \left(-s_{\eta_1}s_{\eta_2}s_{\eta_3}+c_{\eta_1}c_{\eta_3}\right)\mathbf{p_s}_y^{Sh} - s_{\eta_1}c_{\eta_2}\mathbf{p_s}_z^{Sh}\\ \mathbf{p_s}_z^{W} &= \left(-c_{\eta_1}s_{\eta_2}c_{\eta_3}+s_{\eta_1}s_{\eta_3}\right)\mathbf{p_s}_x^{Sh} + \left(c_{\eta_1}s_{\eta_2}s_{\eta_3}+s_{\eta_1}c_{\eta_3}\right)\mathbf{p_s}_y^{Sh} + c_{\eta_1}c_{\eta_2}\mathbf{p_s}_z^{Sh}\end{aligned}$$

4.1.2 Forearm forward kinematics

In the case in which one marker is placed on the forearm, its position does depend also on η_4. Let $\mathbf{M_f}$ a generic marker on the forearm. The aim, as before, is to express it in terms of RF_W coordinates. Observe Fig. 4.1. First, the quantity ${\mathbf{p_f}}^{Sh}$ is computed and then the rotation matrix $\mathbf{R}_{Sh}^{W}$ is applied. Let ${\mathbf{O_{Sh'}}}^{Sh}$ be the origin of frame $RF_{Sh'}$ expressed wrt RF_{Sh}

$$\mathbf{O_{Sh'}}^{Sh} = \begin{bmatrix} 0 \\ -L_{sh} \\ 0 \end{bmatrix}$$

As before, the coordinates of $\mathbf{p_f}^{El} = \left(\mathbf{p_f}_x^{El}, \mathbf{p_f}_y^{El}, \mathbf{p_f}_z^{El}\right)$ are assumed to be known. The joint of the elbow is modeled as 1 DoF and it rotates about axis $z_{Sh'}$ by η_4.

Rotation by η_4

The orientation of frame $RF_{Sh'}$ is the same as RF_{Sh}. Let RF_{El} the resulting reference frame after that the rotation by η_4 is performed about axes $z_{Sh'}$. Hence, the rotation is simply given by

$$\mathbf{R}_{El}^{Sh'}(\eta_4) = \begin{bmatrix} c_{\eta_4} & -s_{\eta_4} & 0 \\ s_{\eta_4} & c_{\eta_4} & 0 \\ 0 & 0 & 1 \end{bmatrix}$$

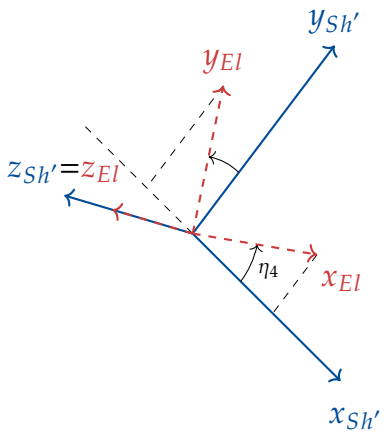

Figure 4.3: Elbow rotation

By summing the translational vector $\mathbf{O_{Sh'}}^{Sh}$ and the quantity $\mathbf{R}_{El}^{Sh'}(\eta_4)\,\mathbf{p_f}^{El}$ one obtains the position of the marker $\mathbf{M_f}$ wrt RF_{Sh}. Thus, one obtains the desired quantity if the rotation matrix $\mathbf{R}_{Sh}^{W}(\eta_1, \eta_2, \eta_3)$ is applied.

$$
\begin{aligned}
{\mathbf{p_f}}^{W} &= \mathbf{\Phi}_{Fo}\left(\eta_1, \eta_2, \eta_3, \eta_4, {\mathbf{p_f}}^{El}\right) \\
&= \mathbf{R}_{Sh}^{W}\left(\eta_1, \eta_2, \eta_3\right)\left(\mathbf{R}_{El}^{Sh'}\left(\eta_4\right){\mathbf{p_f}}^{El} + {\mathbf{O_{Sh'}}}^{Sh}\right) \\
&= \begin{bmatrix} \mathbf{p_f}_x^W \\ \mathbf{p_f}_y^W \\ \mathbf{p_f}_z^W \end{bmatrix}
\end{aligned}
\tag{4.3}
$$

with

$$
\begin{aligned}
\mathbf{p_f}_x^W =& c_{\eta_2}c_{\eta_3}\left(c_{\eta_4}\mathbf{p_f}_x^{El} - s_{\eta_4}\mathbf{p_f}_y^{El}\right) - c_{\eta_2}s_{\eta_3}\left(s_{\eta_4}\mathbf{p_f}_x^{El} + c_{\eta_4}\mathbf{p_f}_y^{El} - L_{sh}\right) + s_{\eta_2}\mathbf{p_f}_z^{El} \\
\mathbf{p_f}_y^W =& \left(s_{\eta_1}s_{\eta_2}c_{\eta_3} + c_{\eta_1}s_{\eta_3}\right)\left(c_{\eta_4}\mathbf{p_f}_x^{El} - s_{\eta_4}\mathbf{p_f}_y^{El}\right) + \left(c_{\eta_1}c_{\eta_3} - s_{\eta_1}s_{\eta_2}s_{\eta_3}\right)\left(s_{\eta_4}\mathbf{p_f}_x^{El} + \right. \\
& \left. c_{\eta_4}\mathbf{p_f}_y^{El} - L_{sh}\right) - s_{\eta_1}c_{\eta_2}\mathbf{p_f}_z^{El} \\
\mathbf{p_f}_z^W =& \left(s_{\eta_1}s_{\eta_3} - c_{\eta_1}s_{\eta_2}c_{\eta_3}\right)\left(c_{\eta_4}\mathbf{p_f}_x^{El} - s_{\eta_4}\mathbf{p_f}_y^{El}\right) + \left(c_{\eta_1}s_{\eta_2}s_{\eta_3} + s_{\eta_1}c_{\eta_3}\right)\left(s_{\eta_4}\mathbf{p_f}_x^{El} + \right. \\
& \left. c_{\eta_4}\mathbf{p_f}_y^{El} - L_{sh}\right) + c_{\eta_1}c_{\eta_2}\mathbf{p_f}_z^{El}
\end{aligned}
$$

4.1.3 Hand forward kinematics

What about ${\mathbf{p_{M_h}}}^{W}$? where $\mathbf{M_h}$ is a generic marker placed on the hand of the human arm. Following the same reasoning as before, one first computes ${\mathbf{p_h}}^{El}$; secondly, ${\mathbf{p_h}}^{Sh}$ is obtained and thereafter the rotation matrix $\mathbf{R}_{Sh}^{W}$ is applied.

$$
{\mathbf{p_h}}^{El} = \mathbf{R}_{Wr}^{El'}\left(\eta_5, \eta_6, \eta_7\right){\mathbf{p_h}}^{Wr} + {\mathbf{O_{El'}}}^{El}
$$

where

$$
{\mathbf{p_h}}^{Wr} = \left({\mathbf{p_h}_x}^{Wr}, {\mathbf{p_h}_y}^{Wr}, {\mathbf{p_h}_z}^{Wr}\right), \quad {\mathbf{O_{El'}}}^{El} = \begin{bmatrix} 0 \\ -L_{fo} \\ 0 \end{bmatrix}
$$

and $\mathbf{R}_{Wr}^{El'}\left(\eta_5, \eta_6, \eta_7\right)$ is obtained as $\mathbf{R}_{Sh}^{W}\left(\eta_1, \eta_2, \eta_3\right)$.

Rotation by η_5

Recalling Fig. 4.3, the orientation of frame RF_{El} is the same as frame $RF_{El'}$. The rotation of $RF_{El''}$ wrt $RF_{El'}$ is given by

$$\mathbf{R}_{El''}^{El'} = \mathbf{R}_z\left(\frac{\pi}{2}\right)\mathbf{R}_x\left(\frac{\pi}{2}\right) = \begin{bmatrix} 0 & 0 & 1 \\ 1 & 0 & 0 \\ 0 & 1 & 0 \end{bmatrix}$$

Let RF_{η_5} the resulting reference frame after that the rotation by η_5 is performed about axes $z_{El''}$.

$$\mathbf{R}_{\eta_5}^{El'}(\eta_5) = \mathbf{R}_{El''}^{El'}\mathbf{R}_z(\eta_5) = \begin{bmatrix} 0 & 0 & 1 \\ c_{\eta_5} & -s_{\eta_5} & 0 \\ s_{\eta_5} & c_{\eta_5} & 0 \end{bmatrix}$$

Rotation by η_6

The rotation of frame $RF_{\eta_5'}$ wrt RF_{η_5} is given by

$$\mathbf{R}_{\eta_5'}^{\eta_5} = \mathbf{R}_y\left(\frac{\pi}{2}\right)\mathbf{R}_z\left(\frac{\pi}{2}\right) = \begin{bmatrix} 0 & 0 & 1 \\ 1 & 0 & 0 \\ 0 & 1 & 0 \end{bmatrix}$$

Let RF_{η_6} the resulting reference frame after that the rotation by η_6 is performed about axes $z_{\eta_5'}$. Hence, the rotation of frame RF_{η_6} wrt RF_{η_5} is given by

$$\mathbf{R}_{\eta_6}^{\eta_5}(\eta_6) = \mathbf{R}_{\eta_5'}^{\eta_5}\mathbf{R}_z(\eta_6) = \begin{bmatrix} 0 & 0 & 1 \\ c_{\eta_6} & -s_{\eta_6} & 0 \\ s_{\eta_6} & c_{\eta_6} & 0 \end{bmatrix}$$

Rotation by η_7

In order to align frame RF_{η_6} to $RF_{\eta_6'}$, the following rotation matrix has to be applied

$$\mathbf{R}_{\eta_6'}^{\eta_6} = \mathbf{R}_y\left(\frac{\pi}{2}\right)\mathbf{R}_z\left(\frac{\pi}{2}\right) = \begin{bmatrix} 0 & 0 & 1 \\ 1 & 0 & 0 \\ 0 & 1 & 0 \end{bmatrix}$$

Let RF_{Wr} the resulting reference frame after that the rotation by η_7 is performed about axes $z_{\eta_6'}$. Hence, the rotation of frame RF_{Wr} wrt RF_{η_6} is given by

$$\mathbf{R}_{Wr}^{\eta_6}(\eta_7) = \mathbf{R}_{\eta_6'}^{\eta_6}\mathbf{R}_z(\eta_7) = \begin{bmatrix} 0 & 0 & 1 \\ c_{\eta_7} & -s_{\eta_7} & 0 \\ s_{\eta_7} & c_{\eta_7} & 0 \end{bmatrix}$$

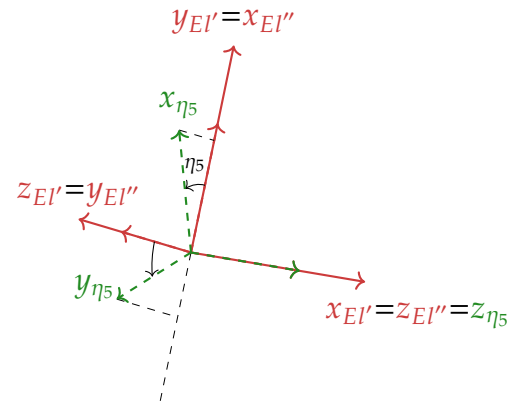

(a) Rotation by η_5 about $z_{El''}$

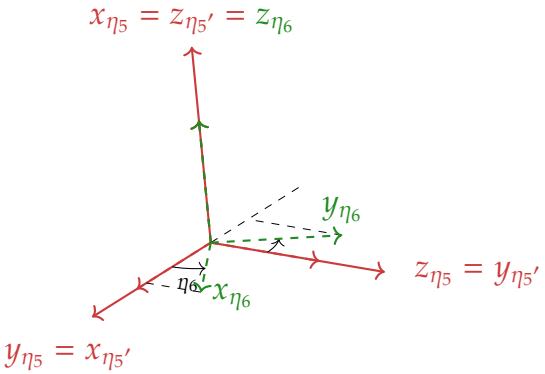

(b) Rotation by η_6 about $z_{\eta_5'}$

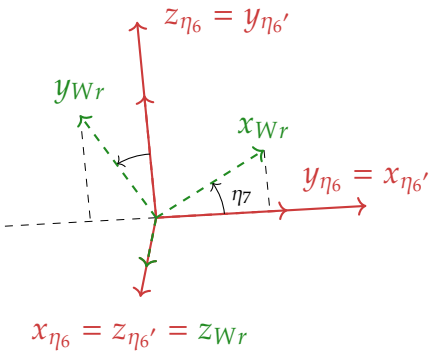

(c) Rotation by η_7 about $z_{\eta_6'}$

Figure 4.4: Wrist rotations

Thus, it is possible to compute $\mathbf{R}_{Wr}^{El'}$

$$\begin{aligned}\mathbf{R}_{Wr}^{El'}(\eta_5, \eta_6, \eta_7) &= \mathbf{R}_{\eta_5}^{El'}(\eta_5)\,\mathbf{R}_{\eta_6}^{\eta_5}(\eta_6)\,\mathbf{R}_{Wr}^{\eta_6}(\eta_7) \\ &= \begin{bmatrix} c_{\eta_6}c_{\eta_7} & -c_{\eta_6}s_{\eta_7} & s_{\eta_6} \\ s_{\eta_5}s_{\eta_6}c_{\eta_7} + c_{\eta_5}s_{\eta_7} & -s_{\eta_5}s_{\eta_6}s_{\eta_7} + c_{\eta_5}c_{\eta_7} & -s_{\eta_5}c_{\eta_6} \\ -c_{\eta_5}s_{\eta_6}c_{\eta_7} + s_{\eta_5}s_{\eta_7} & c_{\eta_5}s_{\eta_6}s_{\eta_7} + s_{\eta_5}c_{\eta_7} & c_{\eta_5}c_{\eta_6} \end{bmatrix}\end{aligned}$$

By combining Eq. 4.3 and the expression for ${\mathbf{p_h}}^{El}$ one obtains, after some computations, the below equations with the notation $\boldsymbol{\eta}_{i-j} = \eta_i, \eta_{i+1}, \ldots, \eta_j,\ j > i$.

$$
\begin{aligned}
{\mathbf{p_h}}^{W} &= \boldsymbol{\Phi}_{Ha}\left(\boldsymbol{\eta}, {\mathbf{p_h}}^{Wr}\right) \\
&= \mathbf{R}_{Sh}^{W}\left(\boldsymbol{\eta}_{1-3}\right) \underbrace{\left(\mathbf{R}_{El}^{Sh'}\left(\eta_4\right) \underbrace{\left(\mathbf{R}_{Wr}^{El'}\left(\boldsymbol{\eta}_{5-7}\right) {\mathbf{p_h}}^{Wr} + {\mathbf{O_{El'}}}^{El} \right)}_{{\mathbf{p_h}}^{El}(\boldsymbol{\eta}_{5-7})} + {\mathbf{O_{Sh'}}}^{Sh} \right)}_{{\mathbf{p_h}}^{Sh}(\boldsymbol{\eta}_{4-7})} \\
&= \begin{bmatrix} {\mathbf{p_h}_x}^{W} \\ {\mathbf{p_h}_y}^{W} \\ {\mathbf{p_h}_z}^{W} \end{bmatrix}
\end{aligned}
\tag{4.4}
$$

with

$$
\begin{aligned}
{\mathbf{p_h}_x}^{W} = &\left(c_{\eta_6}c_{\eta_7}{\mathbf{p_h}_x}^{Wr} - c_{\eta_6}s_{\eta_7}{\mathbf{p_h}_y}^{Wr} + s_{\eta_6}{\mathbf{p_h}_z}^{Wr}\right)\left(c_{\eta_2}c_{\eta_3}c_{\eta_4} - c_{\eta_2}s_{\eta_3}s_{\eta_4}\right) - \big[\left(s_{\eta_5}s_{\eta_6}c_{\eta_7} + \right. \\
&\left. c_{\eta_5}s_{\eta_7}\right){\mathbf{p_h}_x}^{Wr} + \left(-s_{\eta_5}s_{\eta_6}s_{\eta_7} + c_{\eta_5}c_{\eta_7}\right){\mathbf{p_h}_y}^{Wr} - s_{\eta_5}c_{\eta_6}{\mathbf{p_h}_z}^{Wr} - L_{fo}\big]\left(c_{\eta_2}c_{\eta_3}s_{\eta_4} + \right. \\
&\left. c_{\eta_2}s_{\eta_3}c_{\eta_4}\right) + s_{\eta_2}\big[\left(-c_{\eta_5}s_{\eta_6}c_{\eta_7} + s_{\eta_5}s_{\eta_7}\right){\mathbf{p_h}_x}^{Wr} + \left(c_{\eta_5}s_{\eta_6}s_{\eta_7} + s_{\eta_5}c_{\eta_7}\right){\mathbf{p_h}_y}^{Wr} + \\
&c_{\eta_5}c_{\eta_6}{\mathbf{p_h}_z}^{Wr}\big] + c_{\eta_2}s_{\eta_3}L_{sh}
\end{aligned}
$$

$$
\begin{aligned}
{\mathbf{p_h}_y}^{W} = &\left(c_{\eta_6}c_{\eta_7}{\mathbf{p_h}_x}^{Wr} - c_{\eta_6}s_{\eta_7}{\mathbf{p_h}_y}^{Wr} + s_{\eta_6}{\mathbf{p_h}_z}^{Wr}\right)\left(s_{\eta_1}s_{\eta_2}c_{\eta_3}c_{\eta_4} - s_{\eta_1}s_{\eta_2}s_{\eta_3}s_{\eta_4} + c_{\eta_1}s_{\eta_3}c_{\eta_4}\right. \\
&\left. + c_{\eta_1}c_{\eta_3}s_{\eta_4}\right) + \big[\left(s_{\eta_5}s_{\eta_6}c_{\eta_7} + c_{\eta_5}s_{\eta_7}\right){\mathbf{p_h}_x}^{Wr} + \left(-s_{\eta_5}s_{\eta_6}s_{\eta_7} + c_{\eta_5}c_{\eta_7}\right){\mathbf{p_h}_y}^{Wr} - s_{\eta_5}c_{\eta_6}{\mathbf{p_h}_z}^{Wr} \\
&- L_{fo}\big]\left(-s_{\eta_1}s_{\eta_2}c_{\eta_3}s_{\eta_4} - c_{\eta_1}s_{\eta_3}s_{\eta_4} + c_{\eta_1}c_{\eta_3}c_{\eta_4} - s_{\eta_1}s_{\eta_2}s_{\eta_3}c_{\eta_4}\right) - s_{\eta_1}c_{\eta_2}\big[\left(-c_{\eta_5}s_{\eta_6}c_{\eta_7}\right. \\
&\left. + s_{\eta_5}s_{\eta_7}\right){\mathbf{p_h}_x}^{Wr} + \left(c_{\eta_5}s_{\eta_6}s_{\eta_7} + s_{\eta_5}c_{\eta_7}\right){\mathbf{p_h}_y}^{Wr} + c_{\eta_5}c_{\eta_6}{\mathbf{p_h}_z}^{Wr}\big] - \left(c_{\eta_1}c_{\eta_3} - s_{\eta_1}s_{\eta_2}s_{\eta_3}\right)L_{sh}
\end{aligned}
$$

$$
\begin{aligned}
{\mathbf{p_h}_z}^{W} = &\left(c_{\eta_6}c_{\eta_7}{\mathbf{p_h}_x}^{Wr} - c_{\eta_6}s_{\eta_7}{\mathbf{p_h}_y}^{Wr} + s_{\eta_6}{\mathbf{p_h}_z}^{Wr}\right)\left(c_{\eta_1}s_{\eta_2}s_{\eta_3}s_{\eta_4} - c_{\eta_1}s_{\eta_2}c_{\eta_3}c_{\eta_4} + s_{\eta_1}s_{\eta_3}c_{\eta_4}\right. \\
&\left. + s_{\eta_1}c_{\eta_3}s_{\eta_4}\right) + \big[\left(s_{\eta_5}s_{\eta_6}c_{\eta_7} + c_{\eta_5}s_{\eta_7}\right){\mathbf{p_h}_x}^{Wr} + \left(-s_{\eta_5}s_{\eta_6}s_{\eta_7} + c_{\eta_5}c_{\eta_7}\right){\mathbf{p_h}_y}^{Wr} - s_{\eta_5}c_{\eta_6}{\mathbf{p_h}_z}^{Wr} \\
&- L_{fo}\big]\left(c_{\eta_1}s_{\eta_2}c_{\eta_3}s_{\eta_4} + c_{\eta_1}s_{\eta_2}s_{\eta_3}c_{\eta_4} - s_{\eta_1}s_{\eta_3}s_{\eta_4} + s_{\eta_1}c_{\eta_3}c_{\eta_4}\right) + c_{\eta_1}c_{\eta_2}\big[\left(-c_{\eta_5}s_{\eta_6}c_{\eta_7}\right. \\
&\left. + s_{\eta_5}s_{\eta_7}\right){\mathbf{p_h}_x}^{Wr} + \left(c_{\eta_5}s_{\eta_6}s_{\eta_7} + s_{\eta_5}c_{\eta_7}\right){\mathbf{p_h}_y}^{Wr} + c_{\eta_5}c_{\eta_6}{\mathbf{p_h}_z}^{Wr}\big] - \left(s_{\eta_1}c_{\eta_3} + c_{\eta_1}s_{\eta_2}s_{\eta_3}\right)L_{sh}
\end{aligned}
$$

4.2 Differential kinematics

It is desired to express the markers' linear velocity, denoted as $\dot{\mathbf{p}}$, as a function of the joint velocities $\dot{\boldsymbol{\eta}}$. This mapping is described by a matrix, termed Jacobian $\mathbf{J}(\boldsymbol{\eta})$, which depends on the arm configuration, and it can be computed via differentiation of the forward kinematics function with respect to the joint variables. The translational velocity of one marker frame $\mathbf{M_i}$ can be expressed as the time derivative of vector $\mathbf{p_i}$, representing the origin of the marker frame with respect to the base frame. This leads to

$$\dot{\mathbf{p}}_\mathbf{i} = \mathbf{J}_\mathbf{i} \cdot \dot{\boldsymbol{\eta}} = \frac{\partial \boldsymbol{\Phi}_\mathbf{i}}{\partial \boldsymbol{\eta}} \cdot \dot{\boldsymbol{\eta}} = \begin{cases} \frac{\partial \boldsymbol{\Phi}_{Sh}\left(\eta_{1-3}, \mathbf{p_i}^{Sh}\right)}{\partial \boldsymbol{\eta}} \cdot \dot{\boldsymbol{\eta}} = \mathbf{J}_{Sh}\left(\eta_{1-3}, \mathbf{p_i}^{Sh}\right) \cdot \dot{\boldsymbol{\eta}}, & i \in \mathcal{S} \\ \frac{\partial \boldsymbol{\Phi}_{Fo}\left(\eta_{1-4}, \mathbf{p_i}^{El}\right)}{\partial \boldsymbol{\eta}} \cdot \dot{\boldsymbol{\eta}} = \mathbf{J}_{Fo}\left(\eta_{1-4}, \mathbf{p_i}^{El}\right) \cdot \dot{\boldsymbol{\eta}}, & i \in \mathcal{F} \\ \frac{\partial \boldsymbol{\Phi}_{Ha}\left(\eta, \mathbf{p_i}^{Wr}\right)}{\partial \boldsymbol{\eta}} \cdot \dot{\boldsymbol{\eta}} = \mathbf{J}_{Ha}\left(\eta, \mathbf{p_i}^{Wr}\right) \cdot \dot{\boldsymbol{\eta}}, & i \in \mathcal{H} \end{cases}$$

where $\mathbf{J_i} \in \mathbb{R}^{3\times n}$, $n = 7$ is the number of joint variables. As $\boldsymbol{\Phi}_\mathbf{i}$, also $\mathbf{J_i}$ depends on $\left(\eta_{1-3}, \mathbf{p_i}^{Sh}\right)$, $\left(\eta_{1-4}, \mathbf{p_i}^{El}\right)$ or $\left(\eta, \mathbf{p_i}^{Wr}\right)$ but this dependence is dropped for simplicity. Indeed $\boldsymbol{\Phi}_\mathbf{i} = \boldsymbol{\Phi}_{Sh}\left(\eta_{1-3}, \mathbf{p_i}^{Sh}\right)$, $\boldsymbol{\Phi}_\mathbf{i} = \boldsymbol{\Phi}_{Fo}\left(\eta_{1-4}, \mathbf{p_i}^{El}\right)$, or $\boldsymbol{\Phi}_\mathbf{i} = \boldsymbol{\Phi}_{Ha}\left(\eta, \mathbf{p_h}^{Wr}\right)$, depending on where the marker $\mathbf{M_i}$ is placed. In general, one has

$$\dot{\mathbf{p}} = \begin{bmatrix} \dot{\mathbf{p}}_\mathbf{1} \\ \vdots \\ \dot{\mathbf{p}}_\mathbf{m} \end{bmatrix} = \begin{bmatrix} \mathbf{J_1} \\ \vdots \\ \mathbf{J_m} \end{bmatrix} \cdot \dot{\boldsymbol{\eta}} = \begin{bmatrix} \frac{\partial \boldsymbol{\Phi}_\mathbf{1}}{\partial \boldsymbol{\eta}} \\ \vdots \\ \frac{\partial \boldsymbol{\Phi}_\mathbf{m}}{\partial \boldsymbol{\eta}} \end{bmatrix} \cdot \dot{\boldsymbol{\eta}} = \begin{bmatrix} \frac{\partial \boldsymbol{\Phi}_\mathbf{1}}{\partial \eta_1} & \cdots & \frac{\partial \boldsymbol{\Phi}_\mathbf{1}}{\partial \eta_7} \\ \frac{\partial \boldsymbol{\Phi}_\mathbf{2}}{\partial \eta_1} & \cdots & \frac{\partial \boldsymbol{\Phi}_\mathbf{2}}{\partial \eta_7} \\ \vdots & \vdots & \vdots \\ \frac{\partial \boldsymbol{\Phi}_\mathbf{m}}{\partial \eta_1} & \cdots & \frac{\partial \boldsymbol{\Phi}_\mathbf{m}}{\partial \eta_7} \end{bmatrix} \cdot \dot{\boldsymbol{\eta}} = \frac{\partial \boldsymbol{\Phi}\left(\eta, \mathbf{p}^B\right)}{\partial \boldsymbol{\eta}} \cdot \dot{\boldsymbol{\eta}} = \mathbf{J}\left(\eta, \mathbf{p}^B\right) \cdot \dot{\boldsymbol{\eta}} \tag{4.5}$$

where $\mathbf{J}\left(\eta, \mathbf{p}^B\right) \in \mathbb{R}^{(3m)\times n}$.

4.2.1 Shoulder differential kinematics

Let $\mathbf{M_s}$ be a marker on the shoulder. Recalling that $\boldsymbol{\Phi}_{Sh}\left(\eta, \mathbf{p_s}^{Sh}\right) = \begin{bmatrix} \mathbf{p}_{\mathbf{s}_x} \\ \mathbf{p}_{\mathbf{s}_y} \\ \mathbf{p}_{\mathbf{s}_z} \end{bmatrix}$,

$$\dot{\mathbf{p}}_\mathbf{s} = \begin{bmatrix} \dot{\mathbf{p}}_{\mathbf{s}_x} \\ \dot{\mathbf{p}}_{\mathbf{s}_y} \\ \dot{\mathbf{p}}_{\mathbf{s}_z} \end{bmatrix} = \frac{\partial \boldsymbol{\Phi}_{Sh}\left(\eta_{1-3}, \mathbf{p_s}^{Sh}\right)}{\partial \boldsymbol{\eta}} \cdot \dot{\boldsymbol{\eta}} = \mathbf{J}_{Sh}\left(\eta_{1-3}, \mathbf{p_s}^{Sh}\right) \cdot \dot{\boldsymbol{\eta}}$$

Taking the partial derivatives of Eq. 4.2, one obtains

$$
[\mathbf{J}_{Sh}]_{1:1,\dots,n}
\begin{cases}
[\mathbf{J}_{Sh}]_{1,1} = [\mathbf{J}_{Sh}]_{1,4} = [\mathbf{J}_{Sh}]_{1,5} = [\mathbf{J}_{Sh}]_{1,6} = [\mathbf{J}_{Sh}]_{1,7} = 0 \\
[\mathbf{J}_{Sh}]_{1,2} = -s_{\eta_2} c_{\eta_3} \mathbf{p}_{\mathbf{s}_x}^{Sh} + s_{\eta_2} s_{\eta_3} \mathbf{p}_{\mathbf{s}_y}^{Sh} + c_{\eta_2} \mathbf{p}_{\mathbf{s}_z}^{Sh} \\
[\mathbf{J}_{Sh}]_{1,3} = -c_{\eta_2} s_{\eta_3} \mathbf{p}_{\mathbf{s}_x}^{Sh} - c_{\eta_2} c_{\eta_3} \mathbf{p}_{\mathbf{s}_y}^{Sh}
\end{cases}
$$

$$
[\mathbf{J}_{Sh}]_{2:1,\dots,n}
\begin{cases}
[\mathbf{J}_{Sh}]_{2,4} = [\mathbf{J}_{Sh}]_{2,5} = [\mathbf{J}_{Sh}]_{2,6} = [\mathbf{J}_{Sh}]_{2,7} = 0 \\
[\mathbf{J}_{Sh}]_{2,1} = \left(c_{\eta_1} s_{\eta_2} c_{\eta_3} - s_{\eta_1} s_{\eta_3}\right) \mathbf{p}_{\mathbf{s}_x}^{Sh} - \left(c_{\eta_1} s_{\eta_2} s_{\eta_3} + s_{\eta_1} c_{\eta_3}\right) \mathbf{p}_{\mathbf{s}_y}^{Sh} - c_{\eta_1} c_{\eta_2} \mathbf{p}_{\mathbf{s}_z}^{Sh} \\
[\mathbf{J}_{Sh}]_{2,2} = s_{\eta_1} c_{\eta_2} c_{\eta_3} \mathbf{p}_{\mathbf{s}_x}^{Sh} - s_{\eta_1} c_{\eta_2} s_{\eta_3} \mathbf{p}_{\mathbf{s}_y}^{Sh} + s_{\eta_1} s_{\eta_2} \mathbf{p}_{\mathbf{s}_z}^{Sh} \\
[\mathbf{J}_{Sh}]_{2,3} = \left(-s_{\eta_1} s_{\eta_2} s_{\eta_3} + c_{\eta_1} c_{\eta_3}\right) \mathbf{p}_{\mathbf{s}_x}^{Sh} - \left(s_{\eta_1} s_{\eta_2} c_{\eta_3} + c_{\eta_1} s_{\eta_3}\right) \mathbf{p}_{\mathbf{s}_y}^{Sh}
\end{cases}
$$

$$
[\mathbf{J}_{Sh}]_{3:1,\dots,n}
\begin{cases}
[\mathbf{J}_{Sh}]_{3,4} = [\mathbf{J}_{Sh}]_{3,5} = [\mathbf{J}_{Sh}]_{3,6} = [\mathbf{J}_{Sh}]_{3,7} = 0 \\
[\mathbf{J}_{Sh}]_{3,1} = \left(s_{\eta_1} s_{\eta_2} c_{\eta_3} + c_{\eta_1} s_{\eta_3}\right) \mathbf{p}_{\mathbf{s}_x}^{Sh} + \left(-s_{\eta_1} s_{\eta_2} s_{\eta_3} + c_{\eta_1} c_{\eta_3}\right) \mathbf{p}_{\mathbf{s}_y}^{Sh} - s_{\eta_1} c_{\eta_2} \mathbf{p}_{\mathbf{s}_z}^{Sh} \\
[\mathbf{J}_{Sh}]_{3,2} = -c_{\eta_1} c_{\eta_2} c_{\eta_3} \mathbf{p}_{\mathbf{s}_x}^{Sh} + c_{\eta_1} c_{\eta_2} s_{\eta_3} \mathbf{p}_{\mathbf{s}_y}^{Sh} - c_{\eta_1} s_{\eta_2} \mathbf{p}_{\mathbf{s}_z}^{Sh} \\
[\mathbf{J}_{Sh}]_{2,3} = \left(c_{\eta_1} s_{\eta_2} s_{\eta_3} + s_{\eta_1} c_{\eta_3}\right) \mathbf{p}_{\mathbf{s}_x}^{Sh} + \left(c_{\eta_1} s_{\eta_2} c_{\eta_3} - s_{\eta_1} s_{\eta_3}\right) \mathbf{p}_{\mathbf{s}_y}^{Sh}
\end{cases}
$$

4.2.2 Forearm differential kinematics

Let $\mathbf{M}_\mathbf{f}$ be a marker on the forearm. Since $\mathbf{\Phi}_{Fo} = \begin{bmatrix} \mathbf{p}_{\mathbf{f}_x} \\ \mathbf{p}_{\mathbf{f}_y} \\ \mathbf{p}_{\mathbf{f}_z} \end{bmatrix}$,

$$
\dot{\mathbf{p}}_\mathbf{f} = \begin{bmatrix} \dot{\mathbf{p}}_{\mathbf{f}_x} \\ \dot{\mathbf{p}}_{\mathbf{f}_y} \\ \dot{\mathbf{p}}_{\mathbf{f}_z} \end{bmatrix} = \frac{\partial \mathbf{\Phi}_{Fo}\left(\eta_{1-4}, {\mathbf{p}_\mathbf{f}}^{El}\right)}{\partial \eta} \cdot \dot{\eta} = \mathbf{J}_{Fo}\left(\eta_{1-4}, {\mathbf{p}_\mathbf{f}}^{El}\right) \cdot \dot{\eta}
$$

Taking the partial derivatives of Eq. 4.3, one obtains

$$
[\mathbf{J}_{Fo}]_{1:1,\dots,n}\begin{cases}
[\mathbf{J}_{Fo}]_{1,1} = [\mathbf{J}_{Fo}]_{1,5} = [\mathbf{J}_{Fo}]_{1,6} = [\mathbf{J}_{Fo}]_{1,7} = 0 \\
[\mathbf{J}_{Fo}]_{1,2} = -s_{\eta_2}c_{\eta_3}\left(c_{\eta_4}\mathbf{p}_{\mathbf{f}_x}^{El} - s_{\eta_4}\mathbf{p}_{\mathbf{f}_y}^{El}\right) + s_{\eta_2}s_{\eta_3}\left(s_{\eta_4}\mathbf{p}_{\mathbf{f}_x}^{El} + c_{\eta_4}\mathbf{p}_{\mathbf{f}_y}^{El} - L_{sh}\right) + c_{\eta_2}\mathbf{p}_{\mathbf{f}_z}^{El} \\
[\mathbf{J}_{Sh}]_{1,3} = -c_{\eta_2}s_{\eta_3}\left(c_{\eta_4}\mathbf{p}_{\mathbf{f}_x}^{El} - s_{\eta_4}\mathbf{p}_{\mathbf{f}_y}^{El}\right) - c_{\eta_2}c_{\eta_3}\left(s_{\eta_4}\mathbf{p}_{\mathbf{f}_x}^{El} + c_{\eta_4}\mathbf{p}_{\mathbf{f}_y}^{El} - L_{sh}\right) \\
[\mathbf{J}_{Sh}]_{1,4} = c_{\eta_2}c_{\eta_3}\left(-s_{\eta_4}\mathbf{p}_{\mathbf{f}_x}^{El} - c_{\eta_4}\mathbf{p}_{\mathbf{f}_y}^{El}\right) - c_{\eta_2}s_{\eta_3}\left(c_{\eta_4}\mathbf{p}_{\mathbf{f}_x}^{El} - s_{\eta_4}\mathbf{p}_{\mathbf{f}_y}^{El}\right)
\end{cases}
$$

$$
[\mathbf{J}_{Fo}]_{2:1,\dots,n}\begin{cases}
[\mathbf{J}_{Fo}]_{2,5} = & [\mathbf{J}_{Fo}]_{2,6} = [\mathbf{J}_{Fo}]_{2,7} = 0 \\
[\mathbf{J}_{Fo}]_{2,1} = & \left(c_{\eta_1}s_{\eta_2}c_{\eta_3} - s_{\eta_1}s_{\eta_3}\right)\left(c_{\eta_4}\mathbf{p}_{\mathbf{f}_x}^{El} - s_{\eta_4}\mathbf{p}_{\mathbf{f}_y}^{El}\right) - \\
& \left(s_{\eta_1}c_{\eta_3} + c_{\eta_1}s_{\eta_2}s_{\eta_3}\right)\left(s_{\eta_4}\mathbf{p}_{\mathbf{f}_x}^{El} + c_{\eta_4}\mathbf{p}_{\mathbf{f}_y}^{El} - L_{sh}\right) - c_{\eta_1}c_{\eta_2}\mathbf{p}_{\mathbf{f}_z}^{El} \\
[\mathbf{J}_{Fo}]_{2,2} = & s_{\eta_1}c_{\eta_2}c_{\eta_3}\left(c_{\eta_4}\mathbf{p}_{\mathbf{f}_x}^{El} - s_{\eta_4}\mathbf{p}_{\mathbf{f}_y}^{El}\right) - s_{\eta_1}c_{\eta_2}s_{\eta_3}\left(s_{\eta_4}\mathbf{p}_{\mathbf{f}_x}^{El} + c_{\eta_4}\mathbf{p}_{\mathbf{f}_y}^{El} - L_{sh}\right) + \\
& s_{\eta_1}s_{\eta_2}\mathbf{p}_{\mathbf{f}_z}^{El} \\
[\mathbf{J}_{Fo}]_{2,3} = & \left(-s_{\eta_1}s_{\eta_2}s_{\eta_3} + c_{\eta_1}c_{\eta_3}\right)\left(c_{\eta_4}\mathbf{p}_{\mathbf{f}_x}^{El} - s_{\eta_4}\mathbf{p}_{\mathbf{f}_y}^{El}\right) - \\
& \left(c_{\eta_1}s_{\eta_3} + s_{\eta_1}s_{\eta_2}c_{\eta_3}\right)\left(s_{\eta_4}\mathbf{p}_{\mathbf{f}_x}^{El} + c_{\eta_4}\mathbf{p}_{\mathbf{f}_y}^{El} - L_{sh}\right) \\
[\mathbf{J}_{Fo}]_{2,4} = & -\left(s_{\eta_1}s_{\eta_2}c_{\eta_3} + c_{\eta_1}s_{\eta_3}\right)\left(s_{\eta_4}\mathbf{p}_{\mathbf{f}_x}^{El} + c_{\eta_4}\mathbf{p}_{\mathbf{f}_y}^{El}\right) + \\
& \left(c_{\eta_1}c_{\eta_3} - s_{\eta_1}s_{\eta_2}s_{\eta_3}\right)\left(c_{\eta_4}\mathbf{p}_{\mathbf{f}_x}^{El} - s_{\eta_4}\mathbf{p}_{\mathbf{f}_y}^{El}\right)
\end{cases}
$$

$$
[\mathbf{J}_{Fo}]_{3:1,\dots,n}\begin{cases}
[\mathbf{J}_{Fo}]_{3,5} = & [\mathbf{J}_{Fo}]_{3,6} = [\mathbf{J}_{Fo}]_{3,7} = 0 \\
[\mathbf{J}_{Fo}]_{3,1} = & \left(c_{\eta_1}s_{\eta_3} + s_{\eta_1}s_{\eta_2}c_{\eta_3}\right)\left(c_{\eta_4}\mathbf{p}_{\mathbf{f}_x}^{El} - s_{\eta_4}\mathbf{p}_{\mathbf{f}_y}^{El}\right) + \\
& \left(-s_{\eta_1}s_{\eta_2}s_{\eta_3} + c_{\eta_1}c_{\eta_3}\right)\left(s_{\eta_4}\mathbf{p}_{\mathbf{f}_x}^{El} + c_{\eta_4}\mathbf{p}_{\mathbf{f}_y}^{El} - L_{sh}\right) - s_{\eta_1}c_{\eta_2}\mathbf{p}_{\mathbf{f}_z}^{El} \\
[\mathbf{J}_{Fo}]_{3,2} = & -c_{\eta_1}c_{\eta_2}c_{\eta_3}\left(c_{\eta_4}\mathbf{p}_{\mathbf{f}_x}^{El} - s_{\eta_4}\mathbf{p}_{\mathbf{f}_y}^{El}\right) + c_{\eta_1}c_{\eta_2}s_{\eta_3}\left(s_{\eta_4}\mathbf{p}_{\mathbf{f}_x}^{El} + c_{\eta_4}\mathbf{p}_{\mathbf{f}_y}^{El} - L_{sh}\right) - \\
& c_{\eta_1}s_{\eta_2}\mathbf{p}_{\mathbf{f}_z}^{El} \\
[\mathbf{J}_{Fo}]_{3,3} = & \left(s_{\eta_1}c_{\eta_3} + c_{\eta_1}s_{\eta_2}s_{\eta_3}\right)\left(c_{\eta_4}\mathbf{p}_{\mathbf{f}_x}^{El} - s_{\eta_4}\mathbf{p}_{\mathbf{f}_y}^{El}\right) + \\
& \left(c_{\eta_1}s_{\eta_2}c_{\eta_3} - s_{\eta_1}s_{\eta_3}\right)\left(s_{\eta_4}\mathbf{p}_{\mathbf{f}_x}^{El} + c_{\eta_4}\mathbf{p}_{\mathbf{f}_y}^{El} - L_{sh}\right) \\
[\mathbf{J}_{Fo}]_{3,4} = & -\left(s_{\eta_1}s_{\eta_3} - c_{\eta_1}s_{\eta_2}c_{\eta_3}\right)\left(s_{\eta_4}\mathbf{p}_{\mathbf{f}_x}^{El} - c_{\eta_4}\mathbf{p}_{\mathbf{f}_y}^{El}\right) + \\
& \left(c_{\eta_1}s_{\eta_2}s_{\eta_3} + s_{\eta_1}c_{\eta_3}\right)\left(c_{\eta_4}\mathbf{p}_{\mathbf{f}_x}^{El} - s_{\eta_4}\mathbf{p}_{\mathbf{f}_y}^{El}\right)
\end{cases}
$$

4.2.3 Hand differential kinematics

Let $\mathbf{M_h}$ be a marker on the hand.

$$\dot{\mathbf{p}}_\mathbf{h} = \begin{bmatrix} \dot{\mathbf{p}}_{\mathbf{h}_x} \\ \dot{\mathbf{p}}_{\mathbf{h}_y} \\ \dot{\mathbf{p}}_{\mathbf{h}_z} \end{bmatrix} = \frac{\partial \mathbf{\Phi}_{Ha}\left(\boldsymbol{\eta}, {\mathbf{p}_\mathbf{h}}^{Wr}\right)}{\partial \boldsymbol{\eta}} \cdot \dot{\boldsymbol{\eta}} = \mathbf{J}_{Ha}\left(\boldsymbol{\eta}, {\mathbf{p}_\mathbf{h}}^{Wr}\right) \cdot \dot{\boldsymbol{\eta}}$$

Taking the partial derivatives of Eq. 4.4,

$$[\mathbf{J}_{Ha}]_{1:1,\dots,n} \begin{cases} [\mathbf{J}_{Ha}]_{1,1} = & 0 \\ [\mathbf{J}_{Ha}]_{1,2} = & \left(c_{\eta_6}c_{\eta_7}\mathbf{p}_{\mathbf{h}_x}^{Wr} - c_{\eta_6}s_{\eta_7}\mathbf{p}_{\mathbf{h}_y}^{Wr} + s_{\eta_6}\mathbf{p}_{\mathbf{h}_z}^{Wr}\right)\left(-s_{\eta_2}c_{\eta_3}c_{\eta_4} + s_{\eta_2}s_{\eta_3}s_{\eta_4}\right) + \\ & \left[\left(s_{\eta_5}s_{\eta_6}c_{\eta_7} + c_{\eta_5}s_{\eta_7}\right)\mathbf{p}_{\mathbf{h}_x}^{Wr} + \left(-s_{\eta_5}s_{\eta_6}s_{\eta_7} + c_{\eta_5}c_{\eta_7}\right)\mathbf{p}_{\mathbf{h}_y}^{Wr} - s_{\eta_5}c_{\eta_6}\mathbf{p}_{\mathbf{h}_z}^{Wr} - \right. \\ & \left. L_{fo}\right]\left(s_{\eta_2}c_{\eta_3}s_{\eta_4} + s_{\eta_2}s_{\eta_3}c_{\eta_4}\right) + c_{\eta_2}\left[\left(-c_{\eta_5}s_{\eta_6}c_{\eta_7} + s_{\eta_5}s_{\eta_7}\right)\mathbf{p}_{\mathbf{h}_x}^{Wr} + \right. \\ & \left.\left(c_{\eta_5}s_{\eta_6}s_{\eta_7} + s_{\eta_5}c_{\eta_7}\right)\mathbf{p}_{\mathbf{h}_y}^{Wr} + c_{\eta_5}c_{\eta_6}\mathbf{p}_{\mathbf{h}_z}^{Wr}\right] - s_{\eta_2}s_{\eta_3}L_{sh} \\ [\mathbf{J}_{Ha}]_{1,3} = & \left(c_{\eta_6}c_{\eta_7}\mathbf{p}_{\mathbf{h}_x}^{Wr} - c_{\eta_6}s_{\eta_7}\mathbf{p}_{\mathbf{h}_y}^{Wr} + s_{\eta_6}\mathbf{p}_{\mathbf{h}_z}^{Wr}\right)\left(-c_{\eta_2}s_{\eta_3}c_{\eta_4} - c_{\eta_2}c_{\eta_3}s_{\eta_4}\right) - \\ & \left[\left(s_{\eta_5}s_{\eta_6}c_{\eta_7} + c_{\eta_5}s_{\eta_7}\right)\mathbf{p}_{\mathbf{h}_x}^{Wr} + \left(-s_{\eta_5}s_{\eta_6}s_{\eta_7} + c_{\eta_5}c_{\eta_7}\right)\mathbf{p}_{\mathbf{h}_y}^{Wr} - s_{\eta_5}c_{\eta_6}\mathbf{p}_{\mathbf{h}_z}^{Wr} - \right. \\ & \left. L_{fo}\right]\left(-c_{\eta_2}s_{\eta_3}s_{\eta_4} + c_{\eta_2}c_{\eta_3}c_{\eta_4}\right) + c_{\eta_2}c_{\eta_3}L_{sh} \\ [\mathbf{J}_{Ha}]_{1,4} = & \left(c_{\eta_6}c_{\eta_7}\mathbf{p}_{\mathbf{h}_x}^{Wr} - c_{\eta_6}s_{\eta_7}\mathbf{p}_{\mathbf{h}_y}^{Wr} + s_{\eta_6}\mathbf{p}_{\mathbf{h}_z}^{Wr}\right)\left(-c_{\eta_2}c_{\eta_3}s_{\eta_4} - c_{\eta_2}s_{\eta_3}c_{\eta_4}\right) - \\ & \left[\left(s_{\eta_5}s_{\eta_6}c_{\eta_7} + c_{\eta_5}s_{\eta_7}\right)\mathbf{p}_{\mathbf{h}_x}^{Wr} + \left(-s_{\eta_5}s_{\eta_6}s_{\eta_7} + c_{\eta_5}c_{\eta_7}\right)\mathbf{p}_{\mathbf{h}_y}^{Wr} - s_{\eta_5}c_{\eta_6}\mathbf{p}_{\mathbf{h}_z}^{Wr} - \right. \\ & \left. L_{fo}\right]\left(c_{\eta_2}c_{\eta_3}c_{\eta_4} - c_{\eta_2}s_{\eta_3}s_{\eta_4}\right) \\ [\mathbf{J}_{Ha}]_{1,5} = & -\left(c_{\eta_2}c_{\eta_3}s_{\eta_4} + c_{\eta_2}s_{\eta_3}c_{\eta_4}\right)\left[\left(c_{\eta_5}s_{\eta_6}c_{\eta_7} - s_{\eta_5}s_{\eta_7}\right)\mathbf{p}_{\mathbf{h}_x}^{Wr} + \right. \\ & \left.\left(-c_{\eta_5}s_{\eta_6}s_{\eta_7} - s_{\eta_5}c_{\eta_7}\right)\mathbf{p}_{\mathbf{h}_y}^{Wr} - c_{\eta_5}c_{\eta_6}\mathbf{p}_{\mathbf{h}_z}^{Wr}\right] + s_{\eta_2}\left[\left(s_{\eta_5}s_{\eta_6}c_{\eta_7} + \right.\right. \\ & \left.\left.c_{\eta_5}s_{\eta_7}\right)\mathbf{p}_{\mathbf{h}_x}^{Wr} + \left(-s_{\eta_5}s_{\eta_6}s_{\eta_7} + c_{\eta_5}c_{\eta_7}\right)\mathbf{p}_{\mathbf{h}_y}^{Wr} - s_{\eta_5}c_{\eta_6}\mathbf{p}_{\mathbf{h}_z}^{Wr}\right] \\ [\mathbf{J}_{Ha}]_{1,6} = & \left(c_{\eta_2}c_{\eta_3}c_{\eta_4} - c_{\eta_2}s_{\eta_3}s_{\eta_4}\right)\left(-s_{\eta_6}c_{\eta_7}\mathbf{p}_{\mathbf{h}_x}^{Wr} + s_{\eta_6}s_{\eta_7}\mathbf{p}_{\mathbf{h}_y}^{Wr} + c_{\eta_6}\mathbf{p}_{\mathbf{h}_z}^{Wr}\right) - \\ & \left(c_{\eta_2}c_{\eta_3}s_{\eta_4} + c_{\eta_2}s_{\eta_3}c_{\eta_4}\right)\left[s_{\eta_5}c_{\eta_6}c_{\eta_7}\mathbf{p}_{\mathbf{h}_x}^{Wr} - s_{\eta_5}c_{\eta_6}s_{\eta_7}\mathbf{p}_{\mathbf{h}_y}^{Wr} + s_{\eta_5}s_{\eta_6}\mathbf{p}_{\mathbf{h}_z}^{Wr}\right] + \\ & s_{\eta_2}\left[-c_{\eta_5}c_{\eta_6}c_{\eta_7}\mathbf{p}_{\mathbf{h}_x}^{Wr} + c_{\eta_5}c_{\eta_6}s_{\eta_7}\mathbf{p}_{\mathbf{h}_y}^{Wr} - c_{\eta_5}s_{\eta_6}\mathbf{p}_{\mathbf{h}_z}^{Wr}\right] \\ [\mathbf{J}_{Ha}]_{1,7} = & -\left(c_{\eta_2}c_{\eta_3}c_{\eta_4} - c_{\eta_2}s_{\eta_3}s_{\eta_4}\right)\left(c_{\eta_6}s_{\eta_7}\mathbf{p}_{\mathbf{h}_x}^{Wr} + c_{\eta_6}c_{\eta_7}\mathbf{p}_{\mathbf{h}_y}^{Wr}\right) - \\ & \left(c_{\eta_2}c_{\eta_3}s_{\eta_4} + c_{\eta_2}s_{\eta_3}c_{\eta_4}\right)\left[\left(-s_{\eta_5}s_{\eta_6}s_{\eta_7} + c_{\eta_5}c_{\eta_7}\right)\mathbf{p}_{\mathbf{h}_x}^{Wr} + \right. \\ & \left.\left(-s_{\eta_5}s_{\eta_6}c_{\eta_7} - c_{\eta_5}s_{\eta_7}\right)\mathbf{p}_{\mathbf{h}_y}^{Wr}\right] + s_{\eta_2}\left[\left(c_{\eta_5}s_{\eta_6}s_{\eta_7} + s_{\eta_5}c_{\eta_7}\right)\mathbf{p}_{\mathbf{h}_x}^{Wr} + \right. \\ & \left.\left(c_{\eta_5}s_{\eta_6}c_{\eta_7} - s_{\eta_5}s_{\eta_7}\right)\mathbf{p}_{\mathbf{h}_y}^{Wr}\right] \end{cases}$$

$$
[\mathbf{J}_{Ha}]_{2:1,\dots,n}\begin{cases}
[\mathbf{J}_{Ha}]_{2,1} = & \left(c_{\eta_6}c_{\eta_7}\mathbf{p}_{\mathbf{h}x}^{Wr} - c_{\eta_6}s_{\eta_7}\mathbf{p}_{\mathbf{h}y}^{Wr} + s_{\eta_6}\mathbf{p}_{\mathbf{h}z}^{Wr}\right)\left(c_{\eta_1}s_{\eta_2}c_{\eta_3}c_{\eta_4} - c_{\eta_1}s_{\eta_2}s_{\eta_3}s_{\eta_4} - \right. \\
& \left. s_{\eta_1}s_{\eta_3}c_{\eta_4} - s_{\eta_1}c_{\eta_3}s_{\eta_4}\right) + \left[\left(s_{\eta_5}s_{\eta_6}c_{\eta_7} + c_{\eta_5}s_{\eta_7}\right)\mathbf{p}_{\mathbf{h}x}^{Wr} + \right. \\
& \left.\left(-s_{\eta_5}s_{\eta_6}s_{\eta_7} + c_{\eta_5}c_{\eta_7}\right)\mathbf{p}_{\mathbf{h}y}^{Wr} - s_{\eta_5}c_{\eta_6}\mathbf{p}_{\mathbf{h}z}^{Wr} - L_{fo}\right]\left(-c_{\eta_1}s_{\eta_2}c_{\eta_3}s_{\eta_4} + s_{\eta_1}s_{\eta_3}s_{\eta_4} - \right. \\
& \left. s_{\eta_1}c_{\eta_3}c_{\eta_4} - c_{\eta_1}s_{\eta_2}s_{\eta_3}c_{\eta_4}\right) - c_{\eta_1}c_{\eta_2}\left[\left(-c_{\eta_5}s_{\eta_6}c_{\eta_7} + s_{\eta_5}s_{\eta_7}\right)\mathbf{p}_{\mathbf{h}x}^{Wr} + \right. \\
& \left.\left(c_{\eta_5}s_{\eta_6}s_{\eta_7} + s_{\eta_5}c_{\eta_7}\right)\mathbf{p}_{\mathbf{h}y}^{Wr} + c_{\eta_5}c_{\eta_6}\mathbf{p}_{\mathbf{h}z}^{Wr}\right] + \left(s_{\eta_1}c_{\eta_3} + c_{\eta_1}s_{\eta_2}s_{\eta_3}\right)L_{sh} \\
[\mathbf{J}_{Ha}]_{2,2} = & \left(c_{\eta_6}c_{\eta_7}\mathbf{p}_{\mathbf{h}x}^{Wr} - c_{\eta_6}s_{\eta_7}\mathbf{p}_{\mathbf{h}y}^{Wr} + s_{\eta_6}\mathbf{p}_{\mathbf{h}z}^{Wr}\right)\left(s_{\eta_1}c_{\eta_2}c_{\eta_3}c_{\eta_4} - s_{\eta_1}c_{\eta_2}s_{\eta_3}s_{\eta_4}\right) + \\
& \left[\left(s_{\eta_5}s_{\eta_6}c_{\eta_7} + c_{\eta_5}s_{\eta_7}\right)\mathbf{p}_{\mathbf{h}x}^{Wr} + \left(-s_{\eta_5}s_{\eta_6}s_{\eta_7} + c_{\eta_5}c_{\eta_7}\right)\mathbf{p}_{\mathbf{h}y}^{Wr} - s_{\eta_5}c_{\eta_6}\mathbf{p}_{\mathbf{h}z}^{Wr} - \right. \\
& \left. L_{fo}\right]\left(-s_{\eta_1}c_{\eta_2}c_{\eta_3}s_{\eta_4} - s_{\eta_1}c_{\eta_2}s_{\eta_3}c_{\eta_4}\right) + s_{\eta_1}s_{\eta_2}\left[\left(-c_{\eta_5}s_{\eta_6}c_{\eta_7} + s_{\eta_5}s_{\eta_7}\right)\mathbf{p}_{\mathbf{h}x}^{Wr} + \right. \\
& \left.\left(c_{\eta_5}s_{\eta_6}s_{\eta_7} + s_{\eta_5}c_{\eta_7}\right)\mathbf{p}_{\mathbf{h}y}^{Wr} + c_{\eta_5}c_{\eta_6}\mathbf{p}_{\mathbf{h}z}^{Wr}\right] + s_{\eta_1}c_{\eta_2}s_{\eta_3}L_{sh} \\
[\mathbf{J}_{Ha}]_{2,3} = & \left(c_{\eta_6}c_{\eta_7}\mathbf{p}_{\mathbf{h}x}^{Wr} - c_{\eta_6}s_{\eta_7}\mathbf{p}_{\mathbf{h}y}^{Wr} + s_{\eta_6}\mathbf{p}_{\mathbf{h}z}^{Wr}\right)\left(-s_{\eta_1}s_{\eta_2}s_{\eta_3}c_{\eta_4} - s_{\eta_1}s_{\eta_2}c_{\eta_3}s_{\eta_4} + \right. \\
& \left. c_{\eta_1}c_{\eta_3}c_{\eta_4} - c_{\eta_1}s_{\eta_3}s_{\eta_4}\right) + \left[\left(s_{\eta_5}s_{\eta_6}c_{\eta_7} + c_{\eta_5}s_{\eta_7}\right)\mathbf{p}_{\mathbf{h}x}^{Wr} + \right. \\
& \left.\left(-s_{\eta_5}s_{\eta_6}s_{\eta_7} + c_{\eta_5}c_{\eta_7}\right)\mathbf{p}_{\mathbf{h}y}^{Wr} - s_{\eta_5}c_{\eta_6}\mathbf{p}_{\mathbf{h}z}^{Wr} - L_{fo}\right]\left(s_{\eta_1}s_{\eta_2}s_{\eta_3}s_{\eta_4} - c_{\eta_1}c_{\eta_3}s_{\eta_4} - \right. \\
& \left. c_{\eta_1}s_{\eta_3}c_{\eta_4} - s_{\eta_1}s_{\eta_2}c_{\eta_3}c_{\eta_4}\right) + \left(c_{\eta_1}s_{\eta_3} + s_{\eta_1}s_{\eta_2}c_{\eta_3}\right)L_{sh} \\
[\mathbf{J}_{Ha}]_{2,4} = & \left(c_{\eta_6}c_{\eta_7}\mathbf{p}_{\mathbf{h}x}^{Wr} - c_{\eta_6}s_{\eta_7}\mathbf{p}_{\mathbf{h}y}^{Wr} + s_{\eta_6}\mathbf{p}_{\mathbf{h}z}^{Wr}\right)\left(-s_{\eta_1}s_{\eta_2}c_{\eta_3}s_{\eta_4} - s_{\eta_1}s_{\eta_2}s_{\eta_3}c_{\eta_4} - \right. \\
& \left. c_{\eta_1}s_{\eta_3}s_{\eta_4} + c_{\eta_1}c_{\eta_3}c_{\eta_4}\right) + \left[\left(s_{\eta_5}s_{\eta_6}c_{\eta_7} + c_{\eta_5}s_{\eta_7}\right)\mathbf{p}_{\mathbf{h}x}^{Wr} + \right. \\
& \left.\left(-s_{\eta_5}s_{\eta_6}s_{\eta_7} + c_{\eta_5}c_{\eta_7}\right)\mathbf{p}_{\mathbf{h}y}^{Wr} - s_{\eta_5}c_{\eta_6}\mathbf{p}_{\mathbf{h}z}^{Wr} - L_{fo}\right]\left(-s_{\eta_1}s_{\eta_2}c_{\eta_3}c_{\eta_4} - c_{\eta_1}s_{\eta_3}c_{\eta_4} - \right. \\
& \left. c_{\eta_1}c_{\eta_3}s_{\eta_4} + s_{\eta_1}s_{\eta_2}s_{\eta_3}s_{\eta_4}\right) \\
[\mathbf{J}_{Ha}]_{2,5} = & \left[\left(c_{\eta_5}s_{\eta_6}c_{\eta_7} - s_{\eta_5}s_{\eta_7}\right)\mathbf{p}_{\mathbf{h}x}^{Wr} + \left(-c_{\eta_5}s_{\eta_6}s_{\eta_7} - s_{\eta_5}c_{\eta_7}\right)\mathbf{p}_{\mathbf{h}y}^{Wr} - c_{\eta_5}c_{\eta_6}\mathbf{p}_{\mathbf{h}z}^{Wr}\right] \\
& \left(-s_{\eta_1}s_{\eta_2}c_{\eta_3}s_{\eta_4} - c_{\eta_1}s_{\eta_3}s_{\eta_4} + c_{\eta_1}c_{\eta_3}c_{\eta_4} - s_{\eta_1}s_{\eta_2}s_{\eta_3}c_{\eta_4}\right) - \\
& s_{\eta_1}c_{\eta_2}\left[\left(s_{\eta_5}s_{\eta_6}c_{\eta_7} + c_{\eta_5}s_{\eta_7}\right)\mathbf{p}_{\mathbf{h}x}^{Wr} + \left(-s_{\eta_5}s_{\eta_6}s_{\eta_7} + c_{\eta_5}c_{\eta_7}\right)\mathbf{p}_{\mathbf{h}y}^{Wr} - \right. \\
& \left. s_{\eta_5}c_{\eta_6}\mathbf{p}_{\mathbf{h}z}^{Wr}\right] \\
[\mathbf{J}_{Ha}]_{2,6} = & \left(-s_{\eta_6}c_{\eta_7}\mathbf{p}_{\mathbf{h}x}^{Wr} + s_{\eta_6}s_{\eta_7}\mathbf{p}_{\mathbf{h}y}^{Wr} + c_{\eta_6}\mathbf{p}_{\mathbf{h}z}^{Wr}\right)\left(s_{\eta_1}s_{\eta_2}c_{\eta_3}c_{\eta_4} - s_{\eta_1}s_{\eta_2}s_{\eta_3}s_{\eta_4} + \right. \\
& \left. c_{\eta_1}s_{\eta_3}c_{\eta_4} + c_{\eta_1}c_{\eta_3}s_{\eta_4}\right) + \left(s_{\eta_5}c_{\eta_6}c_{\eta_7}\mathbf{p}_{\mathbf{h}x}^{Wr} - s_{\eta_5}c_{\eta_6}s_{\eta_7}\mathbf{p}_{\mathbf{h}y}^{Wr} + s_{\eta_5}s_{\eta_6}\mathbf{p}_{\mathbf{h}z}^{Wr}\right) \\
& \left(-s_{\eta_1}s_{\eta_2}c_{\eta_3}s_{\eta_4} - c_{\eta_1}s_{\eta_3}s_{\eta_4} + c_{\eta_1}c_{\eta_3}c_{\eta_4} - s_{\eta_1}s_{\eta_2}s_{\eta_3}c_{\eta_4}\right) - \\
& s_{\eta_1}c_{\eta_2}\left[-c_{\eta_5}c_{\eta_6}c_{\eta_7}\mathbf{p}_{\mathbf{h}x}^{Wr} + c_{\eta_5}c_{\eta_6}s_{\eta_7}\mathbf{p}_{\mathbf{h}y}^{Wr} - c_{\eta_5}s_{\eta_6}\mathbf{p}_{\mathbf{h}z}^{Wr}\right] \\
[\mathbf{J}_{Ha}]_{2,7} = & \left(-c_{\eta_6}s_{\eta_7}\mathbf{p}_{\mathbf{h}x}^{Wr} - c_{\eta_6}c_{\eta_7}\mathbf{p}_{\mathbf{h}y}^{Wr}\right)\left(s_{\eta_1}s_{\eta_2}c_{\eta_3}c_{\eta_4} - s_{\eta_1}s_{\eta_2}s_{\eta_3}s_{\eta_4} + c_{\eta_1}s_{\eta_3}c_{\eta_4} + \right. \\
& \left. c_{\eta_1}c_{\eta_3}s_{\eta_4}\right) + \left[\left(-s_{\eta_5}s_{\eta_6}s_{\eta_7} + c_{\eta_5}c_{\eta_7}\right)\mathbf{p}_{\mathbf{h}x}^{Wr} + \left(-s_{\eta_5}s_{\eta_6}c_{\eta_7} - c_{\eta_5}s_{\eta_7}\right)\mathbf{p}_{\mathbf{h}y}^{Wr}\right] \\
& \left(-s_{\eta_1}s_{\eta_2}c_{\eta_3}s_{\eta_4} - c_{\eta_1}s_{\eta_3}s_{\eta_4} + c_{\eta_1}c_{\eta_3}c_{\eta_4} - s_{\eta_1}s_{\eta_2}s_{\eta_3}c_{\eta_4}\right) - \\
& s_{\eta_1}c_{\eta_2}\left[\left(c_{\eta_5}s_{\eta_6}s_{\eta_7} + s_{\eta_5}c_{\eta_7}\right)\mathbf{p}_{\mathbf{h}x}^{Wr} + \left(c_{\eta_5}s_{\eta_6}c_{\eta_7} - s_{\eta_5}s_{\eta_7}\right)\mathbf{p}_{\mathbf{h}y}^{Wr}\right]
\end{cases}
$$

$$
[\mathbf{J}_{Ha}]_{3:1,\ldots,n}
\begin{cases}
[\mathbf{J}_{Ha}]_{3,1} = & \left(c_{\eta_6}c_{\eta_7}\mathbf{p}_{\mathbf{h}x}^{Wr} - c_{\eta_6}s_{\eta_7}\mathbf{p}_{\mathbf{h}y}^{Wr} + s_{\eta_6}\mathbf{p}_{\mathbf{h}z}^{Wr}\right)\left(-s_{\eta_1}s_{\eta_2}s_{\eta_3}s_{\eta_4} + s_{\eta_1}s_{\eta_2}c_{\eta_3}c_{\eta_4} + \right. \\
& \left. c_{\eta_1}s_{\eta_3}c_{\eta_4} + c_{\eta_1}c_{\eta_3}s_{\eta_4}\right) + \left[\left(s_{\eta_5}s_{\eta_6}c_{\eta_7} + c_{\eta_5}s_{\eta_7}\right)\mathbf{p}_{\mathbf{h}x}^{Wr} + \left(-s_{\eta_5}s_{\eta_6}s_{\eta_7} + \right.\right. \\
& \left.\left. c_{\eta_5}c_{\eta_7}\right)\mathbf{p}_{\mathbf{h}y}^{Wr} - s_{\eta_5}c_{\eta_6}\mathbf{p}_{\mathbf{h}z}^{Wr} - L_{fo}\right]\left(-s_{\eta_1}s_{\eta_2}c_{\eta_3}s_{\eta_4} - s_{\eta_1}s_{\eta_2}s_{\eta_3}c_{\eta_4} - \right. \\
& \left. c_{\eta_1}s_{\eta_3}s_{\eta_4} + c_{\eta_1}c_{\eta_3}c_{\eta_4}\right) - s_{\eta_1}c_{\eta_2}\left[\left(-c_{\eta_5}s_{\eta_6}c_{\eta_7} + s_{\eta_5}s_{\eta_7}\right)\mathbf{p}_{\mathbf{h}x}^{Wr} + \right. \\
& \left.\left(c_{\eta_5}s_{\eta_6}s_{\eta_7} + s_{\eta_5}c_{\eta_7}\right)\mathbf{p}_{\mathbf{h}y}^{Wr} + c_{\eta_5}c_{\eta_6}\mathbf{p}_{\mathbf{h}z}^{Wr}\right] - \left(c_{\eta_1}c_{\eta_3} - s_{\eta_1}s_{\eta_2}s_{\eta_3}\right)L_{sh} \\
[\mathbf{J}_{Ha}]_{3,2} = & \left(c_{\eta_6}c_{\eta_7}\mathbf{p}_{\mathbf{h}x}^{Wr} - c_{\eta_6}s_{\eta_7}\mathbf{p}_{\mathbf{h}y}^{Wr} + s_{\eta_6}\mathbf{p}_{\mathbf{h}z}^{Wr}\right)\left(c_{\eta_1}c_{\eta_2}s_{\eta_3}s_{\eta_4} - c_{\eta_1}c_{\eta_2}c_{\eta_3}c_{\eta_4}\right) + \\
& \left[\left(s_{\eta_5}s_{\eta_6}c_{\eta_7} + c_{\eta_5}s_{\eta_7}\right)\mathbf{p}_{\mathbf{h}x}^{Wr} + \left(-s_{\eta_5}s_{\eta_6}s_{\eta_7} + c_{\eta_5}c_{\eta_7}\right)\mathbf{p}_{\mathbf{h}y}^{Wr} - \right. \\
& \left. s_{\eta_5}c_{\eta_6}\mathbf{p}_{\mathbf{h}z}^{Wr} - L_{fo}\right]\left(c_{\eta_1}c_{\eta_2}c_{\eta_3}s_{\eta_4} + c_{\eta_1}c_{\eta_2}s_{\eta_3}c_{\eta_4}\right) - c_{\eta_1}s_{\eta_2}\left[\left(-c_{\eta_5}s_{\eta_6}c_{\eta_7} + \right.\right. \\
& \left.\left. s_{\eta_5}s_{\eta_7}\right)\mathbf{p}_{\mathbf{h}x}^{Wr} + \left(c_{\eta_5}s_{\eta_6}s_{\eta_7} + s_{\eta_5}c_{\eta_7}\right)\mathbf{p}_{\mathbf{h}y}^{Wr} + c_{\eta_5}c_{\eta_6}\mathbf{p}_{\mathbf{h}z}^{Wr}\right] - \\
& c_{\eta_1}c_{\eta_2}s_{\eta_3}L_{sh} \\
[\mathbf{J}_{Ha}]_{3,3} = & \left(c_{\eta_6}c_{\eta_7}\mathbf{p}_{\mathbf{h}x}^{Wr} - c_{\eta_6}s_{\eta_7}\mathbf{p}_{\mathbf{h}y}^{Wr} + s_{\eta_6}\mathbf{p}_{\mathbf{h}z}^{Wr}\right)\left(c_{\eta_1}s_{\eta_2}c_{\eta_3}s_{\eta_4} + c_{\eta_1}s_{\eta_2}s_{\eta_3}c_{\eta_4} + \right. \\
& \left. s_{\eta_1}c_{\eta_3}c_{\eta_4} - s_{\eta_1}s_{\eta_3}s_{\eta_4}\right) + \left[\left(s_{\eta_5}s_{\eta_6}c_{\eta_7} + c_{\eta_5}s_{\eta_7}\right)\mathbf{p}_{\mathbf{h}x}^{Wr} + \left(-s_{\eta_5}s_{\eta_6}s_{\eta_7} + \right.\right. \\
& \left.\left. c_{\eta_5}c_{\eta_7}\right)\mathbf{p}_{\mathbf{h}y}^{Wr} - s_{\eta_5}c_{\eta_6}\mathbf{p}_{\mathbf{h}z}^{Wr} - L_{fo}\right]\left(-c_{\eta_1}s_{\eta_2}s_{\eta_3}s_{\eta_4} + c_{\eta_1}s_{\eta_2}c_{\eta_3}c_{\eta_4} - \right. \\
& \left. s_{\eta_1}c_{\eta_3}s_{\eta_4} - s_{\eta_1}s_{\eta_3}c_{\eta_4}\right) - \left(-s_{\eta_1}s_{\eta_3} + c_{\eta_1}s_{\eta_2}c_{\eta_3}\right)L_{sh} \\
[\mathbf{J}_{Fo}]_{3,4} = & \left(c_{\eta_6}c_{\eta_7}\mathbf{p}_{\mathbf{h}x}^{Wr} - c_{\eta_6}s_{\eta_7}\mathbf{p}_{\mathbf{h}y}^{Wr} + s_{\eta_6}\mathbf{p}_{\mathbf{h}z}^{Wr}\right)\left(c_{\eta_1}s_{\eta_2}s_{\eta_3}c_{\eta_4} + c_{\eta_1}s_{\eta_2}c_{\eta_3}s_{\eta_4} - \right. \\
& \left. s_{\eta_1}s_{\eta_3}s_{\eta_4} + s_{\eta_1}c_{\eta_3}c_{\eta_4}\right) + \left[\left(s_{\eta_5}s_{\eta_6}c_{\eta_7} + c_{\eta_5}s_{\eta_7}\right)\mathbf{p}_{\mathbf{h}x}^{Wr} + \left(-s_{\eta_5}s_{\eta_6}s_{\eta_7} + \right.\right. \\
& \left.\left. c_{\eta_5}c_{\eta_7}\right)\mathbf{p}_{\mathbf{h}y}^{Wr} - s_{\eta_5}c_{\eta_6}\mathbf{p}_{\mathbf{h}z}^{Wr} - L_{fo}\right]\left(c_{\eta_1}s_{\eta_2}c_{\eta_3}c_{\eta_4} - c_{\eta_1}s_{\eta_2}s_{\eta_3}s_{\eta_4} - \right. \\
& \left. s_{\eta_1}s_{\eta_3}c_{\eta_4} - s_{\eta_1}c_{\eta_3}s_{\eta_4}\right) \\
[\mathbf{J}_{Fo}]_{3,5} = & \left[\left(c_{\eta_5}s_{\eta_6}c_{\eta_7} - s_{\eta_5}s_{\eta_7}\right)\mathbf{p}_{\mathbf{h}x}^{Wr} + \left(-c_{\eta_5}s_{\eta_6}s_{\eta_7} - s_{\eta_5}c_{\eta_7}\right)\mathbf{p}_{\mathbf{h}y}^{Wr} - c_{\eta_5}c_{\eta_6}\mathbf{p}_{\mathbf{h}z}^{Wr}\right] \\
& \left(c_{\eta_1}s_{\eta_2}c_{\eta_3}s_{\eta_4} + c_{\eta_1}s_{\eta_2}s_{\eta_3}c_{\eta_4} - s_{\eta_1}s_{\eta_3}s_{\eta_4} + s_{\eta_1}c_{\eta_3}c_{\eta_4}\right) + c_{\eta_1}c_{\eta_2}\left[\left(s_{\eta_5}s_{\eta_6}c_{\eta_7}\right.\right. \\
& \left.\left. + c_{\eta_5}s_{\eta_7}\right)\mathbf{p}_{\mathbf{h}x}^{Wr} + \left(-s_{\eta_5}s_{\eta_6}s_{\eta_7} + c_{\eta_5}c_{\eta_7}\right)\mathbf{p}_{\mathbf{h}y}^{Wr} - s_{\eta_5}c_{\eta_6}\mathbf{p}_{\mathbf{h}z}^{Wr}\right] \\
[\mathbf{J}_{Fo}]_{3,6} = & \left(-s_{\eta_6}c_{\eta_7}\mathbf{p}_{\mathbf{h}x}^{Wr} + s_{\eta_6}s_{\eta_7}\mathbf{p}_{\mathbf{h}y}^{Wr} + c_{\eta_6}\mathbf{p}_{\mathbf{h}z}^{Wr}\right)\left(c_{\eta_1}s_{\eta_2}s_{\eta_3}s_{\eta_4} - c_{\eta_1}s_{\eta_2}c_{\eta_3}c_{\eta_4} + \right. \\
& \left. s_{\eta_1}s_{\eta_3}c_{\eta_4} + s_{\eta_1}c_{\eta_3}s_{\eta_4}\right) + \left[s_{\eta_5}c_{\eta_6}c_{\eta_7}\mathbf{p}_{\mathbf{h}x}^{Wr} - s_{\eta_5}c_{\eta_6}s_{\eta_7}\mathbf{p}_{\mathbf{h}y}^{Wr} + \right. \\
& \left. s_{\eta_5}s_{\eta_6}\mathbf{p}_{\mathbf{h}z}^{Wr}\right]\left(c_{\eta_1}s_{\eta_2}c_{\eta_3}s_{\eta_4} + c_{\eta_1}s_{\eta_2}s_{\eta_3}c_{\eta_4} - s_{\eta_1}s_{\eta_3}s_{\eta_4} + s_{\eta_1}c_{\eta_3}c_{\eta_4}\right) + \\
& c_{\eta_1}c_{\eta_2}\left[-c_{\eta_5}c_{\eta_6}c_{\eta_7}\mathbf{p}_{\mathbf{h}x}^{Wr} + c_{\eta_5}c_{\eta_6}s_{\eta_7}\mathbf{p}_{\mathbf{h}y}^{Wr} - c_{\eta_5}s_{\eta_6}\mathbf{p}_{\mathbf{h}z}^{Wr}\right] \\
[\mathbf{J}_{Fo}]_{3,7} = & \left(-c_{\eta_6}s_{\eta_7}\mathbf{p}_{\mathbf{h}x}^{Wr} - c_{\eta_6}c_{\eta_7}\mathbf{p}_{\mathbf{h}y}^{Wr}\right)\left(c_{\eta_1}s_{\eta_2}s_{\eta_3}s_{\eta_4} - c_{\eta_1}s_{\eta_2}c_{\eta_3}c_{\eta_4} + s_{\eta_1}s_{\eta_3}c_{\eta_4} + \right. \\
& \left. s_{\eta_1}c_{\eta_3}s_{\eta_4}\right) + \left[\left(-s_{\eta_5}s_{\eta_6}s_{\eta_7} + c_{\eta_5}c_{\eta_7}\right)\mathbf{p}_{\mathbf{h}x}^{Wr} + \left(-s_{\eta_5}s_{\eta_6}c_{\eta_7} - c_{\eta_5}s_{\eta_7}\right)\mathbf{p}_{\mathbf{h}y}^{Wr}\right] \\
& \left(c_{\eta_1}s_{\eta_2}c_{\eta_3}s_{\eta_4} + c_{\eta_1}s_{\eta_2}s_{\eta_3}c_{\eta_4} - s_{\eta_1}s_{\eta_3}s_{\eta_4} + s_{\eta_1}c_{\eta_3}c_{\eta_4}\right) + \\
& c_{\eta_1}c_{\eta_2}\left[\left(c_{\eta_5}s_{\eta_6}s_{\eta_7} + s_{\eta_5}c_{\eta_7}\right)\mathbf{p}_{\mathbf{h}x}^{Wr} + \left(c_{\eta_5}s_{\eta_6}c_{\eta_7} - s_{\eta_5}s_{\eta_7}\right)\mathbf{p}_{\mathbf{h}y}^{Wr}\right]
\end{cases}
$$

4.3 Human arm model equations

From equations Eq. 4.1 and Eq. 4.5, the *continuous non-linear* model of the 7 DoF RM can be derived, where the dependence from the position of the markers is not reported for simplicity.

$$\begin{cases} \dot{\mathbf{p}} &= \mathbf{J}(\boldsymbol{\eta}) \cdot \dot{\boldsymbol{\eta}} \\ \mathbf{p} &= \boldsymbol{\Phi}(\boldsymbol{\eta}) \end{cases}$$

In the hypothesis in which $m > 2$ and the Jacobian $\mathbf{J} \in \mathbb{R}^{(3m)\times n}$ is full-rank, with reference to A, $\mathbf{J}$ admits the *left presudo-inverse* $\mathbf{J}_L^{\dagger} = \left(\mathbf{J}^T \cdot \mathbf{J}\right)^{-1} \cdot \mathbf{J}^T$. Hence

$$\dot{\boldsymbol{\eta}} = \left(\mathbf{J}^T(\boldsymbol{\eta}) \cdot \mathbf{J}(\boldsymbol{\eta})\right)^{-1} \cdot \mathbf{J}^T(\boldsymbol{\eta}) \cdot \dot{\mathbf{p}}$$

which represent the LS solution for Eq. 4.5. Saying that $\mathbf{J}(\boldsymbol{\eta})$ is full column-rank means that the configuration of the arm $\boldsymbol{\eta}$ is such that there are not *kinematic singularities*. However, it is important to underline that the inversion of the Jacobian can represent a serious inconvenience not only at a singularity but also in the neighbourhood of a singularity. Indeed, in the neighbourhood of a singularity, the determinant takes on a relatively small value which can cause large joint velocities. In order to provide a measure of the distance from a singularity, one can consider the ratio between the minimum and maximum singular values of the Jacobian $\frac{\sigma_1}{\sigma_n}$, assuming rank $[\mathbf{J}(\boldsymbol{\eta})] = n$, which is equivalent to the condition number of matrix $\mathbf{J}(\boldsymbol{\eta})$. The *continuous*-time *non-linear* model of the 7 DoF RM follows:

$$\begin{cases} \dot{\boldsymbol{\eta}}(t) &= \underbrace{\left(\mathbf{J}^T(\boldsymbol{\eta}(t)) \cdot \mathbf{J}(\boldsymbol{\eta}(t))\right)^{-1} \cdot \mathbf{J}^T(\boldsymbol{\eta}(t))}_{\mathbf{J}_L^{\dagger}(\boldsymbol{\eta}(t))} \cdot \dot{\mathbf{p}}(t) \\ \mathbf{p}(t) &= \boldsymbol{\Phi}(\boldsymbol{\eta}(t)) \end{cases} \tag{4.6}$$

As already mentioned, $\mathbf{J}$ and $\boldsymbol{\Phi}$ depend also on the number of markers on the shoulder, forearm and hand $|\mathcal{S}|$, $|\mathcal{F}|$ and $|\mathcal{H}|$ and on the specific markers' position.

5

Matlab simulations

As discussed in Section 1.1, in order to better the estimate of the forces and torques exerted by (**H**) to (**L**) in Eq. 1.3, it is necessary to improve the estimate of $\boldsymbol{\eta}(t)$ by using some different estimation algorithm approaches from that used in [19]. Specifically, the interested quantity is estimated indirectly by making use of some markers placed along the human arm. For this purpose, the Motion Capture System is used. Indeed, the Qualisys Track Manager (QTM) software can measure the linear position and velocity as the cameras observing lightweight markers attached to the object. In particular, three different estimation algorithm are analyzed:

i Least-squares (LS)

ii Linearized Kalman filter (LKF)

iii Extended Kalman filter (EKF)

In all these estimation algorithms, the model of the human arm in Eq. 4.6 is required. Before tackling the *real-world* experimental problem, where the real human arm is used, some simulations are run, in which a Simscape model of the human arm can be exploited, and different estimators can be analyzed theoretically, leading to a first working solution.

By exploiting the Simscape platform, it is possible to develop the 7 DoF model of the right human arm. It can be seen as a composition of:

1. Shoulder
   (a) Shoulder-joint block –> η_1, η_2, η_3
      i. World reference frame RF_W
      ii. Constant rotation $\mathbf{R}^{W}_{W'}$
      iii. Variable rotation $\mathbf{R}^{W'}_{\eta_1}(\eta_1) = \mathbf{R}_z(\eta_1)$
      iv. Constant rotation $\mathbf{R}^{\eta_1}_{\eta_1'}$
      v. Variable rotation $\mathbf{R}^{\eta_1'}_{\eta_2}(\eta_2) = \mathbf{R}_z(\eta_2)$
      vi. Constant rotation $\mathbf{R}^{\eta_2}_{\eta_2'}$
      vii. Variable rotation $\mathbf{R}^{\eta_2'}_{Sh}(\eta_3) = \mathbf{R}_z(\eta_3)$
      viii. Shoulder base reference frame RF_{Sh}
   (b) Shoulder structure: RF_{Sh} –> $RF_{Sh'}$

2. Forearm
   (a) Elbow-joint block –> η_4
      i. Shoulder final reference frame $RF_{Sh'}$
      ii. Variable rotation $\mathbf{R}^{Sh'}_{El}(\eta_4)$
      iii. Elbow base reference frame RF_{El}
   (b) Forearm structure: RF_{El} –> $RF_{El'}$

3. Hand
   (a) Wrist-joint block –> η_5, η_6, η_7
      i. Elbow final reference frame $RF_{El'}$
      ii. Constant rotation $\mathbf{R}^{El'}_{El''}$
      iii. Variable rotation $\mathbf{R}^{El''}_{\eta_5}(\eta_5) = \mathbf{R}_z(\eta_5)$
      iv. Constant rotation $\mathbf{R}^{\eta_5}_{\eta_5'}$
      v. Variable rotation $\mathbf{R}^{\eta_5'}_{\eta_6}(\eta_6) = \mathbf{R}_z(\eta_6)$
      vi. Constant rotation $\mathbf{R}^{\eta_6}_{\eta_6'}$
      vii. Variable rotation $\mathbf{R}^{\eta_6'}_{Wr}(\eta_7) = \mathbf{R}_z(\eta_7)$
      viii. Wrist base reference frame RF_{Wr}
   (b) Hand structure

Each joint block is composed of constant rotations, performed by using the *Rigid Transforms* block, and variable rotations, by making use of the *Revolute Joint* block. As far as the shoulder and the forearm structures are concerned, they are represented by the *Cylindrical Solid* block. In the same library, the block *Brick Solid* is employed to represent the hand structure. The m markers are instead constituted by the *Spherical Solid* block. In order to apply the estimation algorithms, the specific number of markers $|\mathcal{S}|$, $|\mathcal{F}|$, $|\mathcal{H}|$, and the simulated trajectory $\boldsymbol{\eta}^{ref}$ have to be decided.

5.1 Suitable markers' combinations and joint-space trajectory

The markers can be located on the entire shoulder, forearm and hand surfaces. Let $\mathbf{M_s}$, $\mathbf{M_f}$ and $\mathbf{M_h}$ be three markers placed on the shoulder, forearm and hand, respectively. Since the shoulder and forearm are modeled as a cylinder solid while the hand as a brick solid, with reference to Fig. 4.1, it holds:

$$
\begin{array}{lcc}
 & \textit{polar} & \textit{cartesian} \\
\textbf{Shoulder:} & \begin{cases} \theta_s \sim U\left[0, 2\pi\right] \\ \rho_s \sim U\left[-L_{sh}, 0\right] \end{cases} \implies & \begin{cases} \mathbf{p_s}_x^{Sh} = -\left(r_{sh} + r_M\right) \cdot \cos\left(\theta_s\right) \\ \mathbf{p_s}_y^{Sh} = \rho_s \\ \mathbf{p_s}_z^{Sh} = \left(r_{sh} + r_M\right) \cdot \sin\left(\theta_s\right) \end{cases} \\
\textbf{Forearm:} & \begin{cases} \theta_f \sim U\left[0, 2\pi\right] \\ \rho_f \sim U\left[-L_{fo}, 0\right] \end{cases} \implies & \begin{cases} \mathbf{p_f}_x^{El} = -\left(r_{fo} + r_M\right) \cdot \cos\left(\theta_f\right) \\ \mathbf{p_f}_y^{El} = \rho_f \\ \mathbf{p_f}_z^{El} = \left(r_{fo} + r_M\right) \cdot \sin\left(\theta_s\right) \end{cases} \\
\textbf{Hand:} & & \implies \begin{cases} \mathbf{p_h}_x^{Wr} = \sim U\left[-\frac{W_{ha}}{2}, \frac{W_{ha}}{2}\right] \\ \mathbf{p_h}_y^{Wr} = \sim U\left[-L_{ha}, 0\right] \\ \mathbf{p_h}_z^{Wr} = \frac{H_{ha}}{2} + r_M \end{cases}
\end{array}
\tag{5.1}
$$

where r_{sh}, r_{fo}, r_M are the radius of the shoulder, forearm and single marker. Hence, it is possible to generate random markers, which are expressed with respect to the corresponding base reference frame RF_{Sh}, RF_{El} or RF_{Wr}. The two aspects to decide are the number of markers on the 3 links and the reference joint-

space trajectory to use. As far as the former is concerned, various combinations can be analyzed. The whole set of combinations is presented in Tab. 5.1.

Combinations of markers				
#	$\lvert\mathcal{S}\rvert$	$\lvert\mathcal{F}\rvert$	$\lvert\mathcal{H}\rvert$	m
1^{st}	0	1	2	3
2^{nd}	1	0	2	
3^{th}	1	1	1	
4^{th}	0	2	2	4
5^{th}	1	0	3	
6^{th}	1	1	2	
7^{th}	1	2	1	
8^{th}	2	0	2	
9^{th}	1	2	2	5
10^{th}	2	2	1	

Table 5.1: Combination of number of markers on the shoulder, forearm and hand to be analyzed

As it is well described in the next section, a first Matlab simulation is run to analyze the Jacobian behaviour in each of the above markers' combination.

Regarding the trajectory to choose as reference, each joint variable trajectory is chosen by using cubic spline interpolation; a saturation block is added as to constraint the motion. The assigned trajectory is depicted below

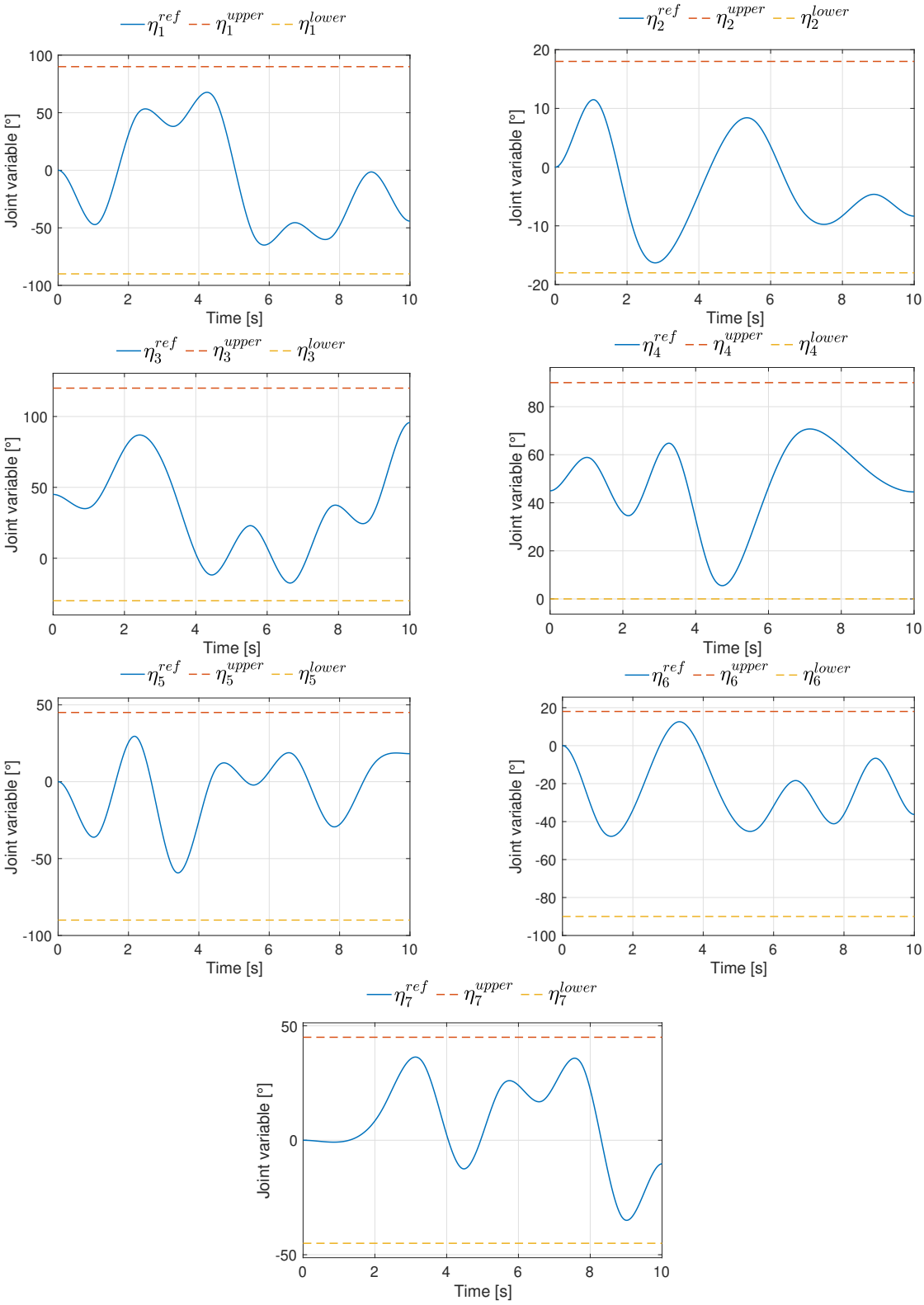

Figure 5.1: LS, EKF: joint variables assigned trajectory

5.2 Preliminary simulation

Given the trajectory $\boldsymbol{\eta}^{ref}(t)$ and a specific combination of number of markers on the 3 links $|\mathcal{S}|, |\mathcal{F}|$ and $|\mathcal{H}|$, a first simulation is run in order to determine if the j^{th} combination, $j = 1, \ldots, 10$, is more likely or not to make the Jacobian singular or close to be singular. In detail, for each combination, 30 simulations are run where, in each one of them, the markers' position are generated randomly, by using eq. 5.1. Let them denote as $\mathbf{p}^B_{j,i}$, where the index i is referred to the i^{th} simulation. At this point, the corresponding Jacobian is evaluated at each time instant of $\boldsymbol{\eta}^{ref}$, therefore one can establish if $\mathbf{J}^{j,i}_{t_k} = \mathbf{J}\left(\boldsymbol{\eta}^{ref}(t_k), \mathbf{p}^B_{j,i}\right)$ is *non-singular*, *singular* or *quasi-singular*, $\forall t_k$. In order to determine if a point of the given trajectory is *quasi-singular*, the condition number of matrix $\mathbf{J}^{j,i}_{t_k}$, $\kappa\left(\mathbf{J}^{j,i}_{t_k}\right) = \frac{\sigma_1\left(\mathbf{J}^{j,i}_{t_k}\right)}{\sigma_n\left(\mathbf{J}^{j,i}_{t_k}\right)}$, is taken into account. The threshold above which $\mathbf{J}^{j,i}_{t_k}$ is considered to be *quasi-singular* is chosen as $\kappa\left(\mathbf{J}^{j,i}_{t_k}\right) > 1000$. This procedure is repeated $\forall j, \forall i$. In the following, for each markers' combination and simulation, the percentage of *non-singular*(NS), *singular*(S) and *quasi-singular*(QS) points of the known trajectory are shown. Before proceeding, the values for the length and radius of the shoulder, L_{sh} and r_{sh}, the length and radius of the forearm, L_{fo} and r_{fo}, the hand dimensions, W_{ha}, L_{ha} and H_{ha}, and the radius of the marker, r_M, are given below.

Human arm parameters	
link	dimensions $[m]$
Shoulder	$L_{sh} = 0.25$
	$r_{sh} = 0.05$
Forearm	$L_{fo} = 0.25$
	$r_{fo} = 0.03$
Hand	$W_{ha} = 0.1$
	$L_{ha} = 0.18$
	$H_{ha} = 0.04$
Markers	$r_M = 0.01$

Table 5.2: Human arm parameters

The L_{sh} and L_{fo} values are necessary for the forward and differential kinematics computation while all the other ones are needed for the markers generation.

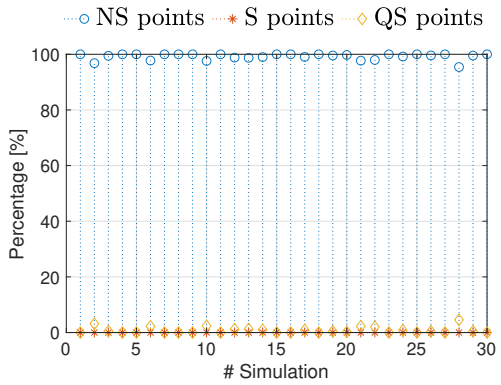

(a) 1^{st} combination

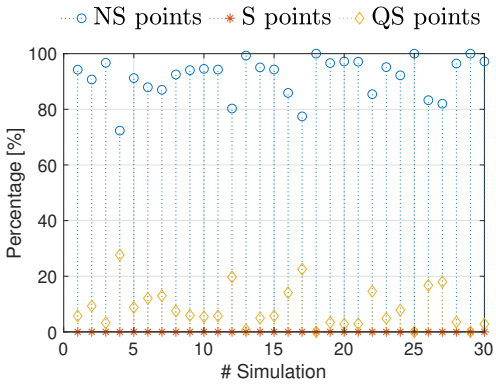

(b) 2^{nd} combination

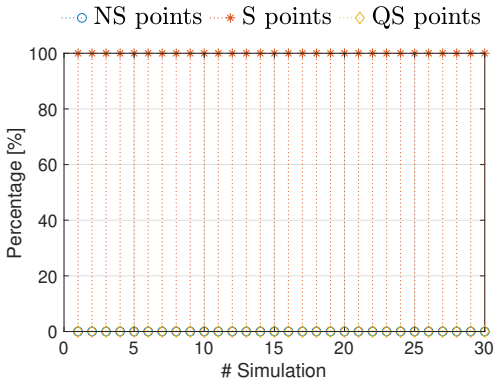

(c) 3^{th} combination

Figure 5.2: 1^{st}, 2^{nd} and 3^{th} combination of $m = 3$ markers

By observing Fig. 5.2, 5.3 and 5.4, one can state that the only markers' combinations for which, for each one of the 30 simulations, all points along the trajectory are singular are the ones with $|\mathcal{H}| = 1$, hence the 3^{th}, the 7^{th} and the 10^{th} combination. At least two markers must be placed on the hand in order not to have singular configurations. In the following, only a specific set of markers is considered. This is chosen as the one, among the 30 simulations of the 6^{th} combination, having the lowest condition number average. Let $\mathbf{p_1}_{6,i}^{Sh}$, $\mathbf{p_2}_{6,i}^{El}$, $\mathbf{p_3}_{6,i}^{Wr}$ and $\mathbf{p_4}_{6,i}^{Wr}$ be the random marker on the shoulder, the random marker on the forearm and the 2 random markers on the hand of the i^{th} simulation ($i = 1, \dots, 30$) of the 6^{th} combination. They are expressed with respect to RF_{Sh}, RF_{El}, RF_{Wr} and RF_{Wr}, respectively. By looking at Fig. 5.3c, each simulation has 100% non-singularities.

One can compute the average condition number of the i^{th} simulation (of the 6^{th} combination) as $\bar{\kappa}_{6,i} = \frac{1}{N} \sum_{k=1}^{N} \kappa \left(\mathbf{J}_{t_k}^{6,i} \right)$.

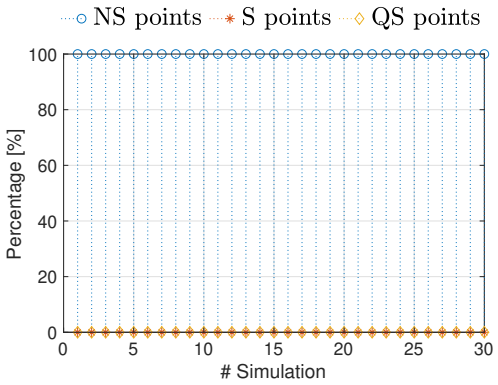

(a) 4^{th} combination

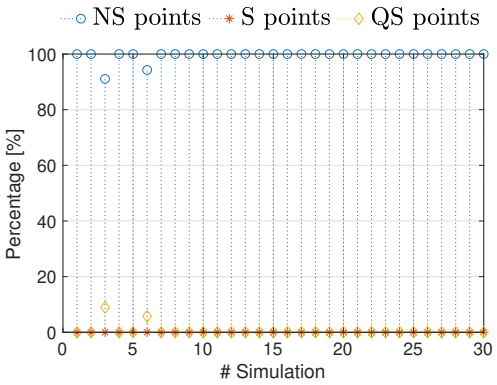

(b) 5^{th} combination

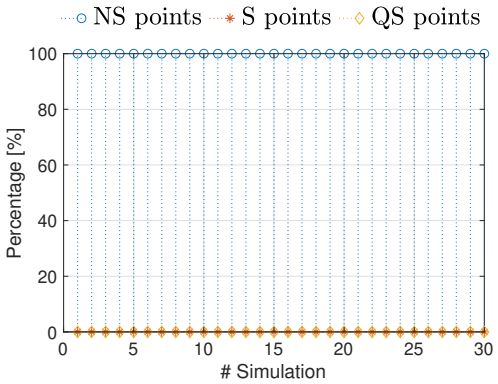

(c) 6^{th} combination

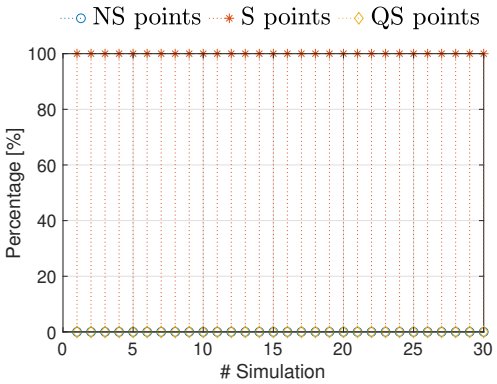

(d) 7^{th} combination

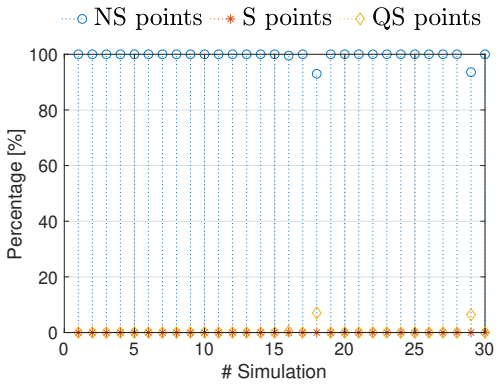

(e) 8^{th} combination

Figure 5.3: 4^{th}, 5^{th}, 6^{th}, 7^{th} and 8^{th} combination of $m = 4$ markers

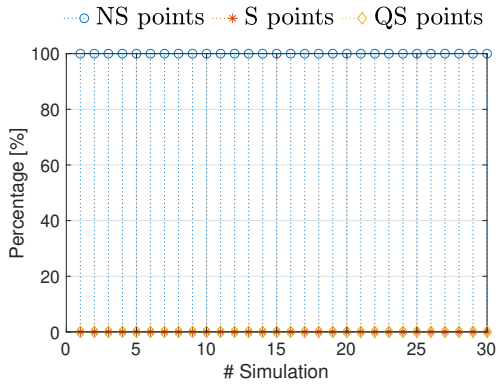

(a) 9^{th} combination

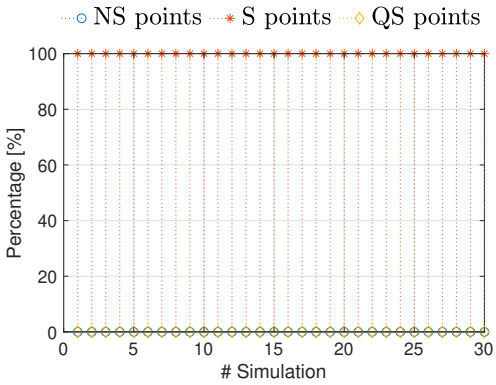

(b) 10^{th} combination

Figure 5.4: 9^{th} and 10^{th} combination of $m = 5$ markers

Let

$$\hat{i} = \underset{i=1,\dots,30}{\operatorname{argmin}} \quad \bar{\kappa}_{6,i}$$

Hence, $\mathbf{p_1}^{Sh}_{6,\hat{i}}$, $\mathbf{p_2}^{El}_{6,\hat{i}}$, $\mathbf{p_3}^{Wr}_{6,\hat{i}}$ and $\mathbf{p_4}^{Wr}_{6,\hat{i}}$ is the chosen set of markers. In Tab. 5.3 their values is shown.

Chosen set of markers	
link	$x-y-z$ coordinates $[m]$
Shoulder	$\mathbf{p_1}^{Sh}_{6,\hat{i}} = \begin{bmatrix} 0.0292 \\ -0.1249 \\ -0.0524 \end{bmatrix}$
Forearm	$\mathbf{p_2}^{El}_{6,\hat{i}} = \begin{bmatrix} -0.0080 \\ -0.1071 \\ 0.0392 \end{bmatrix}$
Hand	$\mathbf{p_3}^{Wr}_{6,\hat{i}} = \begin{bmatrix} -0.0378 \\ -0.0721 \\ 0.0300 \end{bmatrix}$
	$\mathbf{p_4}^{Wr}_{6,\hat{i}} = \begin{bmatrix} 0.0171 \\ -0.1699 \\ 0.0300 \end{bmatrix}$

Table 5.3: Set of markers with minimum condition number average, among the 30 simulations of the 6^{th} combination

In some next simulations, the 2^{nd} combination of markers is used, showing the estimation behaviour in the case in which the corresponding Jacobian is *quasi-singular*. The considered set of markers $\mathbf{p}_{\mathbf{1}_2}^{Sh}$, $\mathbf{p}_{\mathbf{2}_2}^{Wr}$ and $\mathbf{p}_{\mathbf{3}_2}^{Wr}$ can be found in Tab. 5.4.

Chosen set of markers	
link	$x-y-z$ coordinates $[m]$
Shoulder	$\mathbf{p}_{\mathbf{1}_2}^{Sh} = \begin{bmatrix} 0.0336 \\ -0.2072 \\ -0.0497 \end{bmatrix}$
	$\mathbf{p}_{\mathbf{2}_2}^{Wr} = \begin{bmatrix} 0.0206 \\ -0.1302 \\ 0.0300 \end{bmatrix}$
Hand	$\mathbf{p}_{\mathbf{3}_2}^{Wr} = \begin{bmatrix} -0.0468 \\ -0.1717 \\ 0.0300 \end{bmatrix}$

Table 5.4: Set of markers of the 2^{nd} combination

With the choice of markers in Tab.5.3, the human arm model follows, where the dependence from $\mathbf{p}_{6,\hat{i}}^{B}$ is made explicit. The position $\mathbf{p}(t)$ and velocity $\dot{\mathbf{p}}(t)$ of the markers are measured directly. Since these two entities, in the real experiment, are measured by the Motion Capture System, it is plausible to add a white Gaussian noise to the outputs of the human arm , in Simscape, so to generate noisy markers' position and velocity. Let $\mathbf{n}_{\dot{\mathbf{p}}}(t) \sim \mathcal{N}\left(0, \mathbf{N}_{\dot{\mathbf{p}}}\right)$ and $\mathbf{v}(t) \sim \mathcal{N}(0, \mathbf{R})$ be the noises, concerning the markers' velocity and position, respectively.

$$\begin{cases} \dot{\boldsymbol{\eta}}(t) & = \mathbf{J}_L^{\dagger}(\boldsymbol{\eta}(t)) \cdot \dot{\mathbf{p}}(t) \\ \mathbf{p}(t) & = \boldsymbol{\Phi}(\boldsymbol{\eta}(t)) \end{cases} \tag{5.2}$$

with

$$\mathbf{p}(t) = \mathbf{p}_{6,\hat{i}}(t) = \begin{bmatrix} \mathbf{p1}_{6,\hat{i}}(t) \\ \mathbf{p2}_{6,\hat{i}}(t) \\ \mathbf{p3}_{6,\hat{i}}(t) \\ \mathbf{p4}_{6,\hat{i}}(t) \end{bmatrix} \in \mathbb{R}^{3m}$$

$$\mathbf{\Phi}(\boldsymbol{\eta}(t)) = \mathbf{\Phi}\left(\boldsymbol{\eta}(t), \mathbf{p}^{B}_{6,\hat{i}}\right) = \begin{bmatrix} \mathbf{\Phi}_{Sh}\left(\boldsymbol{\eta}_{1-3}(t), \mathbf{p1}^{Sh}_{6,\hat{i}}\right) \\ \mathbf{\Phi}_{Fo}\left(\boldsymbol{\eta}_{1-4}(t), \mathbf{p2}^{El}_{6,\hat{i}}\right) \\ \mathbf{\Phi}_{Ha}\left(\boldsymbol{\eta}(t), \mathbf{p3}^{Wr}_{6,\hat{i}}\right) \\ \mathbf{\Phi}_{Ha}\left(\boldsymbol{\eta}(t), \mathbf{p4}^{Wr}_{6,\hat{i}}\right) \end{bmatrix} \in \mathbb{R}^{3m}$$

$$\mathbf{J}(\boldsymbol{\eta}(t)) = \mathbf{J}\left(\boldsymbol{\eta}(t), \mathbf{p}^{B}_{6,\hat{i}}\right) = \begin{bmatrix} \mathbf{J}_{Sh}\left(\boldsymbol{\eta}_{1-3}(t), \mathbf{p1}^{Sh}_{6,\hat{i}}\right) \\ \mathbf{J}_{Fo}\left(\boldsymbol{\eta}_{1-4}(t), \mathbf{p2}^{El}_{6,\hat{i}}\right) \\ \mathbf{J}_{Ha}\left(\boldsymbol{\eta}(t), \mathbf{p3}^{Wr}_{6,\hat{i}}\right) \\ \mathbf{J}_{Ha}\left(\boldsymbol{\eta}(t), \mathbf{p4}^{Wr}_{6,\hat{i}}\right) \end{bmatrix} \in \mathbb{R}^{(3m)\times n}$$

One question arises, at this point. How to estimate $\mathbf{N}_{\dot{\mathbf{p}}}$ and $\mathbf{R}$? This was possible since the MCS provides also the covariance matrices $\mathbf{M}^{i}_{k}$ and $\dot{\mathbf{M}}^{i}_{k}$ related to the k^{th} measurement (position and velocity, respectively) of the i^{th} marker and gives a measure on how much to trust the specific measurement. Since each marker is assumed to be equal to each other and hence with the same covariances, they can be denoted also as $\mathbf{M}_k$ and $\dot{\mathbf{M}}_k$. Hence, $\mathbf{R}$ and $\mathbf{N}_{\dot{\mathbf{p}}}$, can be estimated as

$$\mathbf{R} = \begin{bmatrix} \mathbf{R}_1 & \dots & 0 \\ \vdots & \ddots & \vdots \\ 0 & \dots & \mathbf{R}_m \end{bmatrix}, \quad \mathbf{N}_{\dot{\mathbf{p}}} = \begin{bmatrix} \mathbf{N}_{\dot{\mathbf{p}}_1} & \dots & 0 \\ \vdots & \ddots & \vdots \\ 0 & \dots & \mathbf{N}_{\dot{\mathbf{p}}_m} \end{bmatrix}$$

$$\mathbf{R}_i = \frac{1}{N}\sum_{k=1}^{N} \mathbf{M}_k = \bar{\sigma}^2_{\mathbf{R}} \cdot \mathbf{I}_{3\times 3}, \quad \bar{\sigma}_{\mathbf{R}} = \sqrt{1.57 \cdot 10^{-6}}\ [\mathrm{m}], \quad i = 1, \cdots, m$$

$$\mathbf{N}_{\dot{\mathbf{p}}_i} = \frac{1}{N}\sum_{k=1}^{N} \dot{\mathbf{M}}_k = \sigma^2_{\mathbf{N}_{\dot{\mathbf{p}}}} \cdot \mathbf{I}_{3\times 3}, \quad \sigma_{\mathbf{N}_{\dot{\mathbf{p}}}} = \sqrt{0.0285}\ [\mathrm{m/s}], \quad i = 1, \cdots, m$$

From these quantities, the goal is to estimate $\boldsymbol{\eta}(t)$. This estimate is indicated as $\hat{\boldsymbol{\eta}}^{LS}(t)$, $\hat{\boldsymbol{\eta}}^{LKF}(t)$ and $\hat{\boldsymbol{\eta}}^{EKF}(t)$, depending on which estimation procedure is used.

5.3 Least-squares estimation

Considering the differential kinematics equation with the presence of the noise $\mathbf{n}_{\dot{\mathbf{p}}}(t)$

$$\dot{\mathbf{p}}(t) = \mathbf{J}(\boldsymbol{\eta}(t)) \cdot \dot{\boldsymbol{\eta}}(t) + \mathbf{n}_{\dot{\mathbf{p}}}(t) \tag{5.3}$$

the LS solution is given by

$$\hat{\boldsymbol{\eta}}^{LS}(t) = \mathbf{J}_L^{\dagger}\left(\hat{\boldsymbol{\eta}}^{LS}(t)\right) \cdot \dot{\mathbf{p}}(t) \tag{5.4}$$

The previous equation can be computed, provided that $\mathbf{J}\left(\hat{\boldsymbol{\eta}}^{LS}(t)\right)$ is *full-column rank* and far from being *singular*. It is possible to observe that, if the initial condition $\hat{\boldsymbol{\eta}}^{LS}(0)$ is provided, one can simply obtain the estimate $\hat{\boldsymbol{\eta}}^{LS}(t)$ as result of the integration of Eq. 5.4. The LS algorithm is shown below.

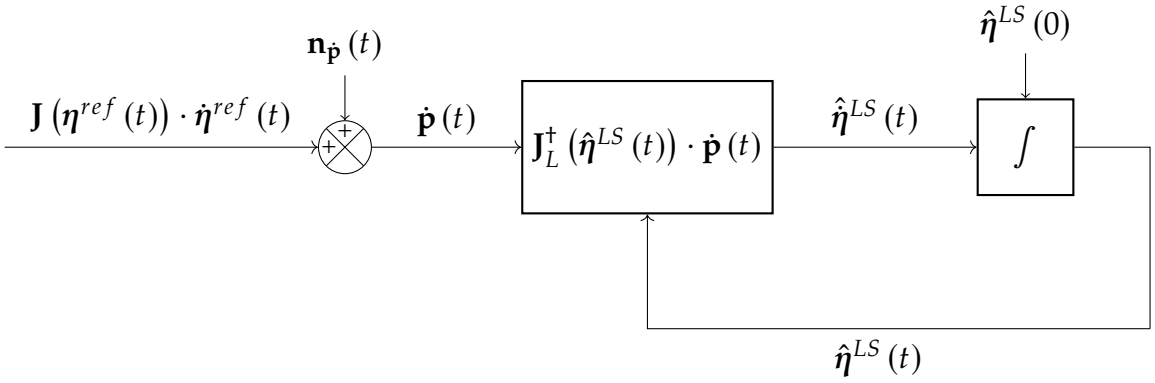

Figure 5.5: LS estimation of joint-space configuration

The Simscape model can be exploited to analyze this estimator. Two parameters must be taken into account before proceeding with the simulations.

1. Initial estimate $\hat{\boldsymbol{\eta}}^{LS}(0)$.
2. Deterministic or noisy $\dot{\mathbf{p}}(t)$.

Different scenarios can be considered. In all the subsequent cases, a measure of the goodness of the estimate is given by the Root Mean Square Error (RMSE), that is:

$$RMSE\left(\hat{\boldsymbol{\eta}}^{LS}\right) = \sqrt{\frac{1}{n} \cdot \frac{1}{N} \sum_{k=1}^{N} \left\| \boldsymbol{\eta}^{ref}(k) - \hat{\boldsymbol{\eta}}^{LS}(k) \right\|^2}$$

The RMSE of all the different scenarios are given below.

Root Mean Squared Error				
Scenario	$\lvert\mathcal{S}\rvert,\lvert\mathcal{F}\rvert,\lvert\mathcal{H}\rvert$	$\boldsymbol{\eta}^{LS}(0)$	$\dot{\mathbf{p}}(t)$	RMSE [rad]
1	1,1,2	$\boldsymbol{\eta}^{LS}(0) = \boldsymbol{\eta}^{ref}(0)$	Deterministic	$RMSE\left(\hat{\boldsymbol{\eta}}^{LS}\right) = 8.05 \cdot 10^{-15}$
2	1,1,2	$\boldsymbol{\eta}^{LS}(0) \neq \boldsymbol{\eta}^{ref}(0)$	Noisy	$RMSE\left(\hat{\boldsymbol{\eta}}^{LS}\right) = 0.1200$
3	1,0,2	$\boldsymbol{\eta}^{LS}(0) = \boldsymbol{\eta}^{ref}(0)$	Deterministic	$RMSE\left(\hat{\boldsymbol{\eta}}^{LS}\right) = 2.52 \cdot 10^{-10}$
4	1,0,2	$\boldsymbol{\eta}^{LS}(0) = \boldsymbol{\eta}^{ref}(0)$	Noisy	$RMSE\left(\hat{\boldsymbol{\eta}}^{LS}\right) = 0.6458$

Table 5.5: Least-squares RMSE

Scenario 1 corresponds to the best-case scenario, since the quantity $\dot{\mathbf{p}}(t)$ that is measured is the true one and the initial estimate $\hat{\boldsymbol{\eta}}^{LS}(0)$ is equal to the initial value of the given trajectory. Moreover, for all the scenarios, the Jacobian is always *full-rank* and hence there exist only one solution to

$$\mathbf{J}^T\left(\hat{\boldsymbol{\eta}}^{LS}\right)\mathbf{J}\left(\hat{\boldsymbol{\eta}}^{LS}\right)\cdot\dot{\hat{\boldsymbol{\eta}}}^{LS} = \mathbf{J}^T\left(\hat{\boldsymbol{\eta}}^{LS}\right)\cdot\dot{\mathbf{p}}$$

Let $\mathbf{J}\left(\hat{\boldsymbol{\eta}}^{LS}(t)\right) = \mathbf{U}\mathbf{S}\mathbf{V}^T$ with $\mathbf{U} = [\mathbf{u}_1 \dots \mathbf{u}_{3m}]$, $\mathbf{V} = [\mathbf{v}_1 \dots \mathbf{v}_n]$ and $\mathbf{S} = \text{diag}[\sigma_1 \dots \sigma_n]$, be the singular value decomposition of $\mathbf{J}\left(\hat{\boldsymbol{\eta}}^{LS}(t)\right)$. Then, it is known that

$$\dot{\hat{\boldsymbol{\eta}}}^{LS}(t) = \sum_{i=1}^{n}\frac{1}{\sigma_i}\mathbf{v}_i\mathbf{u}_i^T\cdot\dot{\mathbf{p}}(t)$$

is the minimum-norm LS solution, leading to $\hat{\boldsymbol{\eta}}^{LS}(t)$.

By looking at the previous equation, when a singularity is approached, the n^{th} singular value tends to zero. In this framework, what if $\mathbf{J}\left(\hat{\boldsymbol{\eta}}^{LS}(t)\right)$ is *ill-conditioned*?

5.3.1 Probabilistic analysis of the *quasi-singular* case

In the case in which the Jacobian is *quasi-singular*, by adopting the notation $\mathbf{J}(\boldsymbol{\eta}(t)) = \mathbf{J}$ and $\dot{\hat{\boldsymbol{\eta}}}^{LS}(t) = \dot{\hat{\boldsymbol{\eta}}}$, substituting the following equation

$$\dot{\mathbf{p}} = \mathbf{J}\cdot\dot{\boldsymbol{\eta}} + \mathbf{n}_{\dot{\mathbf{p}}}$$

into

$$\hat{\dot{\boldsymbol{\eta}}} = \left(\mathbf{J}^T\mathbf{J}\right)^{-1}\mathbf{J}^T \cdot \dot{\mathbf{p}}$$

one has

$$\begin{aligned}\hat{\dot{\boldsymbol{\eta}}} &= \left(\mathbf{J}^T\mathbf{J}\right)^{-1}\mathbf{J}^T \cdot \left[\mathbf{J}\cdot\dot{\boldsymbol{\eta}} + \mathbf{n}_{\dot{\mathbf{p}}}\right] \\ &= \dot{\boldsymbol{\eta}} + \left(\mathbf{J}^T\mathbf{J}\right)^{-1}\mathbf{J}^T \cdot \mathbf{n}_{\dot{\mathbf{p}}}\end{aligned}$$

Defining the estimation error as

$$\tilde{\dot{\boldsymbol{\eta}}} = \hat{\dot{\boldsymbol{\eta}}} - \dot{\boldsymbol{\eta}} = \left(\mathbf{J}^T\mathbf{J}\right)^{-1}\mathbf{J}^T \cdot \mathbf{n}_{\dot{\mathbf{p}}}$$

one can simply obtain its gaussian distribution as

$$\tilde{\dot{\boldsymbol{\eta}}} \sim \mathcal{N}\left(\mathbf{0}, \mathbf{N}_{\dot{\mathbf{p}}} \cdot \left(\mathbf{J}^T\mathbf{J}\right)^{-1}\right)$$

Moreover, by using the SVD of the Jacobian $\mathbf{J} = \mathbf{U}\mathbf{S}\mathbf{V}^T$, it follows

$$\left(\mathbf{J}^T\mathbf{J}\right)^{-1} = (\mathbf{V}\mathbf{S}\underbrace{\mathbf{U}^T\mathbf{U}}_{\mathbf{I}_{(3m)\times(3m)}}\mathbf{S}\mathbf{V}^T)^{-1} = \mathbf{V}\mathbf{S}^{-2}\mathbf{V}^T$$

Hence the variance of the estimation error depends on the singular values of the matrix $\mathbf{J}$

$$\begin{aligned}\text{var}\left[\tilde{\dot{\boldsymbol{\eta}}}\right] &= \mathbf{N}_{\dot{\mathbf{p}}} \cdot \left(\mathbf{J}^T\mathbf{J}\right)^{-1} \\ &= \mathbf{N}_{\dot{\mathbf{p}}} \cdot \mathbf{V}\mathbf{S}^{-2}\mathbf{V}^T\end{aligned}$$

When $\mathbf{J}$ is close to be singular, there are directions (combinations of the parameters which are very difficult to estimate) along which the estimation error has a large variance. Indeed, as it is possible to observe in Fig. 5.8 and Fig. 5.9, the introduced noise heavily affects the LS estimate.

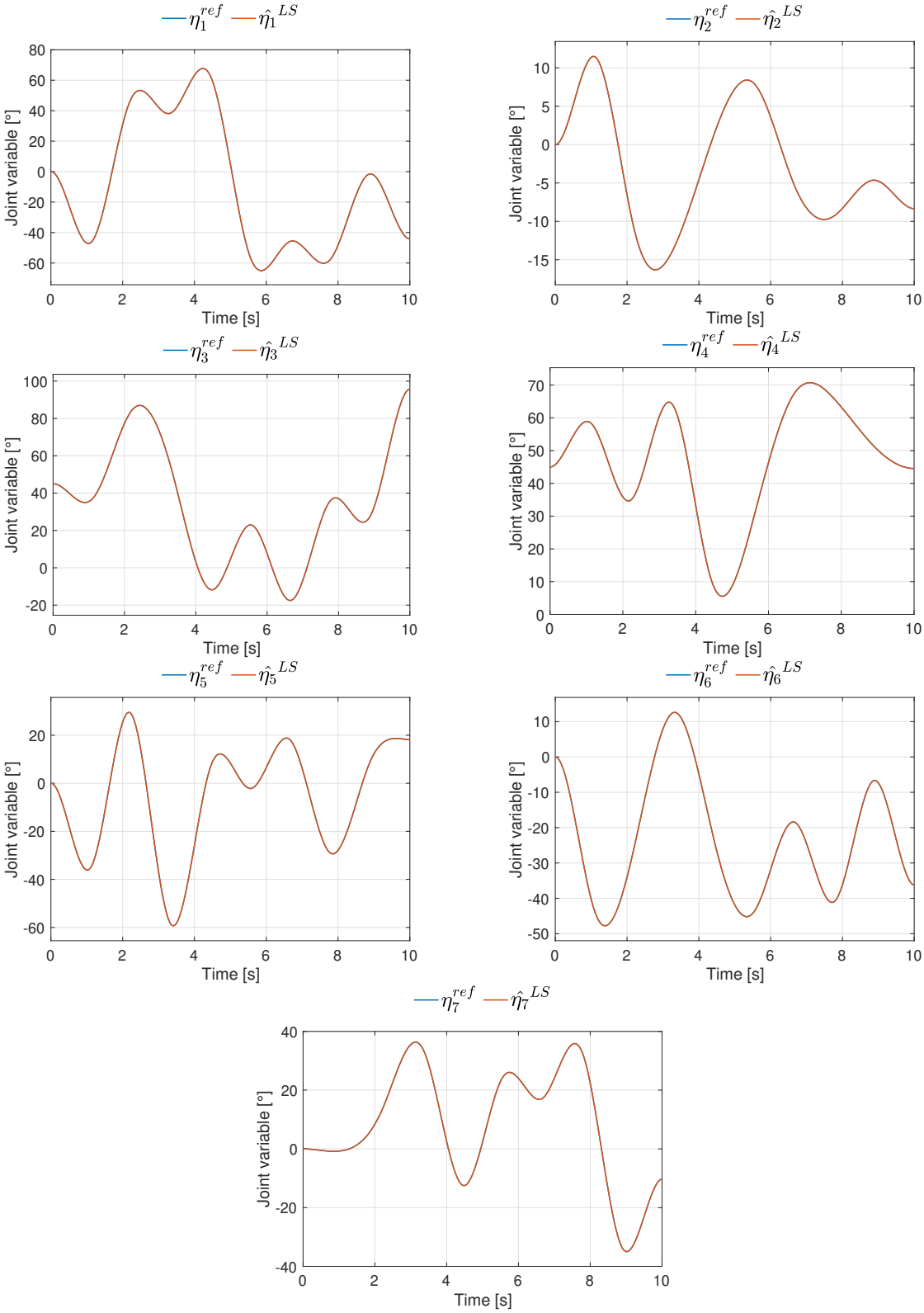

Figure 5.6: LS: scenario 1

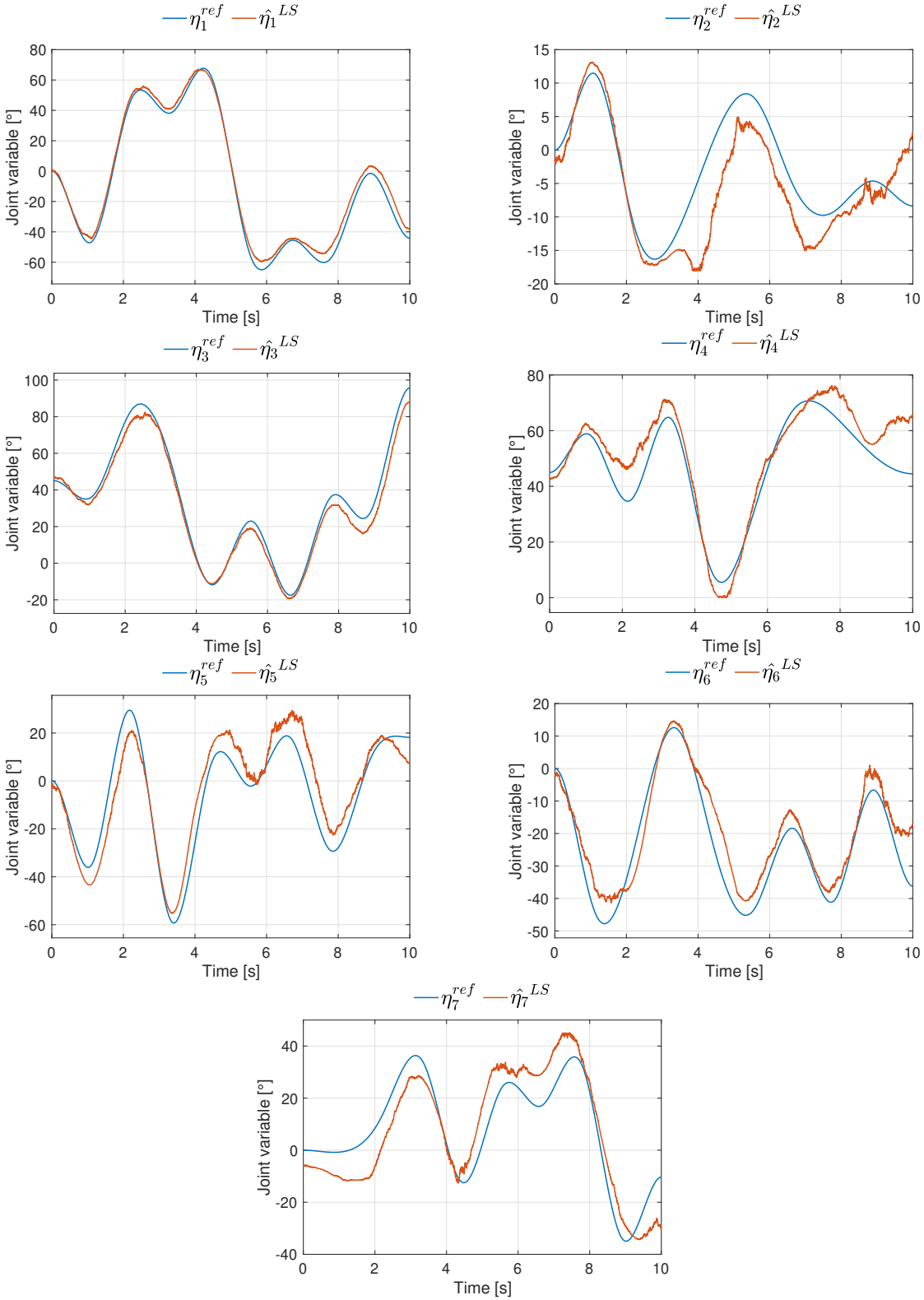

Figure 5.7: LS: scenario 2

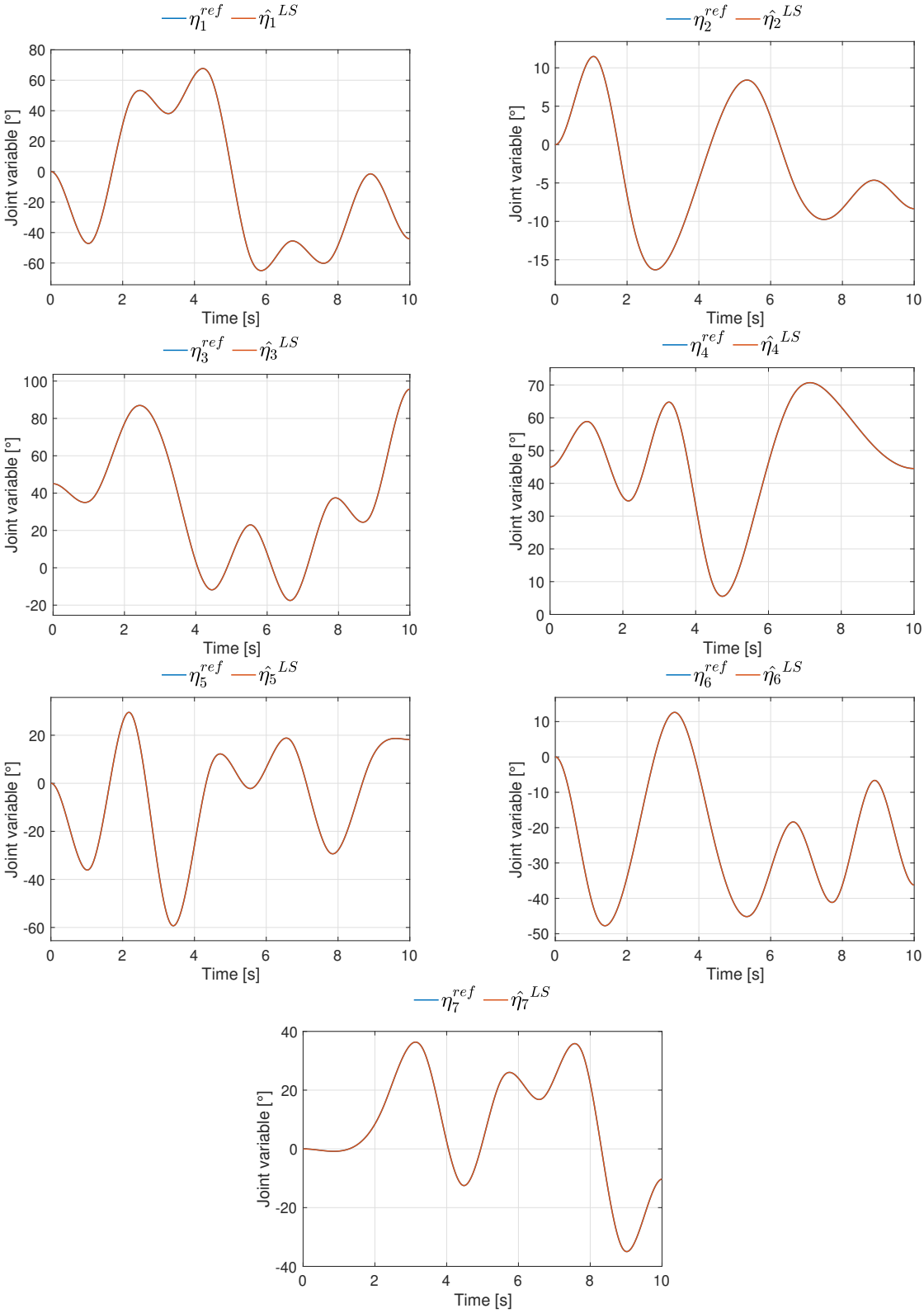

Figure 5.8: LS: scenario 3

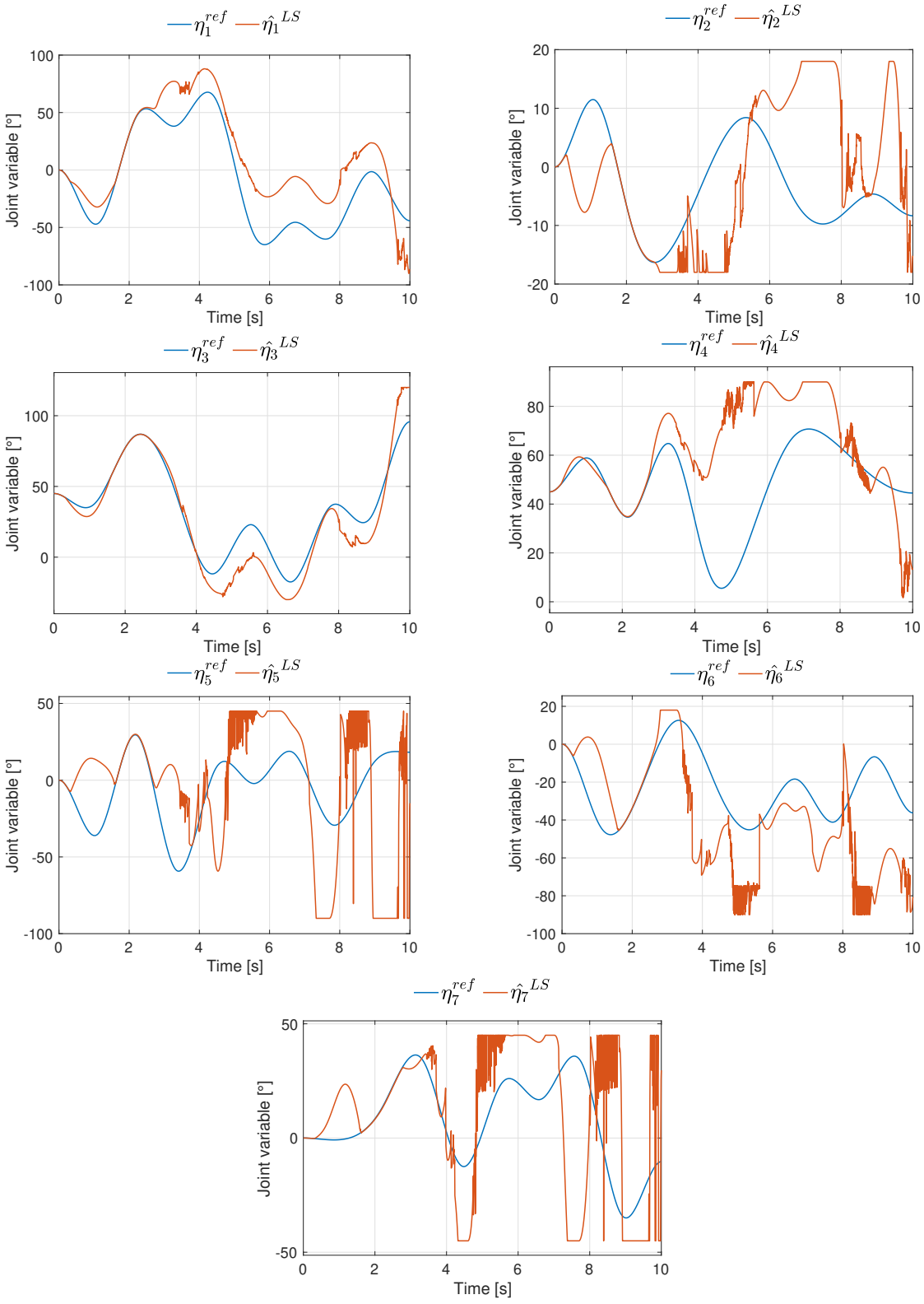

Figure 5.9: LS: scenario 4

5.4 Linearized Kalman filter estimation

In order to apply the KF algorithm, a model as in Eq. 2.11 has to be obtained. Hence, Eq. 5.2 has to be *discretized* and *linearized* around a nominal trajectory.

5.4.1 Runge-Kutta discretization

Recall that the markers' linear velocity and joint velocities are related by

$$\dot{\boldsymbol{\eta}}(t) = \mathbf{J}_L^{\dagger}(\boldsymbol{\eta}(t)) \cdot \dot{\mathbf{p}}(t)$$

To obtain the state $\boldsymbol{\eta}(t_f)$ at any time t_f, the velocities need to be integrated over time. This leads to

$$\boldsymbol{\eta}(t_f) = \boldsymbol{\eta}(0) + \int_0^{t_f} \dot{\boldsymbol{\eta}}(t)\, dt$$

Now suppose that the time interval $[0, t_f]$ is divided into L equally spaced intervals so that $t_i = i \cdot T_s \ \forall\ i = 0, \ldots, L$, and the time-interval $T_s = \frac{t_f}{L}$. Thus, the previous equation can be written as

$$\boldsymbol{\eta}(t_f) = \boldsymbol{\eta}(0) + \sum_{i=1}^{L} \int_{t_{i-1}}^{t_i} \dot{\boldsymbol{\eta}}(t)\, dt$$

More generally, for some $k \in [1, L]$, $\boldsymbol{\eta}(t_{k-1})$ and $\boldsymbol{\eta}(t_k)$ can be written as

$$\boldsymbol{\eta}(t_{k-1}) = \boldsymbol{\eta}(0) + \sum_{i=1}^{k-1} \int_{t_{i-1}}^{t_i} \dot{\boldsymbol{\eta}}(t)\, dt$$

$$\boldsymbol{\eta}(t_k) = \boldsymbol{\eta}(0) + \sum_{i=1}^{k} \int_{t_{i-1}}^{t_i} \dot{\boldsymbol{\eta}}(t)\, dt$$

Hence,

$$\boldsymbol{\eta}(t_k) = \boldsymbol{\eta}(t_{k-1}) + \underbrace{\int_{t_{k-1}}^{t_k} \dot{\boldsymbol{\eta}}(t)\, dt}_{(\star)}$$

By using the notation $\boldsymbol{\eta}(t_k) = \boldsymbol{\eta}_k$, the following fourth-order Runge-Kutta integration represents a way to approximate the integral $(\star)$.

$$\boldsymbol{\eta}_k \approx \mathbf{f}\left(\boldsymbol{\eta}_{k-1}, \dot{\mathbf{p}}_{k-1}\right) = \boldsymbol{\eta}_{k-1} + \underbrace{\frac{T_s}{6} \cdot \left(\mathbf{K_1} + 2\mathbf{K_2} + 2\mathbf{K_3} + \mathbf{K_4}\right)}_{(\star)}$$

where

$$\begin{aligned}
\mathbf{K_1} &= \mathbf{J}_L^{\dagger}\left(\boldsymbol{\eta}_{k-1}\right) \cdot \dot{\mathbf{p}}_{k-1} \\
\mathbf{K_2} &= \mathbf{J}_L^{\dagger}\left(\boldsymbol{\eta}_{k-1} + \mathbf{K_1} \cdot \frac{T_s}{2}\right) \cdot \dot{\mathbf{p}}_{k-1} \\
\mathbf{K_3} &= \mathbf{J}_L^{\dagger}\left(\boldsymbol{\eta}_{k-1} + \mathbf{K_2} \cdot \frac{T_s}{2}\right) \cdot \dot{\mathbf{p}}_{k-1} \\
\mathbf{K_4} &= \mathbf{J}_L^{\dagger}\left(\boldsymbol{\eta}_{k-1} + \mathbf{K_3} \cdot T_s\right) \cdot \dot{\mathbf{p}}_{k-1}
\end{aligned}$$

This leads to the *non-linear discrete*-time model

$$\begin{cases} \boldsymbol{\eta}_k &= \mathbf{f}\left(\boldsymbol{\eta}_{k-1}, \dot{\mathbf{p}}_{k-1}\right) \\ \mathbf{p}_k &= \boldsymbol{\Phi}\left(\boldsymbol{\eta}_k\right) \end{cases} \tag{5.5}$$

In the real experiments, the capture rate that is used in a marker measurement is 100 Hz. For this reason, T_s is set to $T_s = 10\ ms$.

5.4.2 Linearization

The obtained non-linear system in Eq. 5.5 needs to be *linearized* around an equilibrium point. In other words, a linear system that is approximately equal to the non-linear one has to be computed. Specifically, the non-linear system equations $\mathbf{f}\left(\eta_{k-1}, \dot{\mathbf{p}}_{k-1}\right)$ and $\mathbf{\Phi}\left(\eta_k\right)$ can be expanded around the nominal operating point $\left(\bar{\eta}, \bar{\dot{\mathbf{p}}}\right)$ as follows

$$\begin{cases} \eta_k &= \mathbf{f}\left(\eta_{k-1}, \dot{\mathbf{p}}_{k-1}\right) \approx \mathbf{f}\left(\bar{\eta}, \bar{\dot{\mathbf{p}}}\right) + \left.\frac{\partial \mathbf{f}}{\partial \eta}\right|_{\left(\bar{\eta}, \bar{\dot{\mathbf{p}}}\right)} \cdot \left(\eta_{k-1} - \bar{\eta}\right) + \left.\frac{\partial \mathbf{f}}{\partial \dot{\mathbf{p}}}\right|_{\left(\bar{\eta}, \bar{\dot{\mathbf{p}}}\right)} \cdot \left(\dot{\mathbf{p}}_{k-1} - \bar{\dot{\mathbf{p}}}\right) \\ \mathbf{p}_k &= \mathbf{\Phi}\left(\eta_k\right) \approx \mathbf{\Phi}\left(\bar{\eta}\right) + \left.\frac{\partial \mathbf{\Phi}}{\partial \eta}\right|_{\left(\bar{\eta}, \bar{\dot{\mathbf{p}}}\right)} \cdot \left(\eta_k - \bar{\eta}\right) \end{cases}$$

Recall that the equilibrium point is such that $\mathbf{f}\left(\bar{\eta}, \bar{\dot{\mathbf{p}}}\right) = \bar{\eta}$ and $\mathbf{\Phi}\left(\bar{\eta}\right) = \bar{\mathbf{p}}$. Hence, one obtains

$$\begin{cases} \underbrace{\eta_k - \bar{\eta}}_{\Delta\eta_k} &\approx \underbrace{\left.\frac{\partial \mathbf{f}}{\partial \eta}\right|_{\left(\bar{\eta}, \bar{\dot{\mathbf{p}}}\right)}}_{\mathbf{F}} \cdot \underbrace{\left(\eta_{k-1} - \bar{\eta}\right)}_{\Delta\eta_{k-1}} + \underbrace{\left.\frac{\partial \mathbf{f}}{\partial \dot{\mathbf{p}}}\right|_{\left(\bar{\eta}, \bar{\dot{\mathbf{p}}}\right)}}_{\mathbf{G}} \cdot \underbrace{\left(\dot{\mathbf{p}}_{k-1} - \bar{\dot{\mathbf{p}}}\right)}_{\Delta\dot{\mathbf{p}}_{k-1}} \\ \underbrace{\mathbf{p}_k - \bar{\mathbf{p}}}_{\Delta\mathbf{p}_k} &\approx \underbrace{\left.\frac{\partial \mathbf{\Phi}}{\partial \eta}\right|_{\left(\bar{\eta}, \bar{\dot{\mathbf{p}}}\right)}}_{\mathbf{J}} \cdot \underbrace{\left(\eta_k - \bar{\eta}\right)}_{\Delta\eta_k} \end{cases}$$

The *linearized discrete*-time model around the equilibrium point $\left(\bar{\eta}, \bar{\dot{\mathbf{p}}}\right)$ is as follows

$$\begin{cases} \Delta\eta_k &= \mathbf{F} \cdot \Delta\eta_{k-1} + \mathbf{G} \cdot \Delta\dot{\mathbf{p}}_{k-1} + \mathbf{w}_{k-1} \quad , \qquad \mathbf{w}_{k-1} \sim \mathcal{N}\left(0, \mathbf{Q}\right) \\ \Delta\mathbf{p}_k &= \mathbf{J} \cdot \Delta\eta_k + \mathbf{v}_k \quad , \qquad \mathbf{v}_k \sim \mathcal{N}\left(0, \mathbf{R}\right) \end{cases} \tag{5.6}$$

where $\mathbf{w}_k$ and $\mathbf{v}_k$ are the process and measurement noises, respectively. In deriving Eq. 5.6, it was made the important assumption that higher-order terms in the Taylor series expansions of $\mathbf{f}\left(\eta_{k-1}, \dot{\mathbf{p}}_{k-1}\right)$ could be neglected. Of course, this is only correct as long as η_{k-1} is close to $\bar{\eta}$ and $\dot{\mathbf{p}}_{k-1}$ is close to $\bar{\dot{\mathbf{p}}}$. The LKF algorithm use the noise information about the process and measurement equations to estimate the joint-space trajectory.

The Kalman filter algorithm can be applied to Eq. 5.6, leading to the filtered estimate $\Delta\hat{\eta}_{k|k}$. One can observe that, in its implementation, the quantities $\mathbf{K}_k$ and $\mathbf{P}_{k|k}$ can be computed *offline* while $\Delta\hat{\eta}_{k|k-1}$ and $\Delta\hat{\eta}_{k|k}$ must be computed

online, as it is shown in Fig. 5.10. In this context, an other reference trajectory is chosen, depicted in Fig. 5.11, where its first part is close to the nominal trajectory $\bar{\boldsymbol{\eta}}$ while the second one is not. The LKF should return a good estimate only when the joint variables do not move away from the equilibrium. The linear model of Eq. 5.6 which is used in the Kalman equations, was obtained after performing the linearization around a nominal trajectory and nominal input $\left(\bar{\boldsymbol{\eta}}, \bar{\dot{\mathbf{p}}}\right)$. In the following simulations, this is chosen as

$$\begin{cases} \bar{\boldsymbol{\eta}} & = \boldsymbol{\eta}^{ref}\left(0\right) \\ \bar{\dot{\mathbf{p}}} & = \mathbf{0} \end{cases} \tag{5.7}$$

which is indeed an equilibrium point since $\boldsymbol{\eta}^{ref}\left(0\right) = \mathbf{f}\left(\boldsymbol{\eta}^{ref}\left(0\right), \mathbf{0}\right)$.

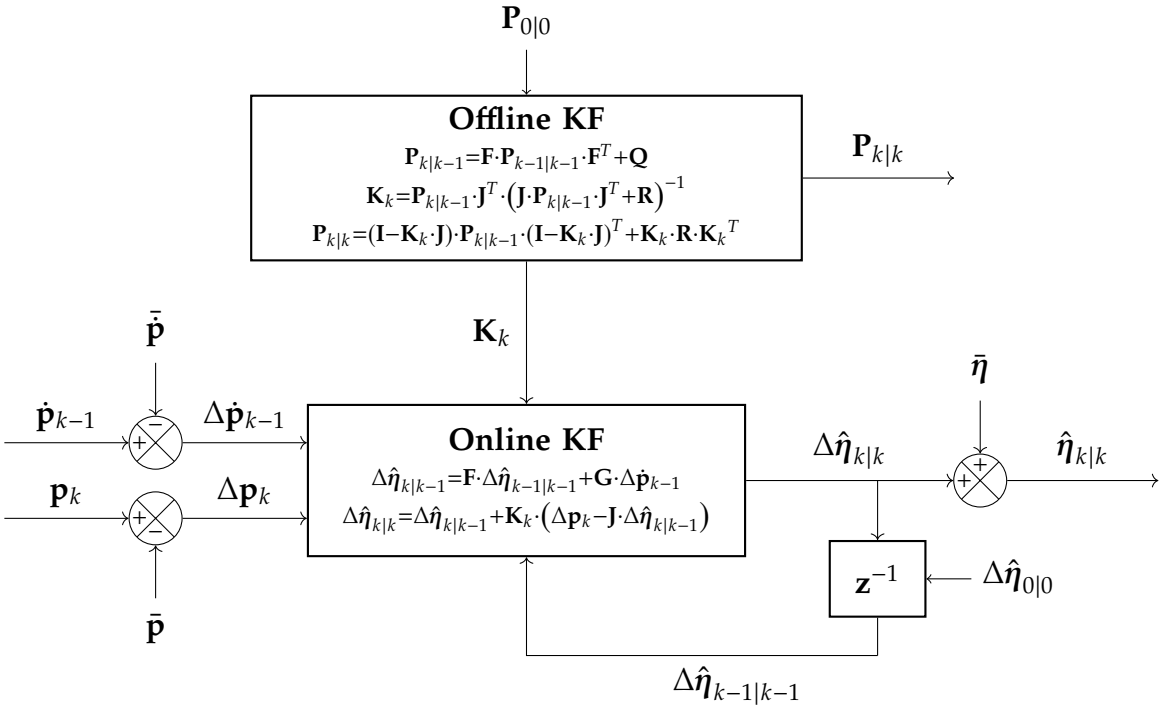

Figure 5.10: LKF estimation of joint-space configuration

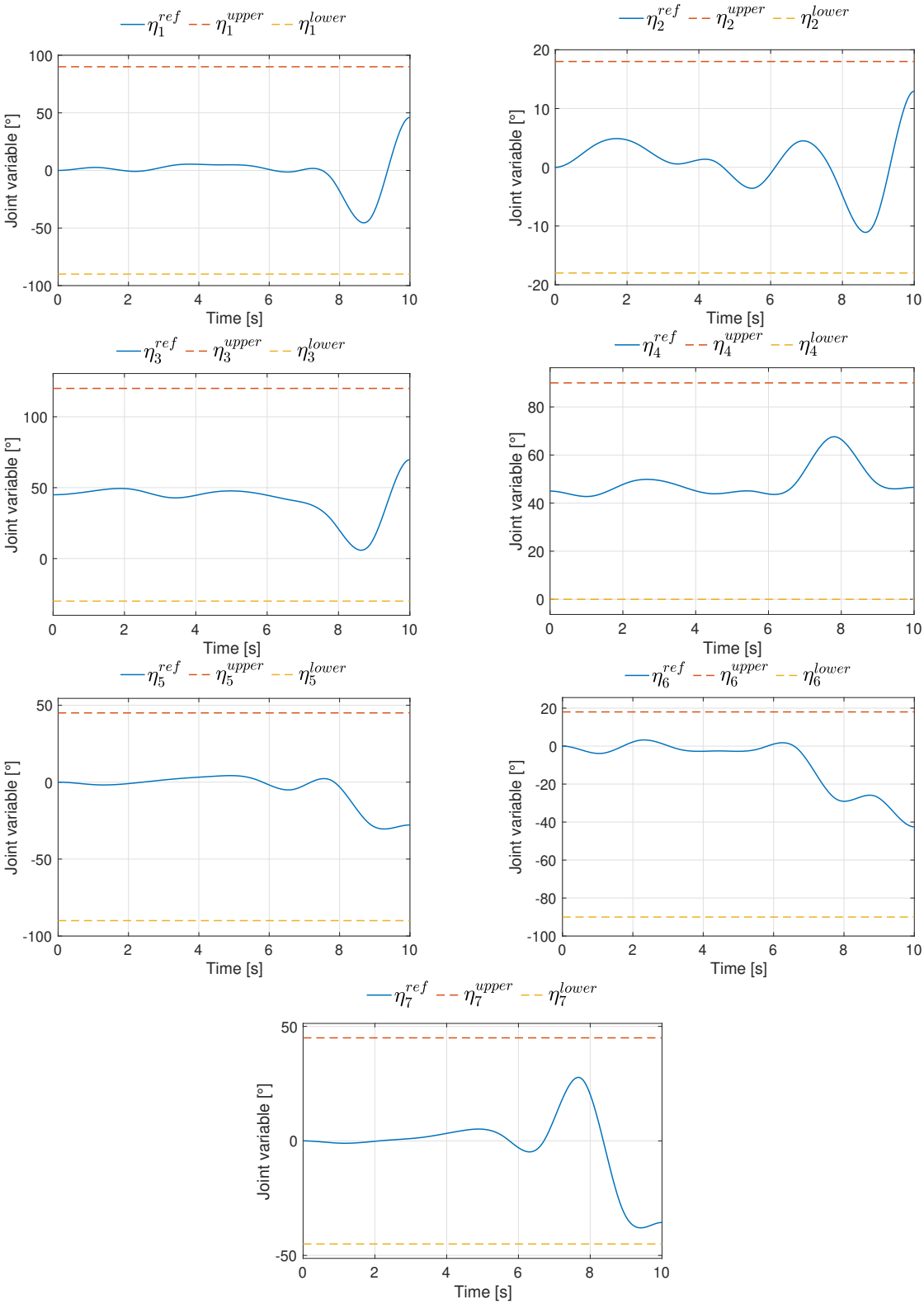

Figure 5.11: LKF: joint variables assigned trajectory

The Linearized Kalman filter algorithm can be applied once the initial estimate $\Delta\hat{\boldsymbol{\eta}}_{0|0}$, the process-measurement noise covariances $\mathbf{Q}$, $\mathbf{R}$ and the initial estimate covariance $\mathbf{P}_{0|0}$ are decided. As before, in the Simscape platform, the gaussian noise $\mathbf{n}_{\dot{\mathbf{p}}}(k) \sim \mathcal{N}\left(0, \mathbf{N}_{\dot{\mathbf{p}}}\right)$ is added to the joint velocities, leading to the corrupted $\dot{\mathbf{p}}_k$. As far as $\hat{\boldsymbol{\eta}}_{0|0}$ is concerned, for each one of the subsequent simulation, it is determined as $\hat{\boldsymbol{\eta}}_{0|0} \neq \bar{\boldsymbol{\eta}}$, hence the initial estimate $\Delta\hat{\boldsymbol{\eta}}_{0|0} \neq \mathbf{0}$. The initial covariance is chosen as $\mathbf{P}_{0|0} = \sigma^2_{\mathbf{P}} \cdot \mathbf{I}_{n\times n}$ with $\sigma_{\mathbf{P}} = \sqrt{10^{-1}}$ [rad]. Let the process noise $\mathbf{Q}$ and the measurement noises $\mathbf{R}$ be

$$\mathbf{Q} = \sigma^2_{\mathbf{Q}} \cdot \mathbf{I}_{n\times n}$$
$$\mathbf{R} = \sigma^2_{\mathbf{R}} \cdot \mathbf{I}_{(3m)\times(3m)}$$

Three different scenarios follow, where, the first two consider the 6^{th} combination while the third scenario deals with the 2^{nd} combination. As far as the first two scenarios are concerned, the value for the process and measurement covariance is left unchanged while the generation of the markers' velocity is changed. This means that the quantity $\mathbf{n}_{\dot{\mathbf{p}}}$ is either added or not at the joint velocities. Specifically, the markers' velocity noise is considered and, as it is depicted in Fig. 5.13, more noise affects the linearized kalman estimate. Especially in the first scenario, the estimate is considered acceptable when the trajectory of the arm maintains close to the equilibrium point.

Root Mean Squared Error					
Scenario	$\lvert\mathcal{S}\rvert,\lvert\mathcal{F}\rvert,\lvert\mathcal{H}\rvert$	$\dot{\mathbf{p}}_k$	$\sigma^2_{\mathbf{Q}}$	$\sigma^2_{\mathbf{R}}$	RMSE [rad]
1	1,1,2	Deterministic	10^{-6}	$\bar{\sigma}^2_{\mathbf{R}}$	$RMSE\left(\hat{\boldsymbol{\eta}}^{LKF}\right) = 0.1690$
2	1,1,2	Noisy	10^{-6}	$\bar{\sigma}^2_{\mathbf{R}}$	$RMSE\left(\hat{\boldsymbol{\eta}}^{LKF}\right) = 0.1824$
3	1,0,2	Deterministic	10^{-6}	$\bar{\sigma}^2_{\mathbf{R}}$	$RMSE\left(\hat{\boldsymbol{\eta}}^{LKF}\right) = 0.4836$

Table 5.6: Linearized Kalman filter RMSE

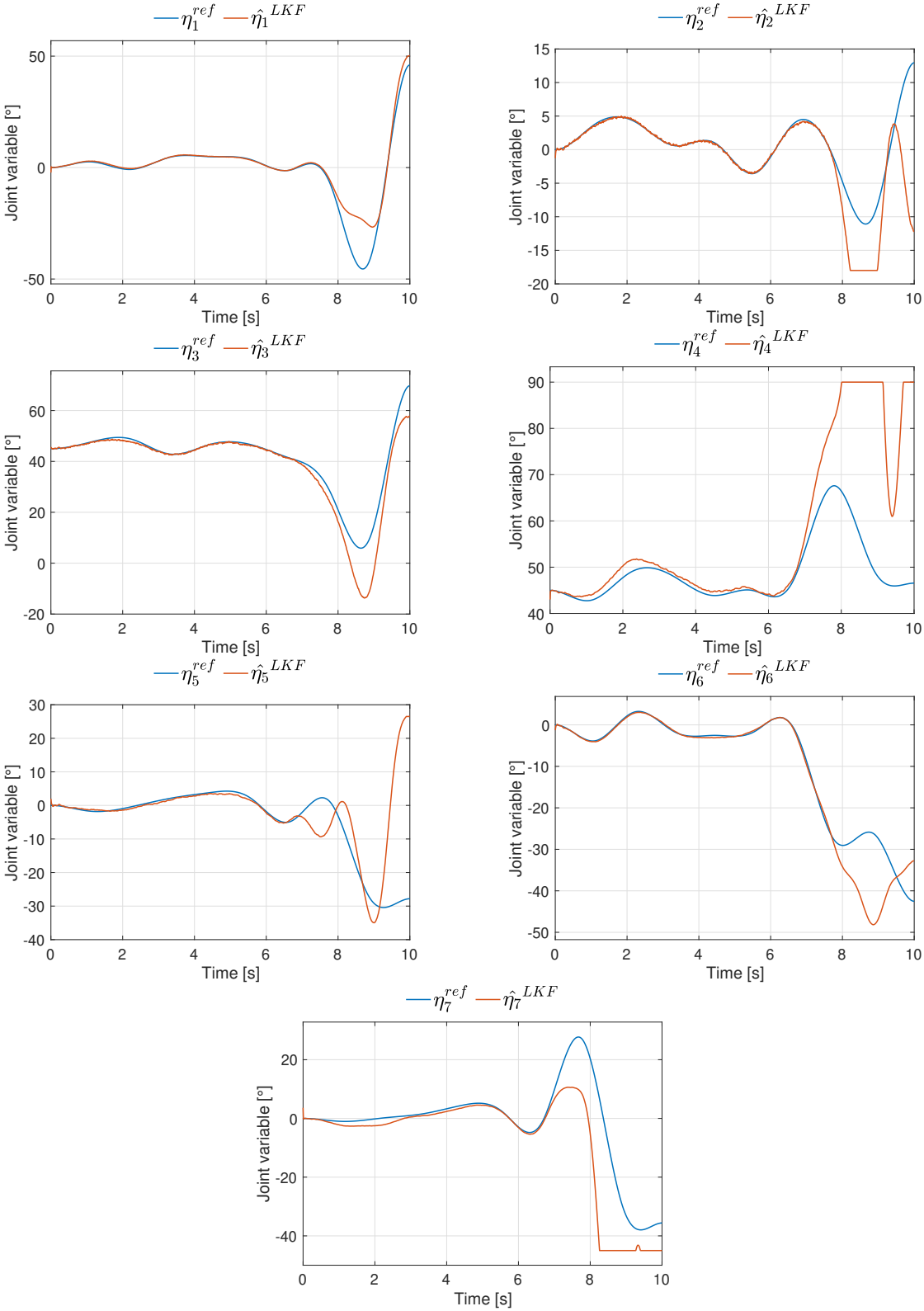

Figure 5.12: LKF: scenario 1

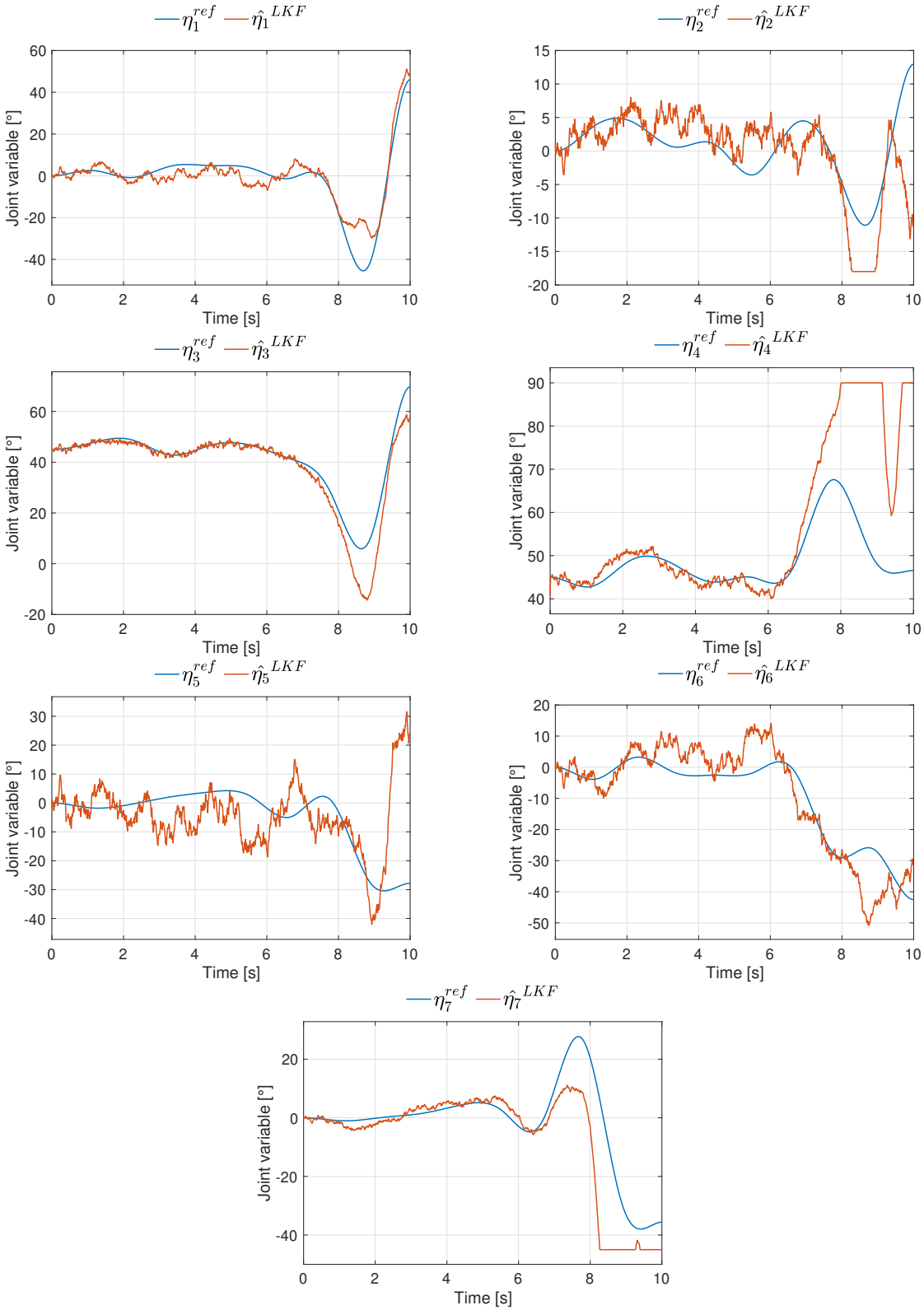

Figure 5.13: LKF: scenario 2

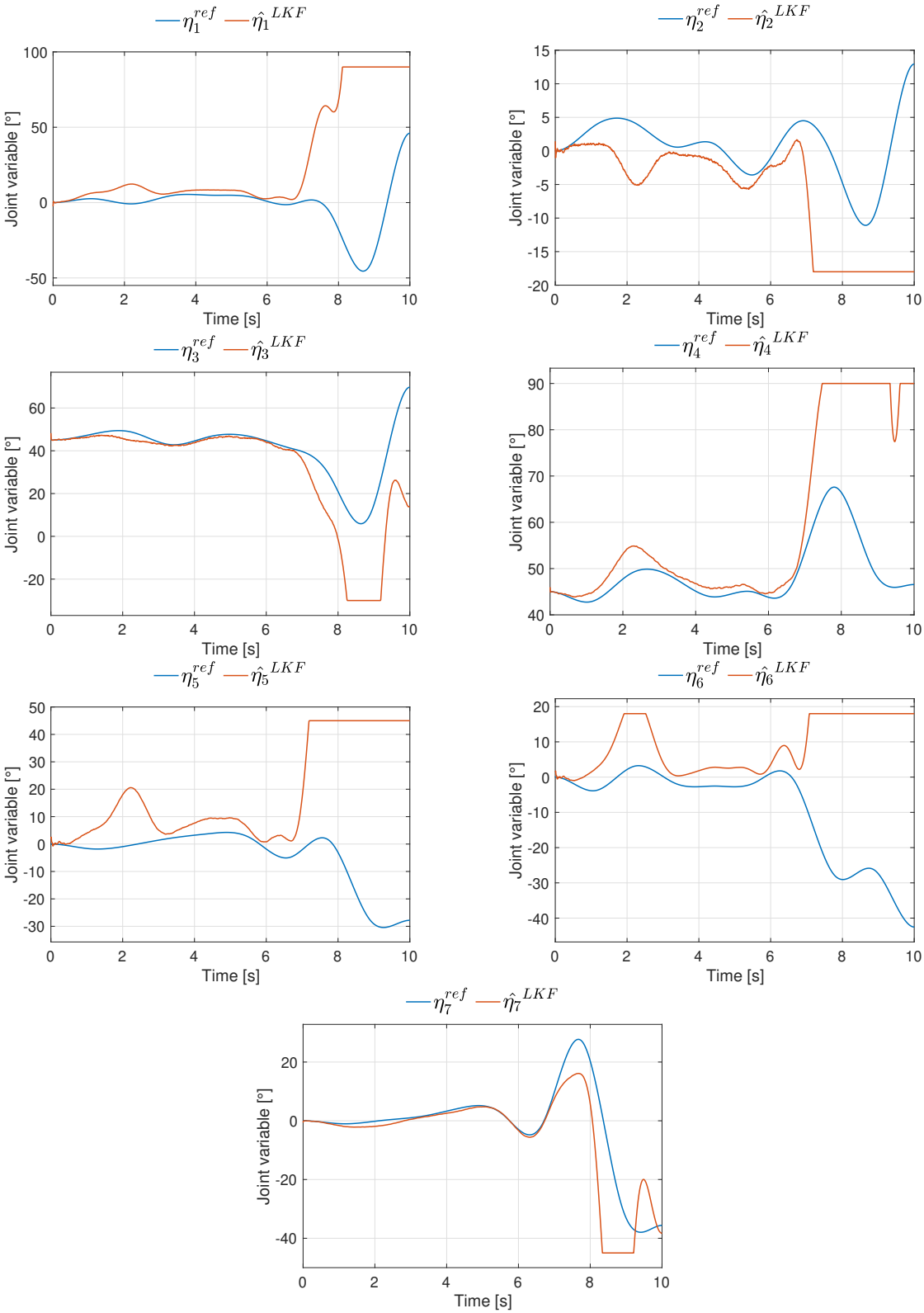

Figure 5.14: LKF: scenario 3

5.5 Extended Kalman filter estimation

In the previous subsection, it was shown that it is possible to apply the Kalman filter algorithm to the linearized model of Eq. 5.6. However, this only works with good results when the trajectory is close to the nominal point around which the model is linearized. This limitation can be overcame by an extension of the regular Kalman filter, known as Extended Kalman filter, which can be applied directly to the *non-linear* model

$$\begin{cases} \boldsymbol{\eta}_k &= \mathbf{f}\left(\boldsymbol{\eta}_{k-1}, \dot{\mathbf{p}}_{k-1}\right) + \mathbf{w}_{k-1}, \quad \mathbf{w}_{k-1} \sim \mathcal{N}\left(0, \mathbf{Q}\right) \\ \mathbf{p}_k &= \boldsymbol{\Phi}\left(\boldsymbol{\eta}_k\right) + \mathbf{v}_k, \quad \mathbf{v}_k \sim \mathcal{N}\left(0, \mathbf{R}\right) \end{cases} \tag{5.8}$$

The detailed derivation of the Extended Kalman filter algorithm can be found in Section 3.1. Its summary is depicted in the following figure.

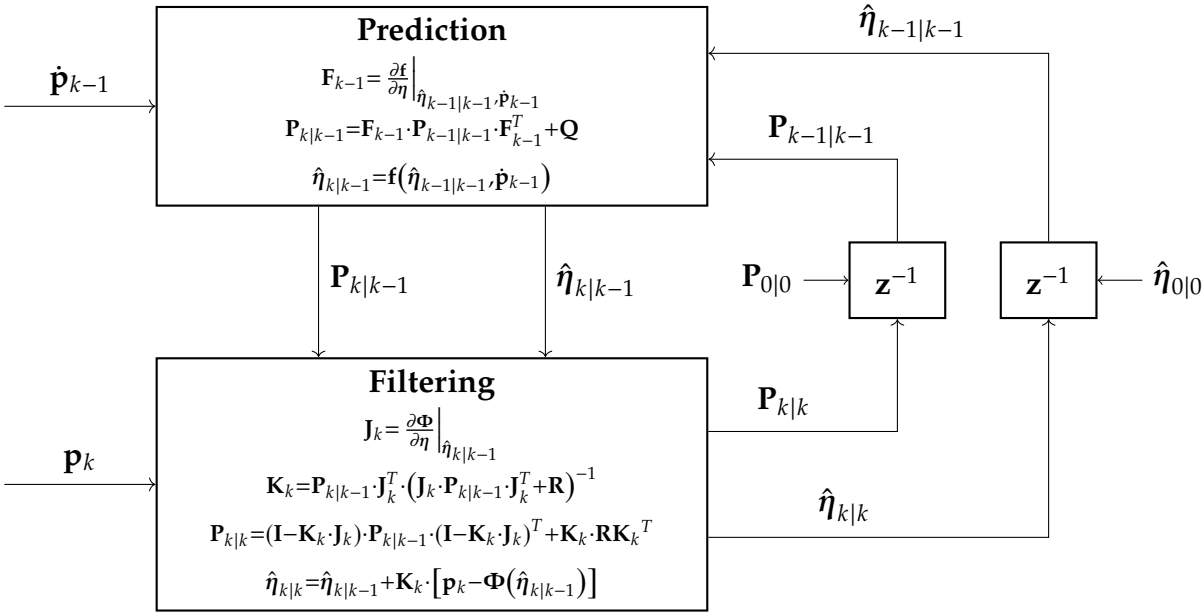

Figure 5.15: EKF estimation of joint-space configuration

In order to apply this extension of the regular Kalman filter, one has to decide the values for the initial estimates $\hat{\boldsymbol{\eta}}_{0|0}$, $\mathbf{P}_{0|0}$ and the covariance matrices $\mathbf{Q}$, $\mathbf{R}$. The initial estimate is chosen slightly different wrt $\boldsymbol{\eta}^{ref}(0)$ and the initial covariance estimate is set as in the LKF case. As before, 3 scenarios are analyzed. The first two scenarios concern the 6^{th} combination while the third one concerns the 2^{nd} combination. The same value for the process and measurement covariances

$\mathbf{Q}$ and $\mathbf{R}$ are used in all the scenarios. The noise related to the linear velocity of the markers $\mathbf{n}_{\dot{\mathbf{p}}}$ is introduced in the second scenario. From the comparison between Fig. 5.16 and 5.17, one can observe a worsening of the EKF estimate. Considering scenario 1, still there is a mismatch between the kalman estimates and the actual joint variables, even though there is no noise affecting the markers' linear velocity. This is due to the value assumed by the process and measurement covariances. The two quantities would perfectly match if either the measurement noise or the process noise was further decreased. In scenario 3 instead the EKF algorithm performs badly. For the same reasoning explained in Section 5.3, since $\mathbf{f}\left(\hat{\boldsymbol{\eta}}_{k-1|k-1}, \dot{\mathbf{p}}_{k-1}\right)$ is a function of $\mathbf{J}_L^{\dagger}\left(\hat{\boldsymbol{\eta}}_{k-1|k-1}\right) \cdot \dot{\mathbf{p}}_{k-1}$, when the Jacobian is *quasi-singular*, small deviation of the previous filtered estimate $\hat{\boldsymbol{\eta}}_{k-1|k-1}$ results in large deviation of the predicted joint variables $\hat{\boldsymbol{\eta}}_{k|k-1}$.
The RMSE, for all the different scenarios, is reported below.

$$RMSE\left(\hat{\boldsymbol{\eta}}^{EKF}\right) = \sqrt{\frac{1}{n} \cdot \frac{1}{N} \sum_{k=1}^{N} \left\| \boldsymbol{\eta}^{ref}(k) - \hat{\boldsymbol{\eta}}_{k|k}^{EKF} \right\|^2}$$

Root Mean Squared Error					
Scenario	$\lvert\mathcal{S}\rvert,\lvert\mathcal{F}\rvert,\lvert\mathcal{H}\rvert$	$\dot{\mathbf{p}}_k$	$\sigma^2_{\mathbf{Q}}$	$\sigma^2_{\mathbf{R}}$	RMSE [rad]
1	1,1,2	Deterministic	10^{-6}	$\bar{\sigma}^2_{\mathbf{R}}$	$RMSE\left(\hat{\boldsymbol{\eta}}^{EKF}\right) = 0.0215$
2	1,1,2	Noisy	10^{-6}	$\bar{\sigma}^2_{\mathbf{R}}$	$RMSE\left(\hat{\boldsymbol{\eta}}^{EKF}\right) = 0.0692$
3	1,0,2	Deterministic	10^{-6}	$\bar{\sigma}^2_{\mathbf{R}}$	$RMSE\left(\hat{\boldsymbol{\eta}}^{EKF}\right) = 0.4051$

Table 5.7: Extended Kalman filter RMSE

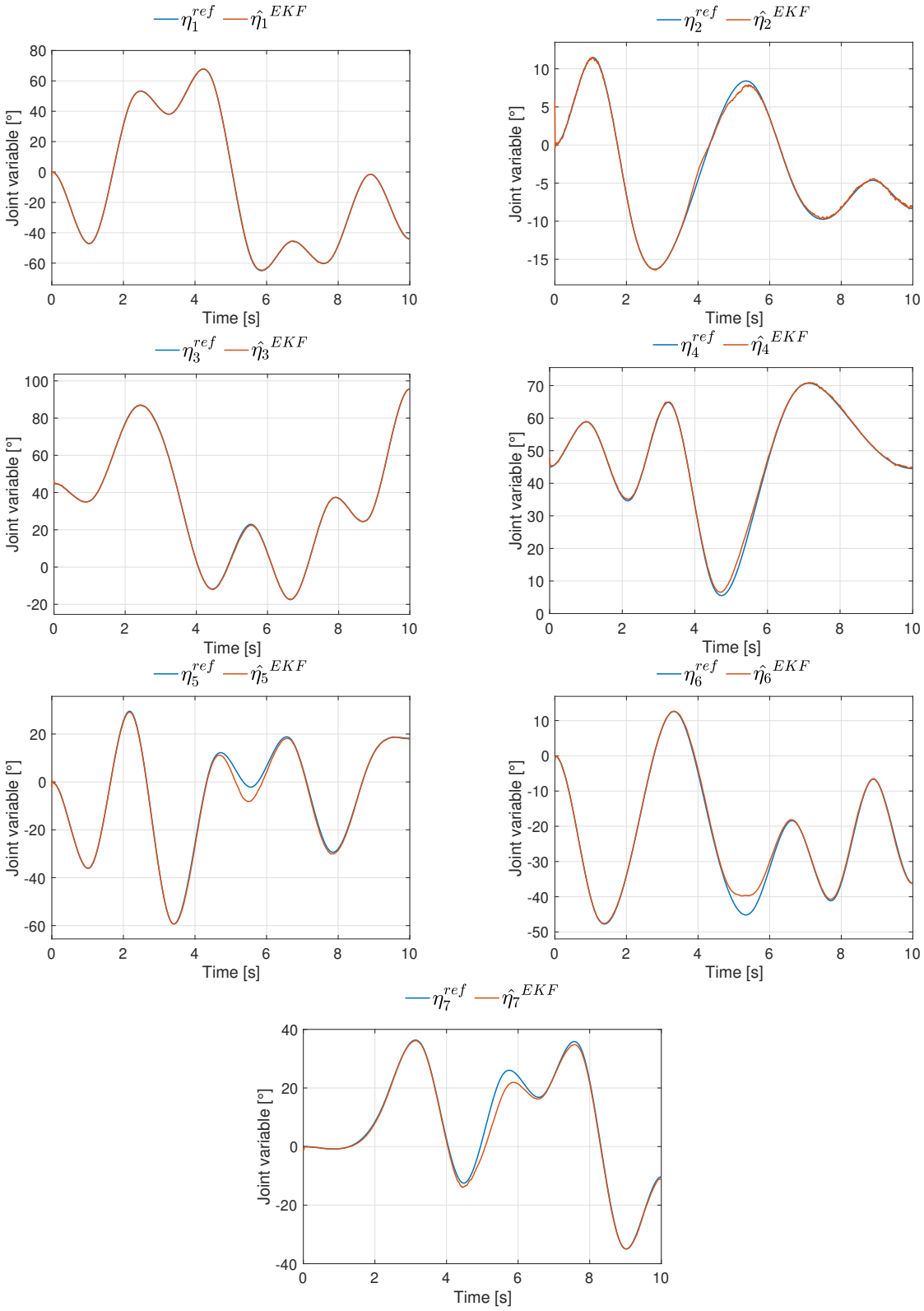

Figure 5.16: EKF: scenario 1

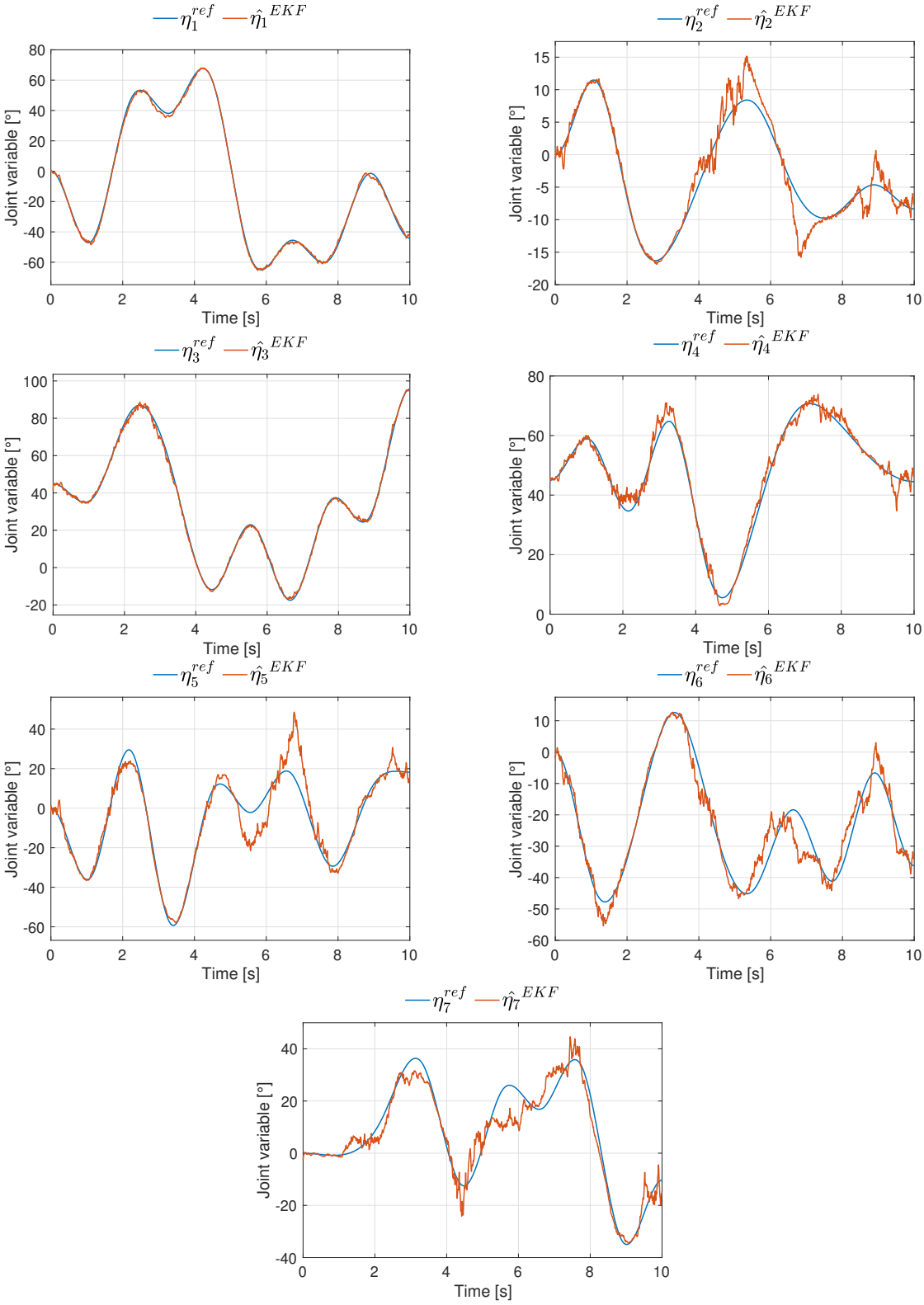

Figure 5.17: EKF: scenario 2

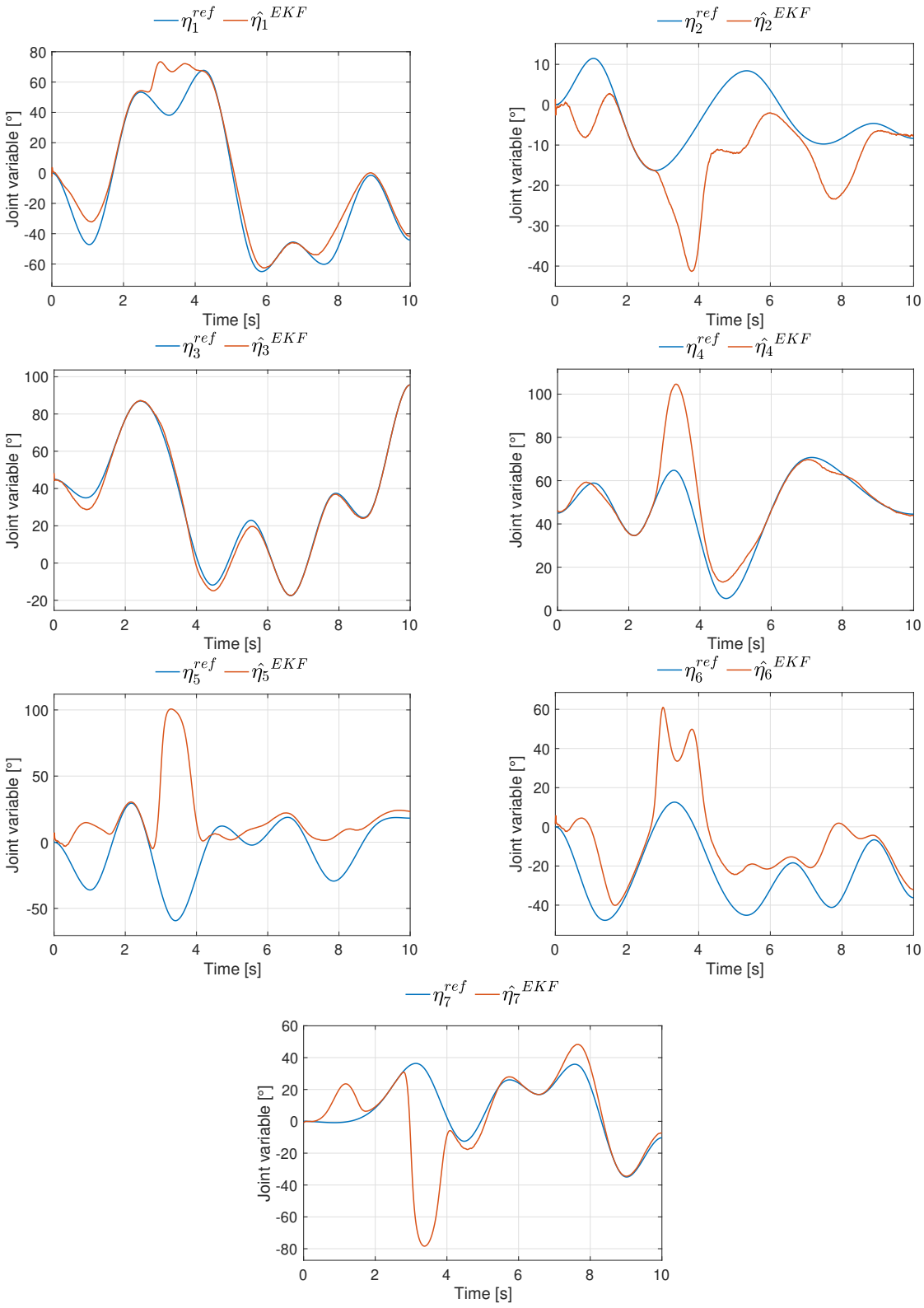

Figure 5.18: EKF: scenario 3

6

Experimental results

All the experiments were carried out at KTH Royal Institute of Technology's SML (Smart Mobility Lab) in Sweden. Through the use of the Motion Capture System (MCS) with twelve cameras arranged over the lab surface, the motion of the involved rigid bodies (markers) could be tracked. Specifically, the Windows-based data acquisition software Qualisys Track Manager (QTM), an interface that allows the user to perform 2D and 3D motion capture, was used. Hence, real-time 2D, 3D, and 6D camera information was displayed during the capture, offering instant confirmation of accurate data acquisition. The data could then be exported to analysis software via several external formats. All markers positions were shared as Robot Operating System (ROS) topics within the ROS framework, and the corresponding data could be accessed from the appropriate topic. The source code of this project can be found at the GitHub repository [1].

Figure 6.1: Smart Mobility Lab

[1]URL GitHub: `https://github.com/Gioo96/Master_thesis`

6.1 Setup of the experiments

The position and velocity of each marker $\mathbf{M_i}$, ${\mathbf{p_i}}^W$ and $\dot{\mathbf{p}}_\mathbf{i}^W$, $i = 1, \cdots, m$, are provided by the MCS. However, these quantities are expressed with respect to the World reference frame RF_W, placed at the center of the laboratory. In order to make the setup of the real experiments equal to the one used in simulation, it is decided to place one more marker $\mathbf{M_0}$ at the origin of the shoulder with arbitrary reference frame RF_0. However, since the movement of the arm makes RF_0 slightly change orientation, the idea is to perform all the experiments by being located in one specific position and to express each marker' position and velocity with respect to $RF_{0'}$, a new reference frame attached to $\mathbf{M_0}$ with the same origin as RF_0 but with fixed orientation obtained after performing a $-\frac{\pi}{2}$ rotation of RF_W about axis z. With reference to Fig. 6.2, the important quantities ${\mathbf{p_i}}^{0'}$ and $\dot{\mathbf{p}}_\mathbf{i}^{0'}$ can be evaluated.

$$
\begin{aligned}
{\mathbf{p_i}}^{0'} &= \mathbf{R}_z\left(\frac{\pi}{2}\right)\left[{\mathbf{p_i}}^W - {\mathbf{p_0}}^W\right] \\
\dot{\mathbf{p}}_\mathbf{i}^{0'} &= \mathbf{R}_z\left(\frac{\pi}{2}\right)\left[\dot{\mathbf{p}}_\mathbf{i}^W - \dot{\mathbf{p}}_\mathbf{0}^W\right]
\end{aligned}
$$

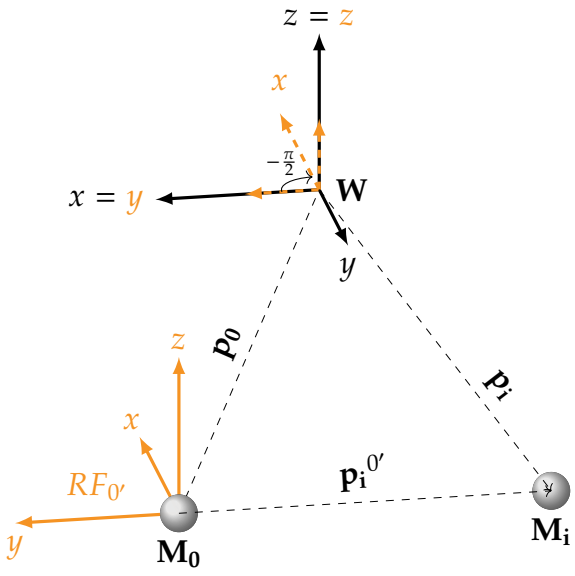

Figure 6.2: Experimental setup

At this point, it is immediate to obtain the quantities $\mathbf{p}^{0'}$ and $\dot{\mathbf{p}}^{0'}$. Moreover, the model of the human arm requires the location of the markers in terms of the

corresponding base frame. While in the simulation step these quantities were perfectly correct, in the experimental phase they are not. In order to evaluate them with enough precision, a first experiment is run, for each specific set of markers. The arm is placed at the **0**-configuration, namely the position for which each joint variable is set to $\eta_j = 0$, $j = 1, \ldots, n$ and it is maintained at that configuration for the whole duration of the experiment. From $\mathbf{p_i}^{0'}$, $\mathbf{p_i}^{B}$ can be computed as follows, where $B = Sh$, $B = El$ or $B = Wr$ depending on the location of marker $\mathbf{M_i}$.

$$\begin{cases} \mathbf{p_i}^{Sh} = & \mathbf{p_i}^{0'}, \quad i \in \mathcal{S} \\ \mathbf{p_i}^{El} = & \mathbf{p_i}^{0'} - \mathbf{O_{Sh'}}^{Sh}, \quad i \in \mathcal{F} \\ \mathbf{p_i}^{Wr} = & \mathbf{p_i}^{0'} - \mathbf{O_{sh'}}^{Sh} - \mathbf{O_{El'}}^{El}, \quad i \in \mathcal{H} \end{cases}$$

Indeed, all the base reference frames RF_{Sh}, RF_{El} and RF_{Wr}, when the arm is at the **0**-configuration, have the same orientation as $RF_{0'}$ but they are translated about y axis of $RF_{0'}$ of 0 $[m]$, L_{sh} and $L_{sh} + L_{fo}$, respectively. By stacking up all $\mathbf{p_i}^{B}$, one obtains $\mathbf{p}^{B}$. The whole set of combinations, described in Tab. 5.1, are analyzed experimentally, except the ones for which singularities, in simulation, have occurred. Hence, all the combination which are tested in the real experiment are reported below.

Combinations of markers				
#	$\lvert\mathcal{S}\rvert$	$\lvert\mathcal{F}\rvert$	$\lvert\mathcal{H}\rvert$	m
1^{st}	0	1	2	3
2^{nd}	1	0	2	
4^{th}	0	2	2	4
5^{th}	1	0	3	
6^{th}	1	1	2	
8^{th}	2	0	2	
9^{th}	1	2	2	5

Table 6.1: Combination of number of markers on the shoulder, forearm and hand to be analyzed in the real experiment

6.2 Noise covariances choice

Once the markers position $\mathbf{p}^B$ is computed, it is possible to compare the performance of the different approaches. As far as LKF and EKF are concerned, one has to decide the covariance matrices $\mathbf{Q}$ and $\mathbf{R}$ to use. For simplicity, they are chosen equal for both in LKF and EKF. One first experiment is run to determine $\mathbf{Q}^i$ and $\mathbf{R}^i$, for each combination of number of markers $i = \{1, 2, 4, 5, 6, 8, 9\}$. Before actually running each experiment, the set of markers is placed along the arm at the $\mathbf{0}$-configuration so that $\mathbf{p}^{B,i}$ can be computed. Once the data related to $\mathbf{p}^{0',i}$, $\dot{\mathbf{p}}^{0',i}$, which corresponds to the i^{th} combination, is obtained, the matrices $\mathbf{Q}^i$ and $\mathbf{R}^i$ are determined as follows.

$$\begin{aligned}\left(\mathbf{Q}^i, \mathbf{R}^i\right) &= \underset{\tilde{\mathbf{Q}}\in\mathcal{S}_\mathbf{Q}, \tilde{\mathbf{R}}\in\mathcal{S}_\mathbf{R}}{\operatorname{argmin}} \ \operatorname{RMSE}\left[\mathbf{\Phi}^i\left(\hat{\boldsymbol{\eta}}^{\mathrm{EKF}(\tilde{\mathbf{Q}},\tilde{\mathbf{R}})}\right)\right] \\ &= \underset{\tilde{\mathbf{Q}}\in\mathcal{S}_\mathbf{Q}, \tilde{\mathbf{R}}\in\mathcal{S}_\mathbf{R}}{\operatorname{argmin}} \sqrt{\frac{1}{3m}\cdot\frac{1}{N}\sum_{k=1}^{N}\left\|\mathbf{p}^{0',i}(k) - \mathbf{\Phi}^i\left(\hat{\boldsymbol{\eta}}_{k|k}^{\mathrm{EKF}(\tilde{\mathbf{Q}},\tilde{\mathbf{R}})}\right)\right\|^2}\end{aligned}$$

Let

$$\begin{aligned}\mathcal{S}_\mathbf{Q} &= \left\{\sigma_{\mathbf{Q}_i}^2\cdot\mathbf{I}_{n\times n}\right\}, \quad \sigma_{\mathbf{Q}_i}^2 = \left\{10^{-3}, 10^{-2}, 10^{-1}, 1, 10, 10^2, 10^3\right\} \\ \mathcal{S}_\mathbf{R} &= \left\{\sigma_{\mathbf{R}_j}^2\cdot\bar{\sigma}_\mathbf{R}^2\cdot\mathbf{I}_{(3m)\times(3m)}\right\}, \quad \sigma_{\mathbf{R}_j}^2 = \left\{10^{-2}, 10^{-1}, 1, 10, 10^2, 10^3, 10^4\right\}\end{aligned}$$

Hence, the process and measurement covariances are chosen as:

$(\mathbf{Q}, \mathbf{R})$ choice		
i	$\mathbf{Q}^i$	$\mathbf{R}^i$
1	$10^{-2}\cdot\mathbf{I}_{n\times n}$	$10\cdot\bar{\sigma}_\mathbf{R}^2\cdot\mathbf{I}_{(3m)\times(3m)}$
2	$10^{-3}\cdot\mathbf{I}_{n\times n}$	$10^4\cdot\bar{\sigma}_\mathbf{R}^2\cdot\mathbf{I}_{(3m)\times(3m)}$
4	$10^{-3}\cdot\mathbf{I}_{n\times n}$	$10^4\cdot\bar{\sigma}_\mathbf{R}^2\cdot\mathbf{I}_{(3m)\times(3m)}$
5	$10^{-3}\cdot\mathbf{I}_{n\times n}$	$10^2\cdot\bar{\sigma}_\mathbf{R}^2\cdot\mathbf{I}_{(3m)\times(3m)}$
6	$10^{-1}\cdot\mathbf{I}_{n\times n}$	$10^4\cdot\bar{\sigma}_\mathbf{R}^2\cdot\mathbf{I}_{(3m)\times(3m)}$
8	$10^{-2}\cdot\mathbf{I}_{n\times n}$	$10^4\cdot\bar{\sigma}_\mathbf{R}^2\cdot\mathbf{I}_{(3m)\times(3m)}$
9	$1\cdot\mathbf{I}_{n\times n}$	$10^4\cdot\bar{\sigma}_\mathbf{R}^2\cdot\mathbf{I}_{(3m)\times(3m)}$

Table 6.2: Choice for $\left(\mathbf{Q}^i, \mathbf{R}^i\right)$ matrices

6.3 Results

In the following, from Fig. 6.3 to Fig. 6.9, the results about the least-squares LS and the Extended Kalman filter EKF approaches are shown, for each combination of number of markers reported in Tab. 6.1. Instead, Fig. 6.10 reports the results about the comparison between the Linearized Kalman filter LKF and the Extended Kalman filter EKF estimates. Specifically, the goodness of the three different joint estimates $\hat{\boldsymbol{\eta}}^{LS}$, $\hat{\boldsymbol{\eta}}^{LKF}$ and $\hat{\boldsymbol{\eta}}^{EKF}$ is reported in terms of RMSE namely, given the estimate $\hat{\boldsymbol{\eta}}_k$, the quantity

$$\sqrt{\frac{1}{3m}\left\|\mathbf{p}^{0\prime}(k)-\boldsymbol{\Phi}\left(\hat{\boldsymbol{\eta}}_k\right)\right\|^2}$$

is plotted $\forall k$. The initial estimates which are fed to the different algorithms are $\hat{\boldsymbol{\eta}}^{LS}(0)=\hat{\boldsymbol{\eta}}_{0|0}^{LKF}=\hat{\boldsymbol{\eta}}_{0|0}^{EKF}=\mathbf{0}$. One can state that the case $|\mathcal{S}|=1,\ |\mathcal{F}|=1,\ |\mathcal{H}|=2$ and $|\mathcal{S}|=1,\ |\mathcal{F}|=2,\ |\mathcal{H}|=2$ leads in general to better joint estimate. Tab. 6.4 shows the corresponding RMSE. Moreover, As far the Linearized Kalman filter is concerned, the nominal point along which the model is linearized is chosen as $\left(\bar{\boldsymbol{\eta}},\bar{\mathbf{p}}\right)=(\mathbf{0},\mathbf{0})$. Since the arm is moved differently in each one of the following first 6 experiments, one more experiment is run, considering the case $|\mathcal{S}|=1,\ |\mathcal{F}|=2,\ |\mathcal{H}|=2$. Fig. 6.10 corresponds to this experiment in which the trajectory of the arm is kept close to the chosen equilibrium point. Only in this case, the performance of the LKF is close to the EKF. The LKF and EKF joint estimates are compared and the corresponding RMSE are reported in Tab. 6.3.

LKF-EKF comparison when $\boldsymbol{\eta} \approx \bar{\boldsymbol{\eta}}$			
$\lvert\mathcal{S}\rvert$	$\lvert\mathcal{F}\rvert$	$\lvert\mathcal{H}\rvert$	Root Mean Squared Error [m]
1	2	2	RMSE $\left[\boldsymbol{\Phi}\left(\hat{\boldsymbol{\eta}}^{\mathrm{LKF}}\right)\right]=0.0059$
			RMSE $\left[\boldsymbol{\Phi}\left(\hat{\boldsymbol{\eta}}^{\mathrm{EKF}}\right)\right]=0.0031$

Table 6.3: LKF-EKF performance when the trajectory of the human arm is close to the equilibrium point in the 5 markers case. The corresponding figure is Fig. 6.10

LS-EKF comparison			
$\lvert\mathcal{S}\rvert$	$\lvert\mathcal{F}\rvert$	$\lvert\mathcal{H}\rvert$	Root Mean Squared Error [m]
0	1	2	RMSE $\left[\mathbf{\Phi}\left(\hat{\eta}^{\mathrm{LS}}\right)\right] = 0.2286$
			RMSE $\left[\mathbf{\Phi}\left(\hat{\eta}^{\mathrm{EKF}}\right)\right] = 0.0261$
1	0	2	RMSE $\left[\mathbf{\Phi}\left(\hat{\eta}^{\mathrm{LS}}\right)\right] = 0.2510$
			RMSE $\left[\mathbf{\Phi}\left(\hat{\eta}^{\mathrm{EKF}}\right)\right] = 0.1498$
0	2	2	RMSE $\left[\mathbf{\Phi}\left(\hat{\eta}^{\mathrm{LS}}\right)\right] = 0.1835$
			RMSE $\left[\mathbf{\Phi}\left(\hat{\eta}^{\mathrm{EKF}}\right)\right] = 0.0263$
1	0	3	RMSE $\left[\mathbf{\Phi}\left(\hat{\eta}^{\mathrm{LS}}\right)\right] = 0.0850$
			RMSE $\left[\mathbf{\Phi}\left(\hat{\eta}^{\mathrm{EKF}}\right)\right] = 0.0596$
1	1	2	RMSE $\left[\mathbf{\Phi}\left(\hat{\eta}^{\mathrm{LS}}\right)\right] = 0.0993$
			RMSE $\left[\mathbf{\Phi}\left(\hat{\eta}^{\mathrm{EKF}}\right)\right] = 0.0085$
2	0	2	RMSE $\left[\mathbf{\Phi}\left(\hat{\eta}^{\mathrm{LS}}\right)\right] = 0.0933$
			RMSE $\left[\mathbf{\Phi}\left(\hat{\eta}^{\mathrm{EKF}}\right)\right] = 0.0326$
1	2	2	RMSE $\left[\mathbf{\Phi}\left(\hat{\eta}^{\mathrm{LS}}\right)\right] = 0.0899$
			RMSE $\left[\mathbf{\Phi}\left(\hat{\eta}^{\mathrm{EKF}}\right)\right] = 0.0052$

Table 6.4: LS-EKF performance in the 3-4-5 markers case. The corresponding figures are Figs. 6.3, 6.4, 6.5, 6.6, 6.7, 6.8, 6.9

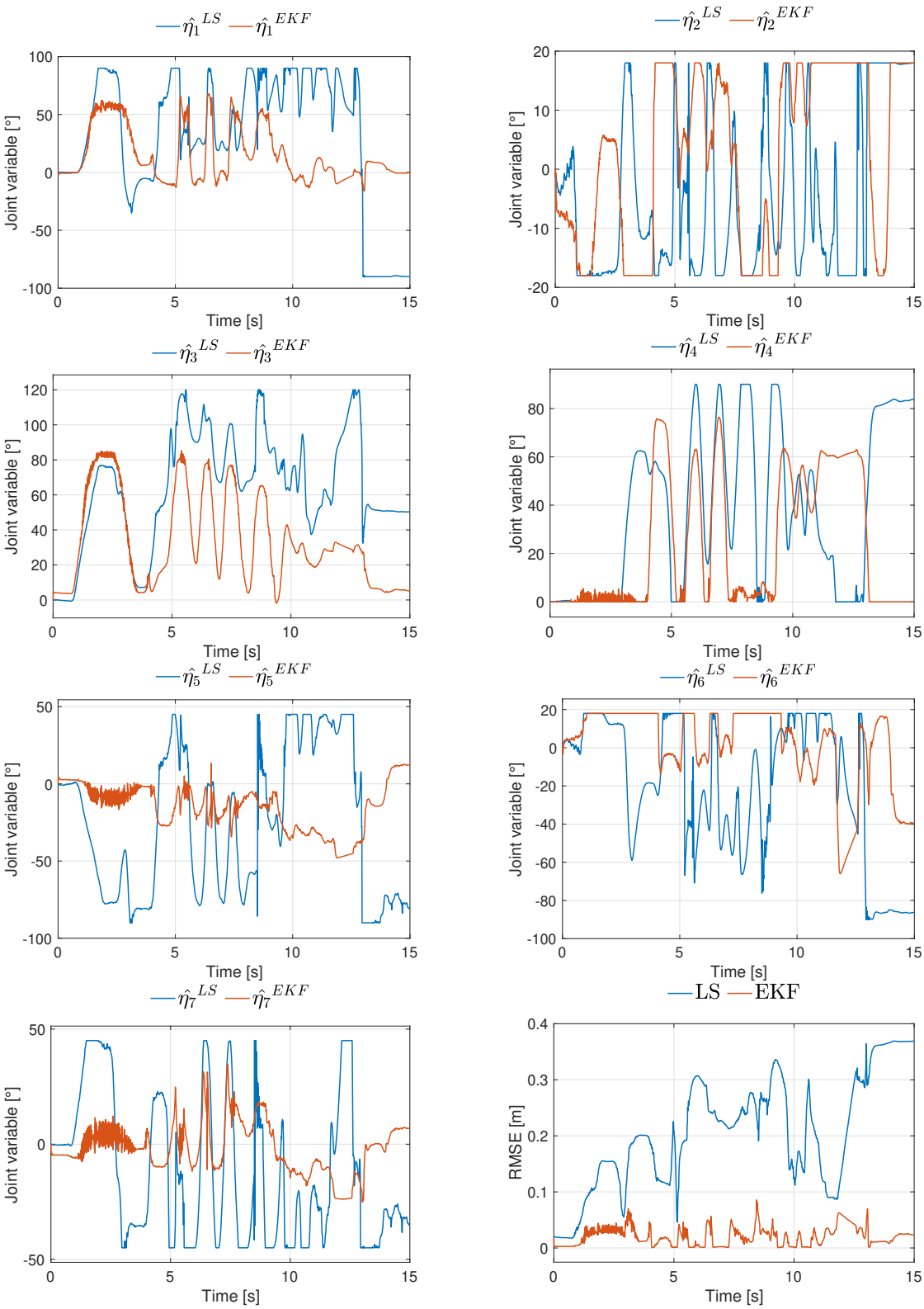

Figure 6.3: $|\mathcal{S}| = 0,\ |\mathcal{F}| = 1,\ |\mathcal{H}| = 2$

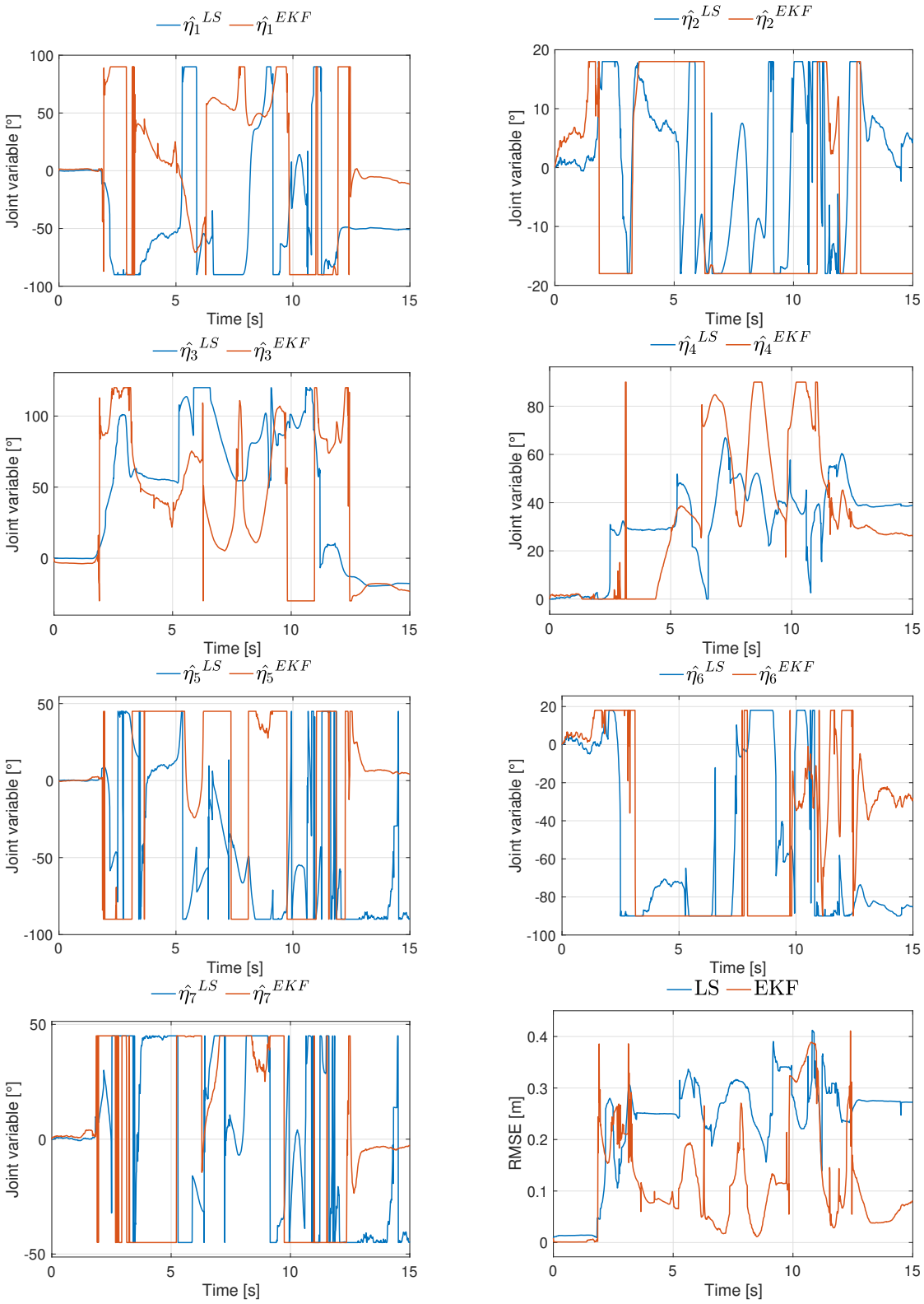

Figure 6.4: $|\mathcal{S}| = 1,\ |\mathcal{F}| = 0,\ |\mathcal{H}| = 2$

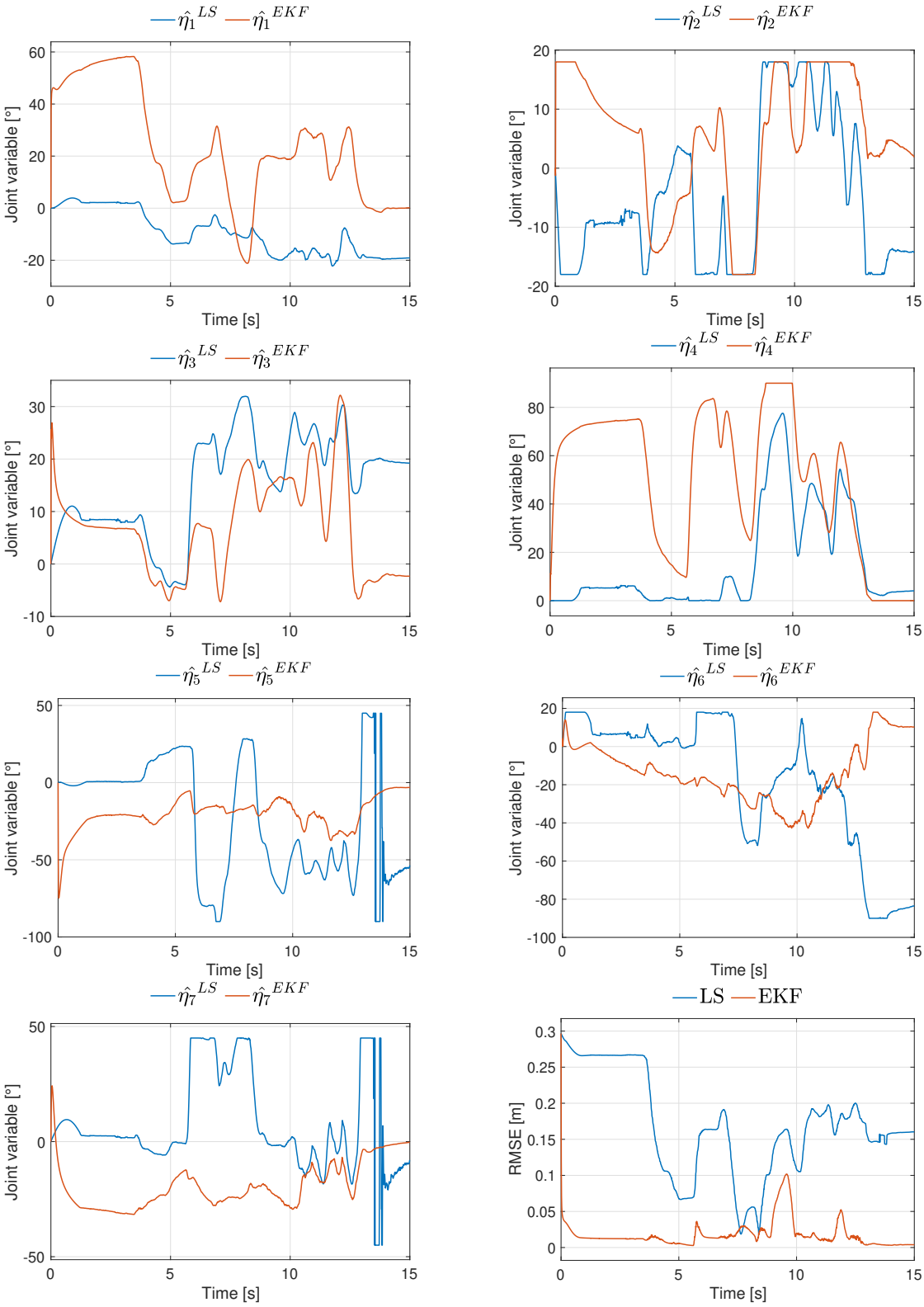

Figure 6.5: $|\mathcal{S}| = 0,\ |\mathcal{F}| = 2,\ |\mathcal{H}| = 2$

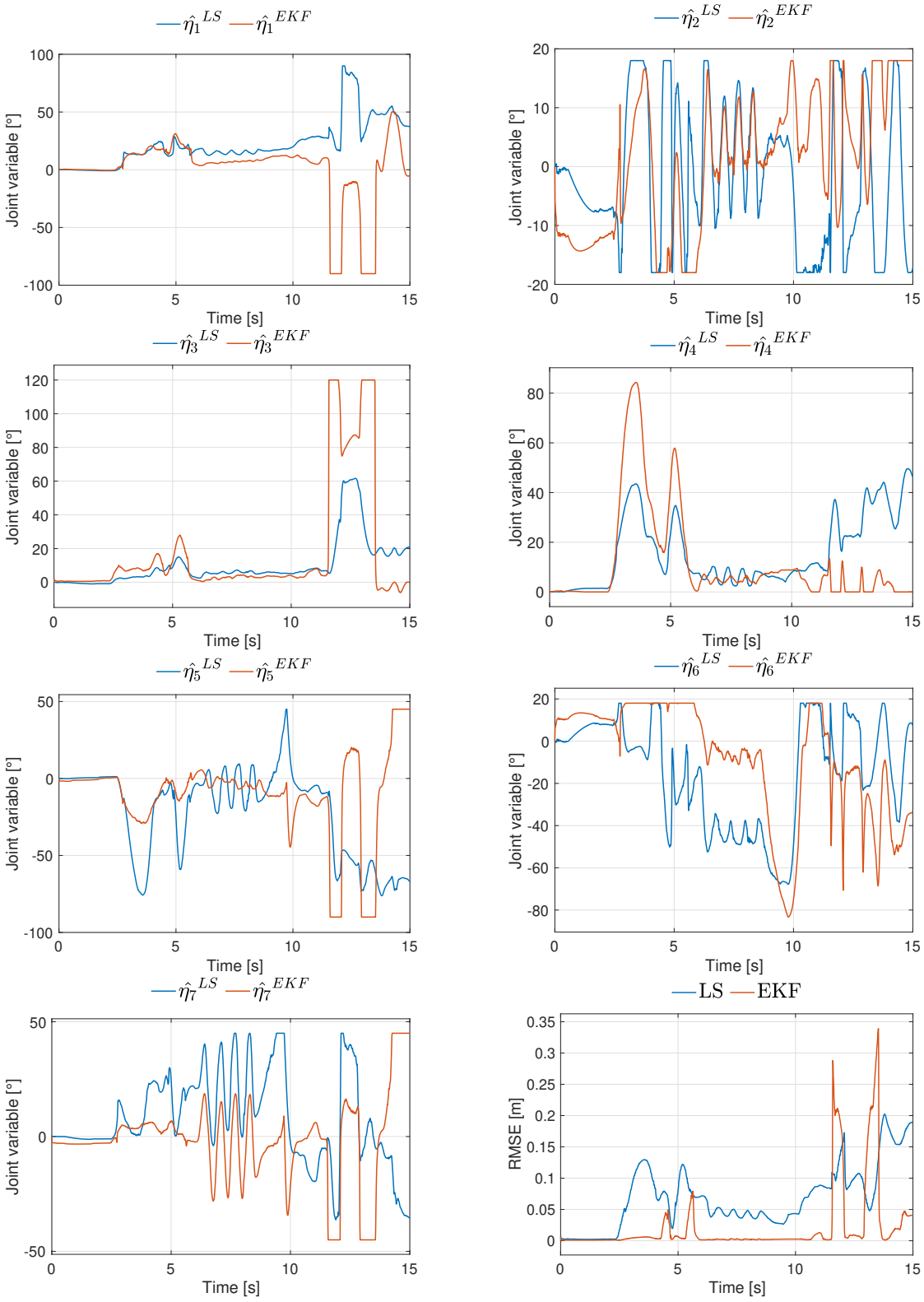

Figure 6.6: $|\mathcal{S}| = 1,\ |\mathcal{F}| = 0,\ |\mathcal{H}| = 3$

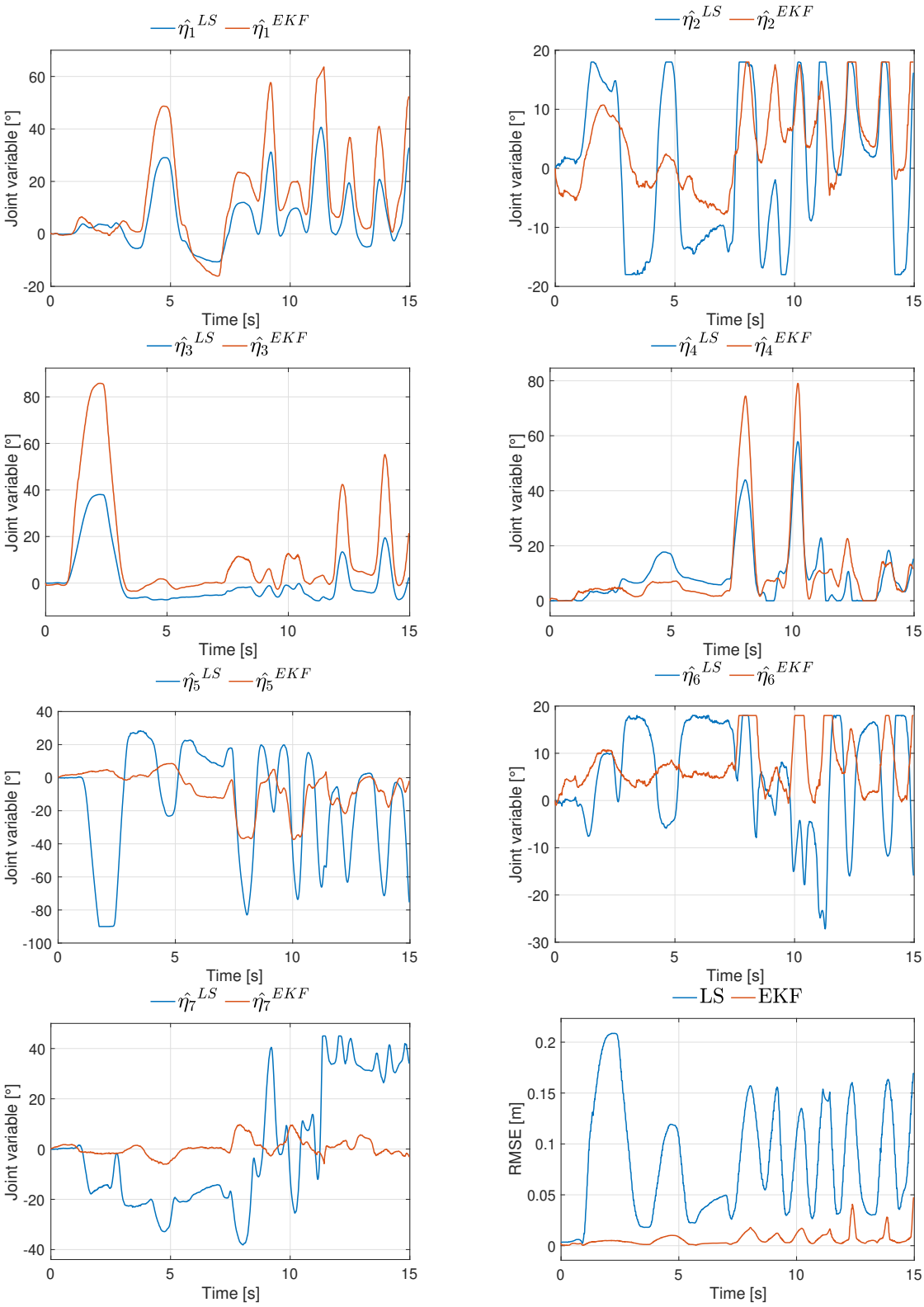

Figure 6.7: $|\mathcal{S}| = 1,\ |\mathcal{F}| = 1,\ |\mathcal{H}| = 2$

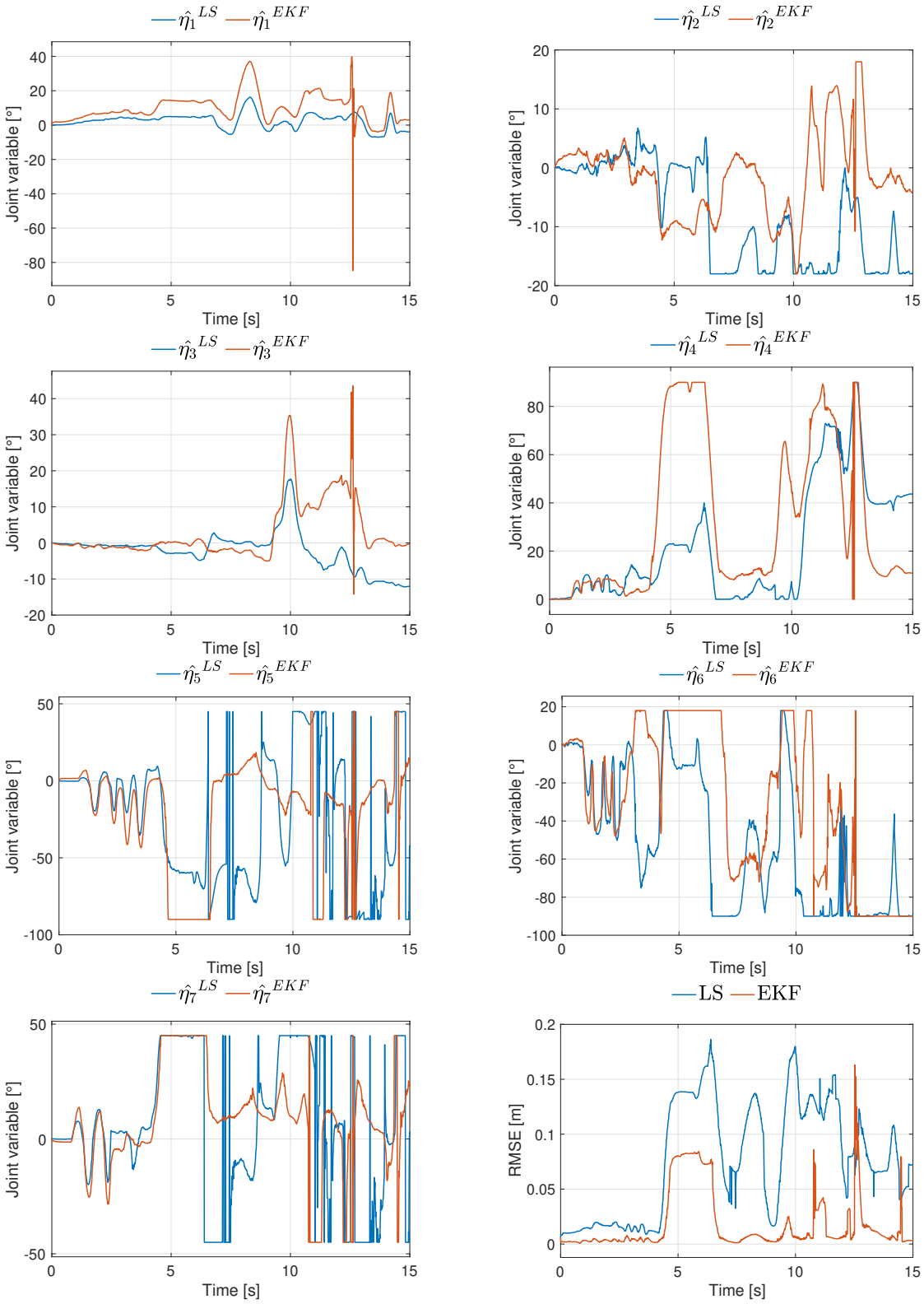

Figure 6.8: $|\mathcal{S}| = 2,\ |\mathcal{F}| = 0,\ |\mathcal{H}| = 2$

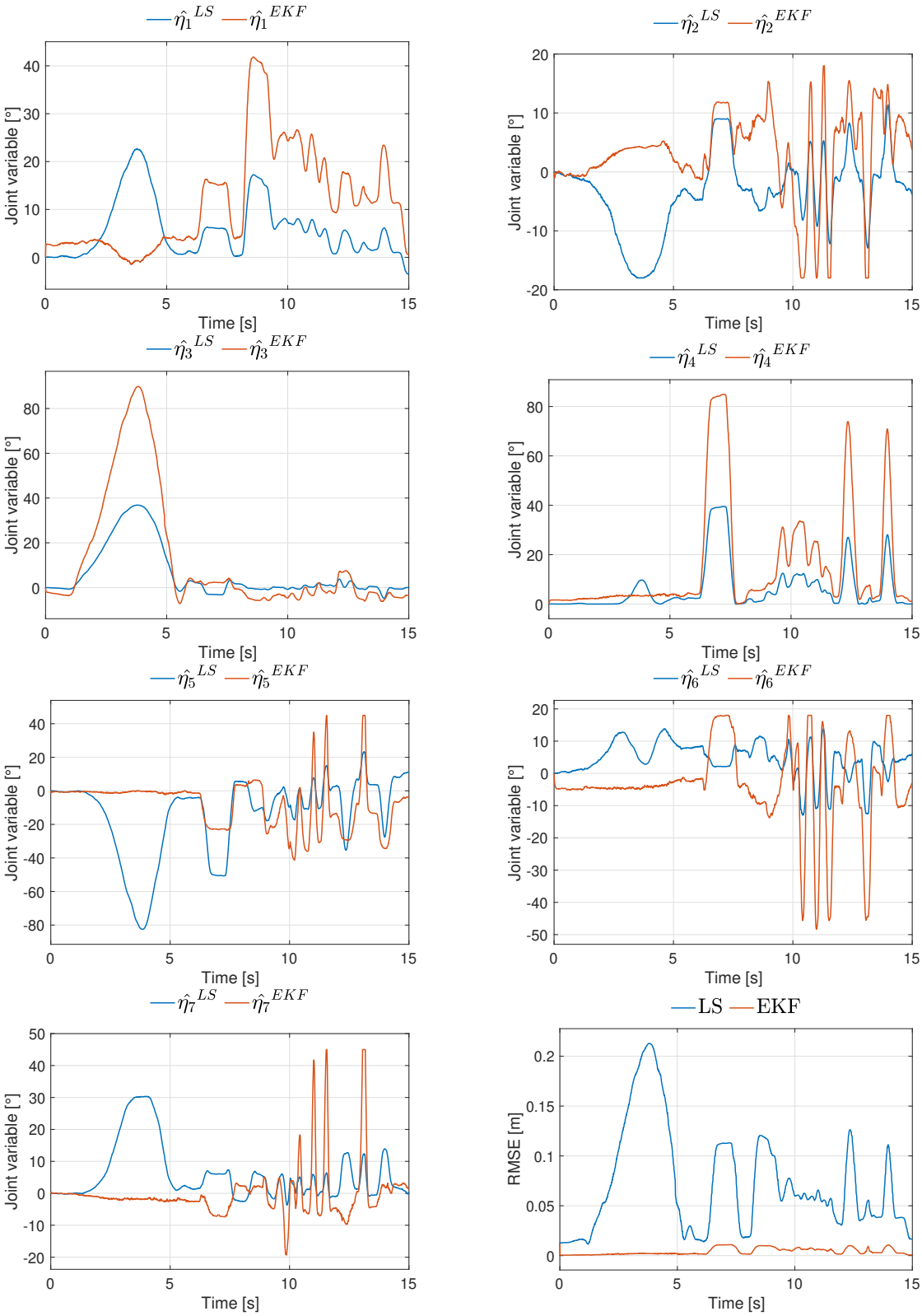

Figure 6.9: $|\mathcal{S}| = 1,\ |\mathcal{F}| = 2,\ |\mathcal{H}| = 2$

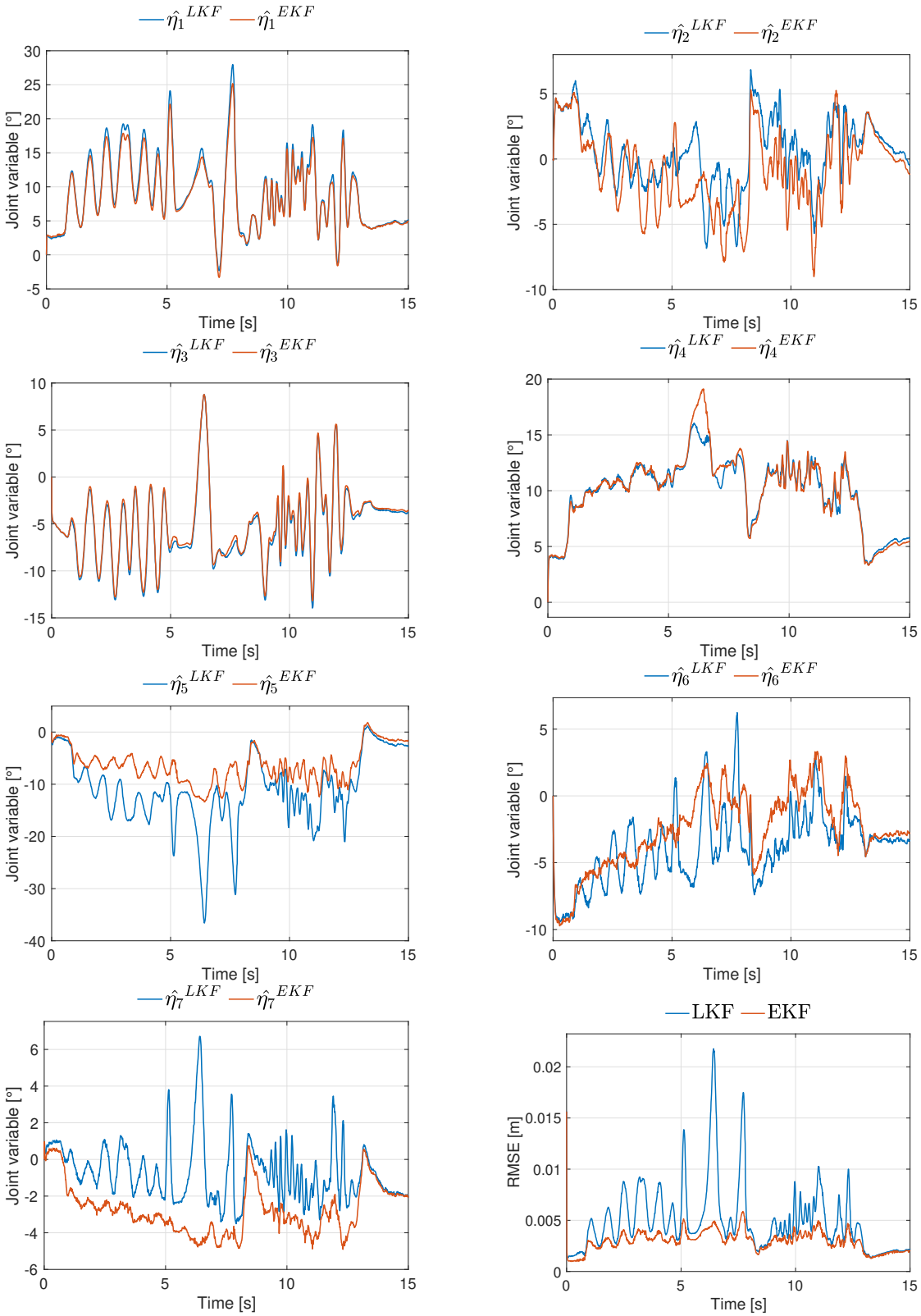

Figure 6.10: $|\mathcal{S}| = 1,\ |\mathcal{F}| = 2,\ |\mathcal{H}| = 2$ when $\boldsymbol{\eta} \approx \bar{\boldsymbol{\eta}}$

6.4 Results discussion

As it is possible to observe in the previous figures, the LS approach does not provide good estimation results as the EKF does. However, the quality of the Extended Kalman filter estimates depend on the number of markers used and, in particular, on $|\mathcal{S}|$, $|\mathcal{F}|$ and $|\mathcal{H}|$. For each combination of markers, the joint variables estimates are shown as well as the corresponding RMSE. As already mentioned, the combinations which produce the best EKF estimates are the following ones:

- $|\mathcal{S}| = 1,\ |\mathcal{F}| = 1,\ |\mathcal{H}| = 2$
- $|\mathcal{S}| = 1,\ |\mathcal{F}| = 2,\ |\mathcal{H}| = 2$

Concerning the LS estimates, it is not as good as the EKF for a number of reasons. First of all, this estimation algorithm does not take into account the noise information. Also, during the simulation step, it was shown that it is not able to return a good estimate whenever there is a mismatch between the initial conditions $\hat{\boldsymbol{\eta}}^{LS}(0)$ and $\boldsymbol{\eta}^{ref}(0)$. Hence, multiple causes makes the LS approach not to perform good.

Regarding Fig. 6.10, the LKF and EKF estimates are quite close since the human arm was moved near the equilibrium along which the *non-linear* model was linearized. Still, there is an improvement of the solution given by the Extended Kalman filter algorithm.

7

Conclusions and Future Works

A suitable algorithm, the Extended Kalman filter (EKF), for the estimation of the joint-space configuration of the human arm, through the data acquisition of some markers placed along, was designed. Other approaches were tested, such as the Least-Squares (LS) and the Linearized Kalman filter (LKF). However, they were shown to lead in general to worse results. In particular, different choices of number of markers on the shoulder, forearm and hand were carefully analyzed during the Matlab simulations, leading good results, both in the simulation and experimental steps, when considering one marker on the shoulder, one on the forearm, two on the hand or one marker on the shoulder, two on the forearm and two on the hand.

However, for different number of markers on the shoulder, forearm and hand, there was the risk of having even bad EKF estimate, due to the use of the *left-pseudoinverse* of the Jacobian in the model of the human arm. The Singular Value Decomposition (SVD) of the Jacobian can represent a valid tool to express the pseudoinverse in terms of only large enough *singular* values so to avoid *quasi-singularities*. This change of model may result in better joint estimates in those cases in which *quasi-singularities* occur. This may be part of future work as well as other extensions of the Kalman filter. Indeed, some limitations of the EKF as, for example, its suboptimality due to the truncation of the higher-order terms when linearizing the system, can be overcame by the Iterated Extended Kalman Filters (IEKF), which is shown to improve the convergence of the first-order filter by iterating at the measurement update step and the Unscented Kalman filter (UKF).

Appendices

A

Pseudo-inverses

In many cases, a vector variable is a linear function of another vector. The proportionality between the two is expressed by the matrix $\mathbf{\Phi}$:

$$\mathbf{y} = \mathbf{\Phi} \cdot \boldsymbol{\theta} \tag{A.1}$$

$\mathbf{\Phi}$ has dimension $(m \times n)$, and it is conformable with $\boldsymbol{\theta} \in \mathbb{R}^n$ and $\mathbf{y} \in \mathbb{R}^m$.
In order to compute the inverse of matrix $\mathbf{\Phi}$, it has to be square $(n = m)$ and *non-singular*. How can an inverse relationship between $\mathbf{y}$ and $\boldsymbol{\theta}$ be defined if m and n are not equal? The answer is found in the generalized inverse or *pseudo-inverse* matrix, denoted by $\mathbf{\Phi}^\dagger$. The *pseudo-inverse* matrix takes one of two forms, depending upon the relative dimensions of $\mathbf{y}$ and $\boldsymbol{\theta}$. If $m > n$, Eq. A.1 represents more scalar equations than unknowns, so the inverse solution may be *over-determined*. On the other hand, if $m < n$, the opposite is true, and the solution for $\boldsymbol{\theta}$ is *under-determined*.

$\mathbf{\Phi}$ is assumed to be a $(m \times n)$ *full-rank* matrix; hence, $\mathbf{\Phi}^T\mathbf{\Phi}$ has dimension $(n \times n)$, while $\mathbf{\Phi}\mathbf{\Phi}^T$ has dimension $(m \times m)$. If $m > n$, $\mathbf{\Phi}^T\mathbf{\Phi}$ is *non-singular*, but $\mathbf{\Phi}\mathbf{\Phi}^T$ is *singular*. Conversely, if $m < n$, $\mathbf{\Phi}\mathbf{\Phi}^T$ is *non-singular*, but $\mathbf{\Phi}^T\mathbf{\Phi}$ is *singular*.

The *left pseudo-inverse* is appropriate for the solution of the *over-determined* case. Pre-multiplying both sides of Eq. A.1 by $\mathbf{\Phi}^T$,

$$\mathbf{\Phi}^T\mathbf{\Phi} \cdot \boldsymbol{\theta} = \mathbf{\Phi}^T \cdot \mathbf{y}$$

it follows that

$$\boldsymbol{\theta} = \underbrace{\left(\boldsymbol{\Phi}^T\boldsymbol{\Phi}\right)^{-1}\boldsymbol{\Phi}^T}_{\boldsymbol{\Phi}_L^\dagger} \cdot \mathbf{y} \tag{A.2}$$

Instead, the *right pseudo-inverse* is appropriate for the solution of the *under-determined* case. By noticing that

$$\left(\boldsymbol{\Phi}\boldsymbol{\Phi}^T\right) \cdot \left(\boldsymbol{\Phi}\boldsymbol{\Phi}^T\right)^{-1} = I_{m\times m}$$

Eq. A.1 can be written as $\boldsymbol{\Phi} \cdot \boldsymbol{\theta} = \boldsymbol{\Phi}\boldsymbol{\Phi}^T \cdot \left(\boldsymbol{\Phi}\boldsymbol{\Phi}^T\right)^{-1} \cdot \mathbf{y}$, therefore

$$\boldsymbol{\theta} = \underbrace{\boldsymbol{\Phi}^T\left(\boldsymbol{\Phi}\boldsymbol{\Phi}^T\right)^{-1}}_{\boldsymbol{\Phi}_R^\dagger} \cdot \mathbf{y} \tag{A.3}$$

B

Singular Value Decomposition

Given a matrix $\mathbf{\Phi}$ of dimensions $(m \times n)$, the scalars $\sigma_1 \geq \sigma_2 \geq \ldots \geq \sigma_n \geq 0$ are said to be its *singular values* and they are related to the eigenvalues of matrix $\mathbf{\Phi}^T\mathbf{\Phi}$, $\lambda_1 \geq \lambda_2 \geq \ldots \geq \lambda_n \geq 0$, as $\lambda_i = \sigma_i^2$. The SVD of matrix $\mathbf{\Phi}$ is given by

$$\mathbf{\Phi} = \mathbf{U}\mathbf{S}\mathbf{V}^T$$

where $\mathbf{U}$ is an $(m \times m)$ orthogonal matrix $\mathbf{U} = [\ \mathbf{u}_1 \quad \mathbf{u}_2 \quad \ldots \quad \mathbf{u}_m\ ]$ and $\mathbf{V}$ is an $(n \times n)$ orthogonal matrix $\mathbf{V} = [\ \mathbf{v}_1 \quad \mathbf{v}_2 \quad \ldots \quad \mathbf{v}_n\ ]$.
Moreover, $\mathbf{S}$ is an $(m \times n)$ matrix

$$\mathbf{S} = \begin{bmatrix} \mathbf{S}_k & \mathbf{O} \\ \mathbf{O} & \mathbf{O} \end{bmatrix} = \underbrace{\left[\begin{array}{cccc|c} \sigma_1 & 0 & \ldots & 0 & \\ 0 & \sigma_2 & \ldots & 0 & \mathbf{0} \\ \vdots & \vdots & \ddots & \vdots & \\ 0 & 0 & \ldots & \sigma_k & \\ \hline & \mathbf{0} & & & \mathbf{0} \end{array}\right]}_{k \qquad n-k} \begin{matrix} \left.\begin{matrix} \\ \\ \\ \\ \end{matrix}\right\} k \\ \left.\begin{matrix} \\ \end{matrix}\right\} m-k \end{matrix}$$

$$, \overbrace{\sigma_1 \geq \sigma_2 \geq \ldots \geq \sigma_k}^{\textit{non-null singular values}} > 0$$

.

The number of non-null *singular values* is equal to the rank k of matrix $\mathbf{\Phi}$ and $k \leq \min(m, n)$. The unit vectors $\mathbf{v}_i \in \mathbb{R}^n$ and $\mathbf{u}_i \in \mathbb{R}^m$ are called *right* and *left* singular vectors of $\mathbf{\Phi}$ with corresponding *singular value* $\sigma_i > 0$ if

$$\mathbf{\Phi}\mathbf{v}_i = \sigma_i \mathbf{u}_i$$
$$\mathbf{\Phi}^T \mathbf{u_i} = \sigma_i \mathbf{v}_i$$

The columns of $\mathbf{U}$ are the eigenvectors of the matrix $\mathbf{\Phi}\mathbf{\Phi}^T$, whereas the columns of V are the eigenvectors of the matrix $\mathbf{\Phi}^T\mathbf{\Phi}$.

The SVD plays an important role when the inverse of the matrix $\mathbf{\Phi}$ does not exist, namely if any of the singular values is zero. Indeed, the *pseudo-inverse* of $\mathbf{\Phi}$, denoted as $\mathbf{\Phi}^\dagger$, can be exploited:

$$\begin{aligned}\mathbf{\Phi}^\dagger &= \mathbf{U}\mathbf{S}^\dagger\mathbf{V}^T \\ &= \mathbf{U}\begin{bmatrix} \frac{1}{\sigma_1} & & & & & \\ & \ddots & & & & \\ & & \frac{1}{\sigma_k} & & & \\ & & & 0 & & \\ & & & & \ddots & \\ & & & & & 0 \end{bmatrix}\mathbf{V}^T\end{aligned}$$

In practical situations, a matrix may have singular values that are very close to zero and it is not possible to accurately compute them. In such cases, the matrix is called *ill-conditioned*, because the division $\frac{1}{\sigma_i}$, where $\sigma_i \approx 0$, will result in numerical errors. Such matrices are theoretically but not practically invertible. The degree to which ill-conditioning prevents a matrix from being inverted accurately depends on the ratio of its largest to smallest singular value, a quantity known as the *condition number* which, in the literature, is defined as

$$\kappa(\mathbf{\Phi}) = \frac{\sigma_1}{\sigma_k}$$

References

[1] Brian D. O. Anderson and John B. Moore. *Optimal Filtering*. 1979.

[2] Simon Dan. *Optimal State Estimation*. 2006.

[3] Alessandro De Luca et al. "Collision Detection and Safe Reaction with the DLR-III Lightweight Manipulator Arm". In: *Proceedings of the 2006 IEEE/RSJ*. 2006.

[4] Cheng Fang et al. "Online Model Based Estimation of Complete Joint Stiffness of Human Arm". In: *IEEE ROBOTICS AND AUTOMATION LETTERS, VOL. 3, NO. 1*. 2018.

[5] L. I. Gliga et al. "A method to estimate the process noise covariance for a certain class of nonlinear systems". In: *Mechanical Systems and Signal Processing 131 (2019) 381–393*. 2019.

[6] Nives Klopcar and Jadran Lenarčič. "Kinematic Model for Determination of Human Arm Reachable Workspace". In: *Meccanica 40: 203–219*. 2005.

[7] H. G. Lee, A. Arapostathis, and S. I. Marcus. "Linearization of discrete time nonlinear systems". In: *Electrical and Computer Engineering Louisiana State University Baton Rouge, LA 70803-5901*.

[8] Jadran Lenarčič and Umek Andreja. "Simple Model of Human Arm Reachable Workspace". In: *IEEE TRANSACTIONS ON SYSTEMS, MAN, AND CYBERNETICS, VOL. 24, NO. 8*. 1994.

[9] Qiang Li et al. "Kalman Filter and Its Application". In: *8th International Conference on Intelligent Networks and Intelligent Systems*. 2015.

[10] Wentao Ma et al. "Linear Kalman Filtering Algorithm With Noisy Control Input Variable". In: *IEEE TRANSACTIONS ON CIRCUITS AND SYSTEMS—II: EXPRESS BRIEFS, VOL. 66, NO. 7*. 2019.

[11] Philippe Martinet and Sukhan Lee. "Damped least square based genetic algorithm with Ggaussian distribution of damping factor for singularity-robust inverse kinematics". In: *Journal of Mechanical Science and Technology*. 2008.

[12] Peter S. Maybeck. "The Kalman Filter: An Introduction to Concepts". In: *I. J. Cox et al. (eds.), Autonomous Robot Vehicles*. 1990.

[13] Jerry M. Mendel. *Lessons in Digital Estimation Theory*. 1897.

[14] Arturo Bertomeu Motos et al. "Human arm joints reconstruction algorithm in rehabilitation therapies assisted by end-effector robotic devices". In: *Journal of NeuroEngineering and Rehabilitation*. 2018.

[15] Dung Phan et al. "A constrained nonlinear optimization solution for 3D orientation estimation of the human limb". In: *The 2017 Biomedical Enginnering International Conference (BMEiCON-2017)*. 2017.

[16] R. A. Prokopenko et al. "Assessment of the accuracy of a human arm model with seven degrees of freedom". In: *Journal of Biomechanics 34 177-185*. 2011.

[17] Isabel Ribeiro. "Kalman and Extended Kalman Filters: Concept, Derivation and Properties". In: *Institute for Systems and Robotics, Lisboa Portugal*. 2004.

[18] Carlos Rodriguez de Cos and J. Á Acosta. "Adaptive Integral Inverse Kinematics Control for Lightweight Compliant Manipulators". In: *IEEE Robotics and Automation Letters*. 2020.

[19] Carlos Rodriguez de Cos and Dimos V. Dimarogonas. "Adaptive Cooperative Control for Human-Robot Load Manipulation". In: *IEEE ROBOTICS AND AUTOMATION LETTERS, VOL. 7, NO. 2*. 2022.

[20] Bruno Siciliano. "Kinematic Control of Redundant Robot Manipulators: A Tutorial". In: *Journal of lntelligent and Robotic Systems 3: 201-212.* 1990.

[21] Bruno Siciliano et al. *Robotics Modelling, Planning and Control*. 2009.

[22] Robert F. Stengel. *Optimal Control and Estimation*. 1994.

[23] Andrea Maria Zanchettin et al. "Kinematic motion analysis of the human arm during a manipulation task". In: *ISR / ROBOTIK*. 2010.